EXPERIMENTAL INVESTIGATIONS OF THERMODYNAMIC PROPERTIES OF ORGANOMETALLIC COMPOUNDS

Von der Fakultät für Ingenieurwissenschaften,

Abteilung Maschinenbau und Verfahrenstechnik

der Universität Duisburg-Essen

zur Erlangung des akademischen Grades

DOKTOR-INGENIEUR

genehmigte Dissertation

von

Rehan Ahmad Siddiqui

aus

Lucknow, Indien

Referent: Uni. Prof. Dr. rer. nat. habil Burak Atakan

Korreferent: Uni. Prof. Dr. rer. nat. Ulrich Zenneck

Tag der mündlichen Prüfung: 10-06-2009

ABSTRACT

Organometallic compounds are often volatile enough to be useful as precursors of the metals in vapor phase deposition process, e.g. chemical vapor deposition (CVD). For this process the precursor molecules are evaporated. To engineer such a process the knowledge of the vapor or sublimation pressures is essential because they determine the maximum theoretical growth rate and the composition. The gaseous diffusion coefficients for organometallic compounds are needed for the calculation of the Sherwood and Lewis numbers used to describe mass transfer process. Such data are either lacking or not well established.

This work reports the thermal stability, vapor pressure and the gaseous diffusion coefficient for numerous organometallic compounds that are used as CVD precursors. These includes

1. Metal acetylacetonates ($[M(acac)_n]$) of aluminium, chromium, iron, thulium, manganese, ruthenium, vanadium, dysprosium, zinc, copper and nickel.
2. Metal 2,2,6,6-tetramethyl-3,5-heptandionate ($[M(tmhd)_n]$) of iron, manganese, aluminium, chromium, europium, nickel, and copper.
3. Metallocene ($[M(cp)_n]$) of nickel and ruthenium.
4. Newly synthesized precursors or non commercial precursors of hafnium, zirconium, ruthenium, tungsten and copper.

Some of the precursors were sensitive towards ambient atmosphere. Therefore, the samples were stored in the glove box. The thermogravimetry analyser (TGA) apparatus was also kept inside the glove box so that an inert atmosphere is always present during handling of the sample. Non isothermal as well as isothermal thermogravimetry was used to study the thermal stability of the precursors. Due attention was being paid to the agreement of the mass loss curve with the theory and the amount of residue. If nearly linear mass loss curve was obtained along with the negligible amount of residue, the substance was considered to be thermally stable. It was then subjected to vapor pressure measurement using a Knudsen cell. A special arrangement was made into the experimental setup to ensure the circulation of nitrogen to prevent the degradation of the sample due to atmospheric air during the heating period. The vapor pressures from 0.01-25 Pa were measured with the Knudsen cell in the temperature range of 317-442K.

The gaseous diffusion coefficients were determined using the TGA. The TGA method of the determination of the gaseous diffusion coefficient is based on the fact that the mass transfer rate at a given total pressure and temperature is mainly a function of the diffusion coefficient and the vapor pressure of the sublimating substance. The vapor pressures determined using the Knudsen cell were combined with the TGA measurements to obtain the diffusion coefficients. The gaseous diffusion coefficients for the organometallic compounds have been reported for the first time.

Apart from the organometallic compounds experiments have been performed with two well studied substances anthracene and pyrene to check the present approach. The measured value of vapor pressure and the gaseous diffusion coefficient values were in good agreement with all the available literature values for these reference substances.

ACKNOWLEDGEMENT

It gives me immense pleasure to express my depth of gratitude and respect toward my supervisor Prof. Dr. rer. nat. habil Burak Atakan for giving me an opportunity to work with him and for his excellent supervision, discussions and suggestions.

I am grateful to Prof. Dr. rer. nat. Ulrich Zenneck for being my co-supervisor.

A grateful acknowledgement is made to Prof. Dr. Anjana Devi (Ruhr-Universität Bochum), Prof. Dr. Heinrich Lang (Technische Universität Chemnitz), Prof. Dr. Stefan Schulz (Universität Duisburg-Essen), Prof. Dr. Matthias Driess (Technische Universität Berlin) and Prof. Dr. rer. nat. Ulrich Zenneck (Universität Erlangen-Nürnberg) for providing me new classes of precursors, which were studied in this work. With reverence, I express my thanks to them.

I place on my record my sincere gratitude to Dr. rer. nat. M. Aslam Siddiqi for his interest, valuable suggestion and keeping a critical eye on my work.

I also take this oppurtunity to thank Dr. rer. nat. Christian Pflitsch his kind help, assistance and suggestions.

I would also like to thanks to all my colleagues for their assistance and generous support received during all the years I spent for the completion of my work.

I am also grateful to Mr. Andreas Görnt and Mr. Manfred Richter for the techinical support.

Last but not the least, my profound thanks to my family and friends for being a constant source of love, support and inspiration to me.

I am also grateful to the Deutsche Forschungsgemeinschaft for the financial support.

Rehan Ahmad Siddiqui

Dedicated to my parents

TABLE OF CONTENTS

CHAPTER 1

INTRODUCTION

1.1 Thin film deposition processes

Thin film deposition involves any process of deposition of thin films of materials on to a substrate by the adhesion of the coating material from a vaporous material using electricity, heat, chemical reactions and other techniques. The thickness of the film is in the range of micrometers. Applications are found in the medical, metallurgical, telecommunication, micro-electronic, optical coating, nanotechnology, semiconductor industries and protective coatings. The thin film deposition processes can be either purely physical such as evaporative method, or purely chemical such as gas or liquid phase chemical process.

In PVD (Physical Vapor Deposition) vapors of the source material or precursors are produced by physical means. The vapors are then transported across a region of low pressure from its source to the substrate to form a thin film. The most widely used methods in PVD of thin films are evaporation, sputtering, and molecular beam epitaxy (MBE). Evaporation method involves generation of vapor from the source material which is then transported to the substrate where it condenses to form a thin film. Sputtering method uses an electrode, which is heated to a temperature high enough to cause the ejection of hot atoms which finally settles down on to a substrate to form thin adherent films. Molecular beam epitaxy is used for growing single crystal epitaxial films in high vacuum. The film is formed by slowly evaporating the source material from an effusion cell and then condensing on to a substrate.

CVD (Chemical Vapor Deposition) is a chemical process for depositing thin films of various materials. It is classified under gas phase chemical processes. In a typical CVD process the substrate is exposed to the vapor of the precursors which react or decompose on the substrate surface to produce the desired thin films which is taking place inside a reaction chamber. In liquid phase chemical processes thin films are obtained from liquid phases by chemical reactions which are carried out by electrochemical processes (anodization and electroplating) or by chemical deposition processes such as sol-gel method. Sol-gel method involves preparation of the precursor sol (colloidal solution). The precursor sol is deposited on to a substrate to form a film by dip coating or spin

coating which is then subjected to thermal treatment. In general, the sol-gel process involves the transition of a system from a liquid sol into a solid gel phase containing metal centres with oxo (M-O-M) or hydroxy (M-OH-M) types of bond. During heat treatment these bonds are broken down to give metal oxides films.
Among the methods described, physical vapor deposition (PVD) and chemical vapor deposition (CVD), methods represent the most commonly used techniques for deposition of thin films.

1.2 Chemical vapor deposition (CVD)

Chemical vapor deposition is a widely used method for depositing thin and high quality films with well defined chemical composition and structural uniformity. For this process the precursor molecules are evaporated. In such a process after the evaporation of one or more precursor molecules that include the elements which shall be present in a deposited thin film (or coating), are mixed and flown to a substrate. There the energy (thermal energy) is provided to initiate a chemical reaction so that films of metal oxides or other compounds are formed on the substrate. In general, the CVD process involves the following steps

1. Vaporization and transport of precursor molecules into the reaction chamber by carrier gas.
2. Chemical reactions in the gas phase leading to new reactive species and by-products.
3. Mass transport of the reaction products through the boundary layer to the surface of the substrate.
4. Decomposition of adsorbed precursor molecules on the heated surface and its incorporation into thin film.
5. Removal of by-product gasses from the reaction chamber through exhaust system.

The schematic of CVD process is shown in figure 1.1.

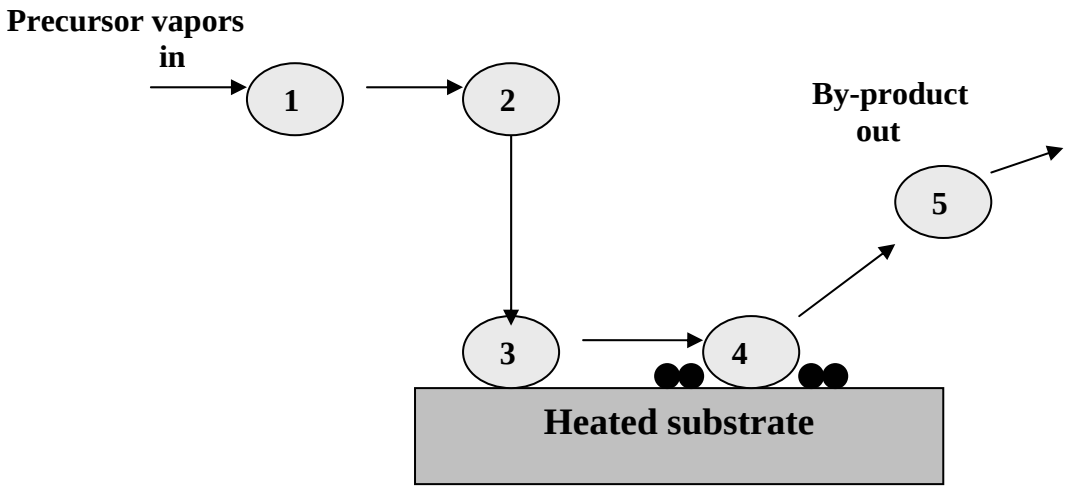

Figure 1.1: Steps in a CVD process.

The main advantages of chemical vapor deposition are the formation of uniform, reproducible and adherent films. Often the main disadvantage of this technique lies in using toxic and dangerous precursors to get a desired film and sometimes very high temperatures are needed for some reactions. The other difficulty is to deposit multi component material with well controlled stoichiometry because different precursors have different vaporization rates but this difficulty can sometimes be overcome by using single source chemical precursors.

CVD can be used to produce a variety of metallic and non metallic coatings, carbides, silicides, nitrides and oxides. CVD is being widely used in coating for wear resistance, corrosion resistance, and high temperature protection, and in the manufacturing of semiconductors, sensors, optoelectronic devices and catalyst [1-3]. The conventional CVD process uses thermal energy to activate the chemical reaction. However, the chemical reaction can also be initiated using different types of energy sources. A number of other forms of CVD processes are widely used and are frequently referenced in the literature as given in the table 1.

	CVD Technique	Principle
1.	Atmospheric pressure CVD	Deposition is done at atmospheric pressure.
2.	Low pressure CVD	Deposition at sub atmospheric pressures in order to reduce unwanted gas phase reaction.
3.	Plasma enhanced CVD	Utilizes plasma to enhance chemical reaction rate of precursors and to produce radicals and ions.
4.	Rapid thermal CVD	Uses heating lamps or other methods to rapidly heat the substrate.
5.	Laser CVD	Precursor is decomposed either photolytically or thermally by contact with a substrate which has been heated by a laser.
6.	Metal-organic CVD	Based on organometallic precursors.
7.	Atomic layer CVD	Two complementary precursors are alternatively introduced into the reaction chamber, the reaction is self-limiting.

Table 1: **Types of CVD processes.**

1.2.1 Metal organic chemical vapor deposition (MOCVD)

In metal organic chemical vapor deposition volatile metal-organic (or organometallic compound) are used as precursor rather than the inorganic precursors which are used in conventional CVD methods. This process offers relatively low deposition temperatures and uniform deposition over large areas; both are significant process advantages, while most metals and their compounds are only volatile at very high temperature.

1.2.2 Precursors for MOCVD

An efficient MOCVD process relies critically on the availability of high purity precursors with appreciable vapor pressures and high thermal stability. The great abundance of organometallic precursors and the selection of suitably tailored organometallic precursor can be successfully applied for an MOCVD process for the production of thin films. Good MOCVD precursors should have the following qualities:

1. Good volatility
2. High purity
3. Good thermal stability during the evaporation and transport process in the gas phase
4. Ability to cleanly decompose on pyrolysis to give the desired material without contamination
5. Good shelf life i.e. must not degrade on exposure to ambient atmosphere
6. Non-toxic and non corrosive

The categories of commercially available metal organic compounds which are frequently used as precursors in MOCVD include

1. Metal β-diketonates - such as metal 2,2,6,6-tetramethyl-3,5-heptandionate (tmhd), metal 2,4-pentanedionate (also known as acetylacetonate (acac)).
2. Alkoxides - such as ethoxides (OEth), isopropoxides (i-OPr) and butaoxide (n-OBut).
3. Alkylmetal - such as ethylzinc and phenylbismuth
4. Metal carbonyl
5. Metal cyclopentadienyl

Each group of precursors has its own advantages and disadvantages e.g. alkylmetal compounds are toxic and flammable, metalcarbonyl are very toxic, alkoxides have the drawback of high air sensitivity. But when it comes to the deposition of a film of desired characterstic and composition, a compromise has to be made on the choice of the precursors. Among the groups, metal β-diketonates and metal cyclopentadienyl compounds often represent the most favourable choice in selection of precursors for MOCVD. The volatility, thermal stability, nontoxicity, good shelf life and moreover the low cost for both the classes are the fundamental factors responsible for their use in the technology of the preparation of films by MOCVD method. The category involving the specially tailored precursors, to suite a particular need in terms of film composition, deposition temperature and environment is unending.

Apart from their use as MOCVD precursors metal β diketonates posses a wide variety of properties of industrial value which are responsible for their wide ranging application such as catalyst in oxidation, addition reactions and polymerization process, separation of lanthanides and gasoline antiknock agents [4-6]. Metal cyclopentadienyl compounds like ferrocene are used as fuel additives, as catalyst for polymerization process and additives for high temperature lubricant and grease [7]. Nicklecoene and Cobaltocene both are used as catalyst in various chemical processes [7]. Ruthenocene is used as photoinitiater for polymerization process [7].

1.3 Motivation and scope of this work

One of the most important thermal parameters of a precursor is its vapor pressure as a function of temperature. It is needed to optimize the delivery of precursor to the deposition chamber. Sufficient precursor vapor density is needed to allow adequate deposition rates. Thus, from the knowledge of the precursor vapor pressure, one can assess its maximum permissible vapor density for the process. The degradation of the precursors could take place by the process of hydrolysis from the trace moisture contamination, thermal pyrolysis and oligomerization. The vapor pressure of a given precursor can be strongly influenced by any degradation that may have occurred.

Since CVD processes are often running for very long times, it becomes increasingly important to quantify the thermal stability at evaporation temperature because during thermal decomposition, the rate of evaporation will vary differently with respect to time

due to the formation of various by-products. Therefore, the rate by which individual molecules which arrive at the substrate for growth would also vary accordingly, in other words the film composition might vary with time and thickness, which would result in poorly reproducible deposition experiment and highly contaminated film. Most of the work for the thermal stability of the precursors using thermogravimetric analyser was done in using temperature ramps (non isothermal mode). This situation does not depict typical evaporator conditions where the precursor is held under isothermal condition for a long period of time. Thus for a complete picture regarding thermal stability, the precursor should be held under isothermal conditions so that one can assess if at a given temperature, the precursor preferably evaporates or decomposes.

This issue was identified in deposition of Co_3O_4 from cobalt (II) acetylacetonate [8,9], reproducibility for the growth rate were obtained only every time with new filling of the evaporator, even though the evaporator temperature was below what was used by other groups [9-11]. Therefore, the evaporation behaviour of cobalt(II) acetylacetonate was studied with respect to time in a thermogravimetric analyser isothermally [12]. It was found that in isothermal experiments for cobalt (II) acetylacetonate evaporation is accompanied by the decomposition of the precursor. Similar observation was also made for cobalt (II) 2,2,6,6-tetramethyl-3,5-heptandionate and only cobalt (III) 2,2,6,6-tetramethyl-3,5-heptandionate evaporated without decomposition. Therefore, it was recommended as a stable MOCVD precursor.

As for unstable compounds vapor pressure measurements are not possible as all the gravimetric approach to measure the vapor pressure of the precursors will fail as soon as the decomposition plays a role because decomposition products will evaporate along with the precursor molecules. Therefore, it is important to have the information regarding thermal stability of the precursor prior to vapor pressure measurements.

Apart from vapor pressure data, diffusion coefficients [13-16] for these metal organic precursors are also needed for Sherwood and Lewis number which are used in mass transfer calculation e.g. degree of saturation of the buffer gas stream in a evaporator. A number of correlations for gaseous diffusion coefficient can be found in the literature for organic compounds but no such correlation or any experimental diffusion data exists even for commonly used precursor like aluminium acetylacetonate. Therefore, it is important to measure the gaseous diffusion coefficient for these precursors.

The present work involves an extensive literature survey for the vapor pressure data for the organometallic compound (metal acetylacetonate, metal 2,2,6,6-tetramethyl-3,5-heptandionate, and metal cyclopentadienyl compounds). It was found that there exist a fair amount of vapor pressure data for these compounds but appreciable discrepancies occur between the experimental vapor pressure data obtained by using different methods and sometimes using the same method by different workers. The reason for these discrepancies can in part be explained in terms of using impure substances, thermal instability of the substance and the use of measurement technique which are not recommended for vapor pressure measurements. Apart from commercially available precursors, some new organometallic precursors have been synthesized by various groups and have been successfully applied in CVD application. Absence of any thermodynamic data for these precursors restricts their further use under different conditions for deposition; therefore, some of these precursors were also studied.

The department of thermodynamics of University of Duisburg-Essen for the last few years has been extensively engaged in studying the thermodynamic properties of organometallic compounds [12, 17-19] used in CVD processes. Due to very low vapor pressure the reliable data were scarce for MOCVD precursors. The aim of this study is to give a systematic account of the available literature data and point out the discrepancies and present experimental result regarding thermal stability, vapor pressure and diffusion coefficient for the precursors. As sublimation rates strongly depend upon diffusion, equilibrium vapor pressure data alone cannot be used to find optimal temperature for a given transport rate. This will be explained in the theory section (Chapter 2). Therefore, the present measurements can be used to obtain reliable data for the design of evaporators. Vapor pressure and diffusion coefficient were also measured for some of the organic compounds such as anthracene and pyrene as these compounds are used as reference substances for vapor pressure measurement. A good quality reliable data for vapor pressure were available in literature for both compounds while experimental diffusion coefficients are still lacking at higher temperatures. Since both compounds are considered to be pollutants the gaseous diffusion coefficients are needed to understand the pollutant movement into the atmosphere.

CHAPTER 2

EXPERIMENTAL TECHNIQUES AND THEORY

2.1 Thermal analysis

Thermal analysis refers to a group of techniques in which the properties of a substance under study is monitored with respect to time and temperature in a specified atmosphere. Thermal analysis of the precursors is important for CVD processes, as one of the prerequisite of the process is the production of vapors from the volatile precursor. This is often done by heating the presurcors in an evaporator isothermally. Volatization of solid in a broad sense includes any process which result in conversion of matter from the solid state to the vapor phase. Volatization process can be accomplished by two ways

1. Sublimation process in which the gaseous phase composed of the same type of atoms or molecules supplied by the solid phase i.e. the composition of the gaseous phase and the solid phase remain the same - a true vaporization process.
2. A chemical reaction between the solid phase and another species to form gaseous products. The additional species may be environmental gases, adsorbed water, or some some solid like container material. In both cases the composition of the gaseous phase is always different from the solid phase. This is often termed as decomposition or pyrolysis.

As solid is heated, the extent of lattice vibrations within the solid are increased and a temperature would be reached during heating where following changes can occur

1. Melting: the forces of attraction between the constituents decrease which maintain an orderly arrangement of the solid and comes down to a more disordered system called liquid state.
2. Phase transition: a new arrangement of the lattice structure.
3. Sublimation: direct transformation from the solid state to the gas phase occurs.
4. Decomposition: sometimes the molecular rearrangements of bonds within the solid during heating also result in formation products chemically different from the solid. These products can be a solid or gasses. This occurs over a range of temperature.

Thus if we are able to obtain gravimetric data of heating a solid sample with time or temperature in a specified atmosphere, we would be able to say about the volatility, thermal stability, physical state of the sample at a particular temperature.

2.1.1 Thermogravimetry

Thermogravimetric analysis covers a wide spectrum of thermo analytical techniques, which monitor one or more physical properties of a substance that is undergoing a temperature programmed heating as a function of time and temperature. It provides a quantative measurement of any weight changes associated with thermally associated changes. Thermogravimetric analysers can be called as a thermo balance which is a combination of a suitable electronic microbalance with a furnace, which is operated with a computer controlled heating programm. It allows the sample to be weighed and heated or cooled in a temperature controlled manner and the mass, time and temperature data to be recorded under specific atmosphere.

The thermogravimetry analyser (TGA) system, which combines thermogravimetry (TG) and differential thermal analyser (DTA), is widely used in the fields of gas–solid interactions, fuels, catalysis, polymers and chemical synthesis. Thermogravimetric analysis is used to determine the material's thermal stability and its fraction of volatile components by monitoring the weight change that occurs as a sample is heated. This is explained later in detail. The measurement is normally carried out in an inert atmosphere, such as Helium or Argon, and the weight is recorded as a function of temperature. In addition to weight changes, some instruments also record the temperature difference between the specimen and the reference pan (differential thermal analysis, or DTA) or the heat flow into the specimen crucible compared to that of the reference crucible (differential scanning calorimetry, or DSC). The latter can be used to monitor the energy released or absorbed via chemical reactions during the heating process. A DTA apparatus consists of a sample holder comprising thermocouples, sample containers and a ceramic or metallic block; a furnace; a temperature programmer; and a recording system. The key feature is the existence of two thermocouples connected to a voltmeter. One thermocouple measures the temperature of an inert material such as Al_2O_3, while the other is used for measurement for the sample temperature under study. As the temperature is increased, there will be a deflection of the voltmeter if the sample is undergoing a phase transition. This occurs

because the input of heat will raise the temperature of the inert substance, but be incorporated as latent heat in the material changing phase. In DTA, the differential temperature is plotted against the time, or against the temperature (DTA curve or thermogram). Changes in the sample, either exothermic or endothermic, can be detected relative to the inert reference. Thus, a DTA curve provides data on the transformations that have occurred, such as glass transitions, crystallization, melting and sublimation. The area under a DTA peak is related to the enthalpy change of the sample. Generally a sharp endothermic (negative peak) DTA peak at particular temperature indicates the melting point of the sample as the temperature of the sample at this particular temperature would lag behind the temperature of reference substance where as an exothermic peak indicate the onset of decomposition process.

Interpretation of Thermogravimetric data

For interpreting the volatility and thermal stability of sample one needs to use different temperature program and record mass loss versus time data as the decomposition is a time and temperature dependent process. Generally following types of mass loss curves are obtained in the standard temperature gradient program in which temperature is raised continuously with a constant heating rate as shown in figure 2.1.

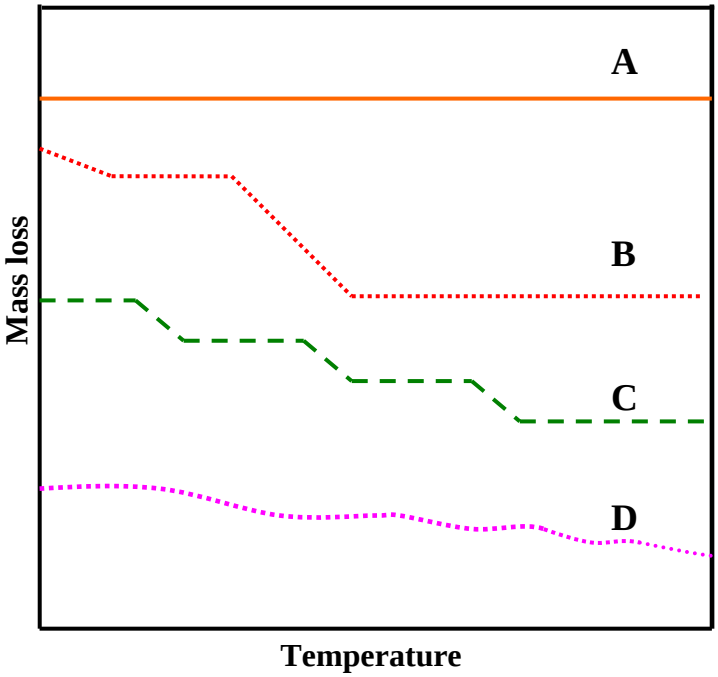

Figure 2.1: Different types of thermogravimetric curves.

Type **A** curve indicate that no mass loss was observed even as temperature is increasing meaning that no vaporization is taking place.

Type **B** curve indicate that initially some absorbed water or some associated solvent is lost which is shown by a rapid mass loss and thereafter evaporation process begins in the second step. But this could also be a two step decomposition reaction. So in order to confirm this one has to use some other analytical techniques.

Type C indicates a multi step decomposition mechanism like decomposition of $CaC_2O_4.H_2O$. Each step representing elimination of H_2O, CO and CO_2 according to the usual reaction scheme $CaC_2O_4.H_2O \longrightarrow CaC_2O_4 \longrightarrow CaCO_3$

Type D also indicates a multi step decomposition mechanism with the formation relatively unstable intermediates due to a high heating rate.

2.1.2 Thermal stability from thermogravimetric data

For a clear cut picture regarding thermal stability one should always rely upon the isothermal mode experiment where the sample is held under a constant temperature for a long period of time in the range of hours depending upon the volatility of sample as decomposition is a time and temperature dependent process. If nearly linear slope are obtained for mass loss versus time plot and substance evaporates completely without leaving residue then the substance is considered to be showing clean vaporization process without any decomposition. Even when one observes a linear mass for some period of time and after that no further mass loss occurs and whatever amount is left (as residue), a decomposition process is indicated. As some chemical changes had happened during the vaporization which had led to the formation of residue as a product of the decomposition process. In the past most of the thermal stability for the CVD precursors studies were done in the non isothermal mode and attention was paid only to a single step mass loss curve which was considered to be a criteria for thermal stability. It's worthwhile to note that the non isothermal mode can provide only an idea about vaporization temperature and first impression whether the decomposition is taking place or not. Since decomposition is a time dependent process and for some substances it may happen that the substance remains stable for a short period of time particularly at low temperature and only after this time period decomposition begins. And in non isothermal or temperature gradient mode, the temperature is raised as function of time, it is not possible to observe the decomposition at low temperatures. If the precursor left

some residue in the non isothermal mode experiment, it was attributed to the decomposition caused during heating at high temperature. Such kind of measurement does not represent a typical evaporator condition and therefore, should not be applied for thermal stability measurements.

The drawback of thermogravimetric method is that it cannot distinguish the actual nature of the material evolved in the course of the process and is also handicapped in resolving overlapped thermal events. So it is not always possible to describe the process under study completely. However, some technique which can provide additional information, particularly on the nature and content of the liberated gases, will be able to describe the process more precisely but in this study this is not a matter of concern as we need only qualitative information regarding thermal stability which is an important factor prior to vapor pressure measurement.

2.2 Thermal stability studies using FTIR (Fourier transform infrared) spectroscopy

Thermal stability can also be studied using FTIR provided with the arrangement of heated gas cell. The IR spectra of sample vapors are monitored as a fuction of time. The collimated IR beam from FTIR spectrophotometer is passed through a heated gas cell equipped with transparent KBr windows. The sample to be examined is heated isothermally in a sublimator and the vaporized sample is carried to the heated gas cell with the help of an inert carrier gas through a heated gas line from the sublimator to the inlet of the cell. If any change in spectrum of the substance occurs with time, this indicates that the substance has changed during the vaporization process. The set up consists of FTIR spectrophotometer provided with heated gas cell, a sublimator, and transfer lines as shown in figure 2.2

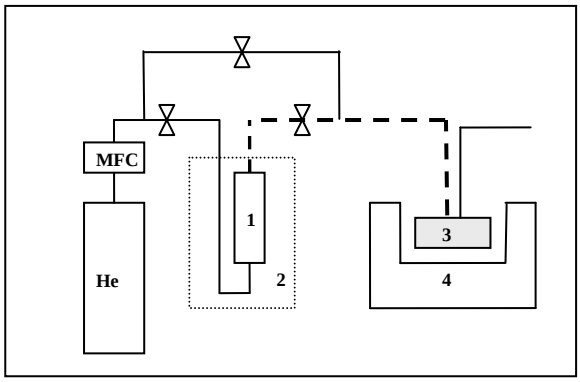

Figure 2.2: Schematic of the experimental setup
(1: sublimator, 2: thermostat, 3: heated gas cell, 4: FTIR, ----heated transfer line)

Attempts have been made to establish the thermal stability of the sample using mass spectrometry to see the gas phase composition as a function of time above the sublimating substance, to see if the composition is constant for a period of time or it changes. In mass spectrometry a sample undergoes chemical fragmentation forming charged particles (ions) which are seperated in a mass analyzer according to the ratio of mass to charge of the ions and finally to a detector which measures the abundances of each ion fragment present. Changes in the intensites of ion peak could occur due to further fragmentation of the parent ion due to high ionization energy in the ionization chamber. Therefore, it would be difficult to infer the thermal stability based on intensites of the ion peak which could also change due to the decomposition of the compound.

If one is interested only in getting the information regarding the thermal stability and not for decomposition pathways or product, then the thermogravimetric analysis is the most straight forward technique.

2.3 Vapor pressure measurement

The vapor pressure of a liquid or the sublimation pressure of a solid is the pressure of a vapor in equilibrium with its condensed phases. Liquids and solids have a tendency to evaporate to a gaseous form, and all gases have a tendency to condense back into their original form (either liquid or solid). For a substance at any given temperature, there is a partial pressure at which the vapor of the substance is in dynamic equilibrium with its condensed form in the saturation regime. This is the equilibrium vapor pressure of that substance at that temperature. Thus the equilibrium vapor pressure can be defined as the pressure reached when a condensed phase is in equilibrium with its own vapor. In the

case of an equilibrium solid, such as a crystal, this can be defined as the pressure when the rate of sublimation of a solid matches the rate of deposition of its vapor phase. This is often termed as sublimation pressure. Under equilibrium condition the pressure exerted by the vapor above the condensed phase is dependent on temperature only and independent of fraction of the condensed phase which has vaporized. If the sample consists of more than one component (degraded sample) then the pressure is not independent of the fraction vaporized since the component and composition of the condensed phase will differ from vapor phase as high volatile component evaporate more fast than less volatile one. Therefore, the measured vapor pressure would not be the true vapor pressure of the substance.

The vapor pressure of a substance in equilibrium with its liquid or solid phase at a given temperature can be regarded as a measurement of maximum achievable amount of the substance in the vapor phase. The corresponding concentration of the vapor can be obtained from the gas law P/RT (mol m^{-3}). A substance with a high vapor pressure at normal temperatures is often referred to as volatile.

2.3.1 Techniques for vapor pressure measurement

The various techniques for determining vapor pressure data were reviewed by Ambrose [20] and recently by Verevkin [21]. The experimental methods are generally classified as "static" or "dynamic" method. The static methods measure directly the pressure exerted by the vapor in equilibrium with its liquid or solid phase while with the dynamic methods a sample of saturated vapor is removed and vapor pressure is determined from the mass loss of the sample.

Direct static method measurement of vapor pressure can be used over a wide range of pressure down to 1Pa. The main experimental techniques in determining vapor pressure data in the low pressure regime are gas saturation or transpiration method using a carrier gas and the molecular effusion method using a Knudsen cell or torsion effusion method. Gas saturation and effusion are generally considered the most accurate experimental method for vapor pressure lower than ~ 1Pa. It has to be pointed out that basically no new method have been developed and whatever the development has taken place is generally the modification or refinement of well established methods [21] which are discussed in this section.

2.3.1.1 Effusion method

2.3.1.1.1 The Knudsen effusion method

Effusion is a process by which molecules of a gas pass through a small hole into the vacuum. Gases at low pressures behave very differently from gases at normal pressure. In vacuum the gas in the system will pass through different flow regimes which are characterized by the Knudsen number. The Knudsen number (K_n), is a dimensionless ratio of mean free path length (average distance that a molecule travels between collisions) of the molecule to the characterstic dimension of the flow system i.e diameter of the hole and is represented as

$$K_n = \frac{\lambda}{d} \tag{2.1}$$

where d is the characteristic dimension of the flow system and λ is the mean free path length of the molecule given by the relation

$$\lambda = \frac{kT}{\sqrt{2}\pi d^2 p} \tag{2.2}$$

where k is the Boltzmann's constant, T is the temperature, p is the pressure and d is the diameter of the gas particles.

Gas flow regimes classified on the basis of the Knudsen number can be classified as

1. Continuum / viscous flow for $K_n < 0.01$
2. Transitional flow for $0.01 < K_n < 1$
3. Molecular flow for $K_n > 1$

To summarize, when the ratio of the average mean free path length of the molecule to the radius of the hole is less than 0.01, the flow is continuum/ viscous. When the ratio is greater than 1, the flow is molecular. The transition flow exists between the viscous and molecular flow regimes.

In the Knudsen effusion method, the sample effuses out through a small orifice of known diameter under molecular flow conditions. This requires that the pressure inside and outside the cell is sufficiently low enough (high vacuum) so that the frequency of collision of vapor molecules in the gas phase is low. The effusion method is based on the molecular effusion of a vapor of the substance through an orifice held in a closed Knudsen cell. Under normal conditions the molecules evaporates from the surface of condensed phase but do not move very far because they collide with other molecules in the gas phase, while the molecules moving in the gas phase strike the surface and are

reabsorbed. Knudsen [22] established the fact that in the low pressure regime the molecule passing through the orifice has no appreciable effect on the equilibrium between vapor and the condensed phase, if the mean path length of the effusing molecule is much greater than diameter of the orifice. Since the vapor effuses into high vacuum and having the species with long mean path, the effusate behave like a well defined molecular beam of atoms or molecules moving in nearly collision free trajectories with particle distribution easily calculated from kinetic theory. The number of molecules escaping can be found from the mass loss of the sample and its molecular weight. The frequency of collision of gas molecules with the wall per unit wall area is given by [23]

$$Z_{wall} = \frac{n\bar{c}}{4} \tag{2.3}$$

where, $\bar{c}$ is the average speed of molecules, and n is the number density. The ideal gas law (using the number density and the number of particles) is

$$P = nkT \tag{2.4}$$

where, k is Boltzmann's constant and T is temperature in Kelvin and also

$$\bar{c} = \sqrt{\frac{8RT}{\pi M}} \tag{2.5}$$

The number of molecules leaving the orifice of area A in time t, if the orifice does not disturb the velocity and density distribution in gas phase would be given by

$$N_{escape} = Z_{wall}\, A\, t \tag{2.6}$$

If the molecules leaving the orifice are permanently lost from the gas phase to a vacuum space on the other side of the orifice, then the total mass lost is given as

$$\text{Mass lost } (\Delta m) = M\, N_{escape} = M\, Z_{wall}\, A\, t \tag{2.7}$$

$$\frac{\Delta m}{\Delta t} = p^{vap} A \sqrt{\frac{M}{2\pi RT}} \tag{2.8}$$

Equation (2.8) is strictly valid for an ideal hole, which means a hole in the sheet of infinitely small thickness. For the finite sheet thickness, where the height of the orifice is not negligible, an additional correction factor which is known as the Clausing factor [24], K, is taken into account. If the thickness of the sheet is not infinitely small, some molecules which strike the orifice wall will suffer non-specular reflection and return to the effusion cell [25]. Clausing [24] calculated a factor giving the probability that a molecule impinging on an orifice of finite thickness will pass through it. Thus, Equation (2.8) is written after applying the correction factor

$$\frac{\Delta m}{\Delta t} = p^{vap} A \sqrt{\frac{M}{2\pi RT}} \times K \tag{2.9}$$

$$p^{vap} = \frac{\Delta \mathrm{m}}{\mathrm{KA}\Delta \mathrm{t}} \sqrt{\frac{2\pi RT}{M}} \tag{2.10}$$

The main presuppositions for the application of this formula are the very low pressure regime and the evaporation of non-associated molecules. The following facts must also be taken into account

1. The cell must be isothermal (absence of any temperature gradient) and the temperature has to be accurately known.
2. The cell must be inert i.e. the only interaction with wall are random reflection.
3. The area of orifice must be considerably less than the effective evaporating area of the sample. This is to ensure that the rate of evaporation always exceed the effusion rate and equilibrium between the vapor and the condensed phase is not disturbed by the loss of molecule through the orifice.

This method utilizes a conventional mass loss technique; i.e. the weight loss from the cell is measured as function of time with help of some gravimetric method or by simply weighing the cell before and after the experiment. The mass loss equals the effusion rate out of the cell. Measurements are typically made under isothermal conditions.

2.3.1.1.1.1 Complication inherent in the Knudsen effusion method

Many workers had mentioned the possible sources of error introduced into the measurement by considering the evaporation coefficient (defined as the ratio of observed rate of evaporation to the maximum theoretically possible), shape of the orifices, temperature gradient effect, and the surface diffusion effect.

According to Motzfeld [26], in order to interpret the weight loss in terms of equilibrium vapor pressure of the evaporating substance, consideration of the following facts must be taken into account

1. The possible resistance to evaporation represented by low evaporation coefficient *"α"* for the evaporating substance. As the number of molecules condensing under the equilibrium conditions cannot exceed the number striking the surface, it may be always less than this number.Thus the rate of evaporation into vacuum will be less than the rate at which vapor molecules are computed to strike the surface at equilibrium i.e low evaporation coefficient.
2. The resistance exerted on the effusing vapors by the main body of the cell, represented in terms of area of the cell B and Clausing probability factor "W_A" for the cell.
3. The resistance represented by the hole with area A and Clausing factor K.

Motzfeld [26] gave relation for the equilibrium vapor pressure, p^{eq}, represented as

$$p^{eq} = \left[1 + f\left(\frac{1}{\alpha} + \frac{1}{W_A} - 2\right)\right] p^{m} \qquad (2.11)$$

$$f = \frac{KA}{B} = \frac{\text{Effective orifice area}}{\text{Area of the cell or sample}} \qquad (2.12)$$

where p^{m} is the measured pressure using the equation (2.10).

The term f (equation 2.12) may be made small by minimizing the size the product KA and maximizing the surface area of the sample and therefore, the effect of cell area diminishes by keeping f as small as possible and similarly the effect of evaporation coefficient also diminishes on keeping f as small as possible. According to Whitman [27] the effect of evaporation coefficient on p^{vap} in the case of equation (2.11) where α = 0.7 and f = 0.1, the effect caused by neglecting f would be 5% at the most and for f = 0.01, this error becomes 0.5 percent. Thus the effect of α can be made negligible by the

use of small f . Thus it can be suggested that the inaccuracies are too small to impair the general validity of the equation. Similar observation was also made by Carlson [28].

In many vapor pressure studies using effusion method, knife edge orifices were used having the shape of a cone and the rate of effusion is taken to be the same as that of ideal orifices or corrected empirically. Searcy [29] stated that the Clausing equation assumes that specular reflection can be neglected but he found that it was not always valid and therefore, in his study he used cone shaped orifice. Iczkowski [30] stated that failure to account for the effect of the conical geometry makes the vapor pressure measurements doubtful. Most of the workers have used cylindrical shape orifices for which the correction factor was given by Clausing. As already it had been mentioned that the vapor pressure equation is only valid under ideal condition of infinitesimally small or zero thickness orifices but for orifices of finite thickness correction factors must be taken into account. Therefore, whatever the shape of the orifice is, the correction factor must be used for precise vapor pressure measurements.

Morecroft [31] had shown that the vapor pressure measurements were independent of orifice sizes within the assumption that the mean free path length of molecules are larger than the orifice diameters and good results can, however be obtained when the diameter is same that of mean free path length. Suuberg and Oja [32] observed the same and recommended the diameter range of 0.6 mm-1.1mm. On the other hand if the effusion rates are very small, a large orifice diameter is required to give reasonable results [33] but on the other hand very large holes can give considerably lower vapor pressure values owing to self cooling of the sample especially for substances having high vapor pressure which evaporates rapidly so that the energy is carried away rapidly by vapor leading to self cooling of the sample and the failure to maintain equilibrium conditions. In addition to slow effusion rates from the orifices of small sizes, a small leak in the cell assembly can cause problem in terms of enhanced effusion rate leading to considerably higher mass losses. Winterbottom and Hirth [34] have reported that the surface diffusion increases as the radius of the orifice decreases.

Care should be taken in measuring the cell temperature, as according to Clausius Clapeyron equation, vapor pressure is a strong function of temperature. Maintaining an effusion cell at a uniform temperature is a complicated process. The requirement of open space for the effusing gas above the cell may lead to a lid temperature considerably lower than the temperature of the sample unless special arrangement are fore seen to counter this effect. The best solution to this problem would be to heat the

entire vacuum chamber to the temperature of measurement. Sufficient heating time should be given so that the thermal equilibrium between the cell and the content of the cell is achieved before starting an experiment.

Sometimes lower mass losses could also be observed due to the restriction of free molecular flow by a small vacuum chamber surrounding the cell. A fraction of molecules which initially evaporates may strike the container wall and recondense upon the effusion cell rather than escaping to pumping system or to a condenser.

Sample purity is also an important factor to be taken care of due to the need to study clean pure and uncontaminated surface. A little amount of a non volatile impurity can lead to lowering of the calculated vapor pressure values, so before starting vapor pressure measurement attention should be also paid to check if substance leaves some residue on evaporation. Presence of some high volatile impurities like some associated solvent or chemically combined / absorbed water should also checked prior to the experiment. Some substances tend to deteriorate on exposure to air which can happen during the heating period of the sample in the vacuum chamber so an arrangement of circulating some inert gas through the set up should be made so that the sample could be heated in absence of air.

Uncertainites in the measurements can also come in reporting the observed mass loss. As in the conventional method, a weight balance is used for weighing the Knudsen cell which is usually done before and after the experiment to get the mass loss. For precise measurement of mass loss, a high precision weight balance must be used. A high precision vacuum microbalance is prefered for vapor pressure measurements. Experiments involving vacuum balance, measurements are made under isothermal conditions with mass loss from the cell being recorded as a function of time in a thermogravimetric type apparatus results in high precision. The sample cell is held in high vacuum and must receive heat purely by radiation and therefore, the heat transfer is a key concern. A long time is generally required to reach the thermal equilibrium in an isothermal experiment. Since isothermal experiments are time consuming in terms of reaching thermal equilibrium, a speedy modification of this method is to measure the mass loss rate in non isothermal mode with some constant heating ramp. The chamber enclosing the cell will rise in temperature at a rate somewhat similar to the rise in the heating block. The temperature difference between the heating block and cell is measured. The information of mass as a function of time was converted to a derivative,

so that it is possible to relate each recorded sample temperature to an instantaneous value of mass loss rate.

Suuberg and Oja [32] found a significant deviation of non isothermal results from isothermal results for vapor pressure of anthracene, napthalene and attributed this to temperature differences between the cell and the chamber which encloses the cell. Even by using slow heating rates, they could still find about 10% difference between the values measured by isothermal and non isothermal techniques.

Thus the main area of concern in using vacuum microbalance is of temperature measurement, since the temperature of the effusing cell generally cannot be directly measured and what is measured, is the temperature in the vicinity of cell and it is assumed that this would be the temperature of the cell but if there exist some temperature difference between the cell and its surrounding, it should be taken into account. Therefore, a proper temperature calibration of the apparatus is necessary for precise measurements.

The Knudsen effusion method is a reliable technique to measure the vapor pressures. Inaccuracies in the measurement due to the evaporation coefficient of the sample, area of the cell and orifice sizes could be minimized when we choose correct parameters for constructing the Knudsen cell for effusion measurements. For precise measurements attention should be given to temperature measurement, determination of Clausing factor and purity of the sample which are the main and important requirement of this method. Some technical consideration includes

1. Maintenance of high quality vacuum quickly so that the beginning of an experiment can be registered with sufficient temporal accuracy.
2. Installation of a cooling trap to condense the vaporized substance and also for maintenance of high quality vacuum.
3. Precise temperature control.
4. Proper orifice diameter selection.

2.3.1.2 Torsion effusion method

In the torsion effusion method, an effusion cell is suspended in vacuum furnace by a fine wire. Upon heating, vapor escapes through two eccentrically placed orifices in the cell, there by exerting a torsional force or torque on the wire. The angle through which the cell is turned is measured by a mirror attached to suspension and from this angle, the vapor pressure can be calculated by the means of formula

$$p^{vap} = \frac{2\phi D}{d_1 f_1 A_1 + d_2 f_1 A_1} \tag{2.13}$$

where, ϕ is the angle of twist, D is the torsion constant for the cell, d is the perpendicular distance from the cell centre to the axis of the effusion hole, A is the area of orifice, and f is the correction factor (ratio of the force in the effusion of vapor through a hole of finite length to the force expected if the hole had infinitesimal length). Torsion constant of the wire is determined by the method of observing the periods of the suspended assembly when cylinders of known but different moment of inertia are added. Since the geometric factors ϕ, and f are difficult to determine with sufficient precision, the apparatus is calibrated using a compound with known vapor pressure at different temperatures, therefore, the equation (2.13) becomes

$$P = C^i \phi \tag{2.14}$$

The main drawback of this method is that the temperature of the effusing cell is not measured directly but in the vicinity of the effusing cell thus far away from the effusing sample, as discussed before for vacuum balance exact determination of sample temperature is not possible.

Other drawbacks of this method as stated by Rosen [35] are

1. The torsional constant of the wire is subjected to change and also to hysteresis effect.
2. Only a small fraction of possible rotation of the suspension is visible in most the equipments.
3. Separate torsion wires must be used for different pressures in order to stay within given angular displacements.

In some experiments torque, which is directly proportional to the vapor pressure, in a torsion-effusion apparatus is counterbalanced electromagnetically [35], so

$$P = C^i I \tag{2.15}$$

where, I is the electrical compensation current, C^i is the constant in which physical and chemical parameter of the cell and the torsion wire are included. If heating is done by induction, the effusion cell must be shielded sufficiently by a large susceptor so that additional deflection and oscillation are not introduced into the system.

The torsion effusion method can also be used to determine simultaneously vapor pressure and molecular weight of the sample in a setup in which the torsion effusion measurement is combined with measurements of the weight of the effusion cell with time. The method of weighing is based on the equation

$$P_{mass\,loss} = C\frac{\Delta m}{\Delta t} \tag{2.16}$$

The constant C contains the orifice area, molar mass and the temperature of effusing species. The details of the method are mentioned elsewhere [36]. The advantage of this method that the decomposition dissociation or association of the sample would be immediately noticed as the $p_{mass\,loss}/p_{\text{torsion}}$ would be different, in principle it should be unity. The limitation of exact measurement of sample temperature is the major drawback. The schematic diagram of the set up is shown in figure 2.3.

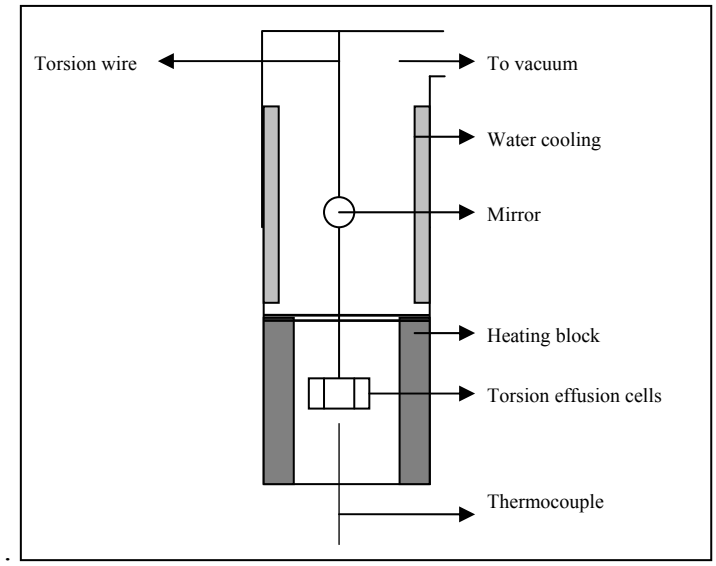

Figure 2.3: Schematic of the torsion effusion method.

2.3.1.3 The effusion method using a quartz cyrstal microbalance

In this method a piezoelectric quartz crystal is used as weighing device instead of using conventional gravimetric device. Molecules escaping from the orifice of Knudsen cell are trapped onto an externally cooled quartz crystal microbalance. In this case the mass loss through orifice is the mass gain on QCM. The relationship between resonance frequency of the quartz crystal Δf and the surface density, ρ of the deposited substance is expressed as [37]

$$\Delta f = \frac{f^2 mk}{n \rho A} \qquad (2.17)$$

where, f is the average resonance frequency, m is the mass of deposited sample on QCM , n is the crystal constant, k is the constant dependent on mass distribution on the crystal surface, ρ is the surface density of the deposited substance and A area of the quartz crystal.

From this equation one can clearly see that Δf , is directly proportional to the mass of the substance deposited on the crystal surface with the assumption that the total change in frequency change is small, $\Delta f << f$ and the substance is deposited on the crystal surface. Therefore, the experimentally measured rate υ, of resonance frequency change in time Δt for the quartz crystal

$$\upsilon = \frac{\Delta f}{\Delta t} \tag{2.18}$$

is proportional to the sublimation rate of the investigated substance

$$\upsilon = \frac{\Delta f}{\Delta t} = \frac{\Delta m}{\Delta t} \tag{2.19}$$

and the vapor pressure can be obtained by using the Knudsen equation (2.10). This method could be applied to the substances which have very low pressure as the QCM has the sensitivity of less than 1ng, therefore, very low mass losses can be observed with great accuracy within short span of time. When compared to other measurement techniques which would have surely taken longer time to get some measurable values of mass loss. High sensitivity and insensitivity to vibrational noise are the main advantages of the QCM [38].

This method however could not be applied to the substances having high vapor pressure at ambient temperature. As the desorption rate from the crystal surface at ambient temperature being comparable with condensation rates of the molecular stream at the surface.

2.3.1.4 The Knudsen cell mass spectrometry

A Knudsen cell can also be employed as the "gas source" of a high-temperature mass spectrometer, and the effusing molecular beam is directed into the ionisation chamber of the connected mass spectrometer. The ionized vapor beam is then directed into a high voltage accelerating region and then into a magnetic field for selection according to the mass to charge ratio. The other common techniques for ion selection such as quadrupole filters and time of flight instrument have also been used. However the magnetic field ion selector is most desirable due to its stability and lack of mass discrimination. Detecting the ionized vapor beam by means of an electron multiplier yields the intensities of the composing species of the vaporized sample. The output of the mass spectrometer is in ion intensities I_i of species i. Thermodynamic evaluation can then be based upon the relation between the vapor pressures of the species *i* as

$$P_i = \frac{k_m I_i T}{\psi} \tag{2.20}$$

I_i is the ion intensity of species i
k_m is the apparatus constant
Ψ is the ionization crossection.

To calculate the vapor pressure the value of both k_m and Ψ must be known. The apparatus constant is a combination of numerous factors involved in the formation of the molecular beam, the ionization process, ion collection efficiency, transmission efficiency of the analyser and the collection efficiency of the detector.
One advantage of this method is that the measurement can be made despite of the presence of impurities provided the impurities do not contribute to the peaks chosen for study. Comparison of several peaks in different parts of the spectrum will assist in checking this because, if they are due to a single component only, their ratio should remain constant as the temperature of the equilibrium chamber is changed.
The mass spectrometer is not suitable for precise measurement of the absolute vapor pressure at a single temperature. The measurement depend upon the positive ion current for a particular species which in turn depends upon on the ion collection efficiency of the instrument and ionization cross section of the species concerned so systematic uncertainties in these will make the vapor pressure data imprecise. Modern Knudsen cell mass spectrometry is a well established method for high-temperature investigations of the thermodynamic properties of both gaseous and condensed phases and is being employed specifically in alloy thermodynamics with great success.

2.3.2 The transpiration method or gas saturation method

In this technique the mass loss of the sample maintained at a constant temperature is measured in the presence of an inert carrier gas flowing over it at a constant rate. The main idea of this method is that the flowing inert gas has to be totally saturated by the evaporating substance. By applying Dalton's law for the carrier gas and knowing the flow rate of the inert gas, the vapor pressure of the substance can be calculated with the formula below [20]

$$P = \frac{\dot{m}RT_a}{\dot{V}M} \tag{2.21}$$

where $\dot{m}$ is the mass loss rate of the transported compound, T_a is the temperature at which the mass flow rate is measured, $\dot{V} =$ the volumetric flow rate of the inert gas, M is the molecular mass of the substance and R is the gas constant.

The flow rate of the carrier gas is chosen so that the thermodynamic equilibrium between the vapor and the vaporizing substance is virtually undisturbed. This can be established experimentally. The vapor pressure P of the substance under investigation is then calculated from equation (2.21) which is based on the following assumptions [20, 39]

1. The vapor behaves ideally.
2. The thermodynamic equilibrium between the vapor and the vaporizing substance is undisturbed by the flow of the carrier gas.
3. All the vapor is transported by the carrier gas.

Transpiration experiments are generally performed at a total pressure of one atmosphere, for which the ideal gas equation can be assumed to be valid for many inert gases. Experiments are also designed to meet closely the criteria in assumptions (2) and (3) by choosing the appropriate flow rates of the carrier gas swept over the sample. The range of flow rates is such that the relative contribution to the mass loss of the sample due to other processes such as diffusion is insignificant compared to the mass loss caused by the vapor transported by the carrier gas. Furthermore, it is ensured that the flow rates chosen are not too fast to disturb the thermodynamic equilibrium between the sample and the vapor.

However, it is difficult to find a flow range at which the 100% saturation of the sample vapor in the carrier gas is reached. At most of the time, the carrier gas is either unsaturated due to the fast flow rate or is super saturated due to the slow flow rate of the carrier gas.

The mass loss of the sample contained in the crucible or evaporator ranges from a few milligrams to hundreds of micrograms and is monitored by any one of the following method:

1. Weighing the sample with the crucible or evaporator before and after the experiment.
2. Weighing the condenser before and after the experiment to give the mass of the vapor transported into it during the experiment and hence the mass loss of the sample.

3. Analyzing the vapor deposited in the condenser chemically employing sensitive analytical techniques.

Of the above three methods, the chemical analysis of the condensate in the condenser provides the most accurate information, however, it is quite time consuming. In the first of these methods, there is an inevitable error due to vaporization of the sample during attainment of the temperature of the experiment, which can be minimized only by increasing the total time of the experiment. Moreover, the total weight of the sample with the crucible is too large compared to the mass loss of the sample involved in the experiment. The determination of the mass loss from the vapor deposited in the condenser by weighing it before and after the experiment also gives results of poor accuracy because of the relatively small increase in the weight of the collector compared to its total weight. Further, there can also be considerable weighing error caused by the characteristic of the sample (sometimes the sample may be hygroscopic) if adequate care is not exercised during cooling of the sample. Use of gravimetric devices such as a thermobalance are becoming common these days for transpiration method, as one gets precise information regarding mass loss of the sample. A commercial thermo balance appears to have great advantage over conventional transpiration system in many ways:

1. Mass versus time data can be easily acquired through computers at any desired intervals of time and at any programmed heating
2. Mass versus time data at various flow rates can be obtained in a quick period of time
3. Both the above mentioned possibilities without having to change the sample during the course of flow dependence or temperature dependence measurements

Thus the time of measurements is reduced from days to hours. Though certain points still need some considerations, as observed by Siddiqi and Atakan [44] that the flow geometries of a typical thermobalances is not optimum for the transpiration method or in other words that it is not optimized for ensuring total saturation of the carrier gas with the evaporating substance. This is due to the fact that the mass loss of the substance depends upon the diffusion coefficient of the substance and the effective height of the sample in the crucible. The carrier gas flow rate has no effect on the mass loss rate of the sample in a thermobalance. Viswanathan [40] took these considerations into account by optimizing the geometry of the crucible in a way to fill the sample up to the brim of the crucible and by constricting the outlet of carrier gas so as to increase the

residence time of the carrier gas to get complete saturation. Regarding the identification of the saturation region, that most of the worker used the concept of identifying saturation region by plotting apparent vapor pressure (*P*) vs. flow rate ($\dot{V}$) plot. This is shown in figure 2.4

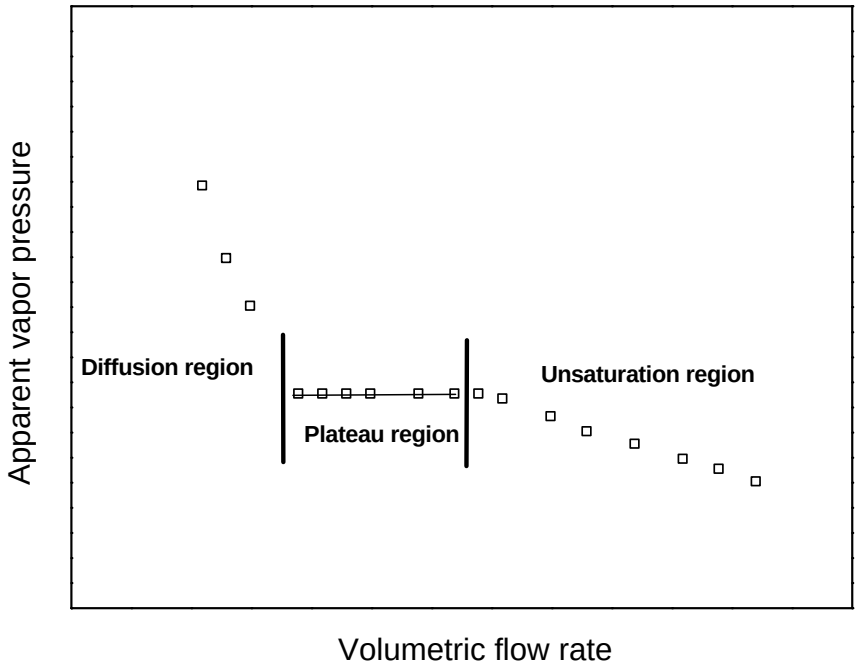

Figure 2.4: Variation of apparent vapor pressure with volumetric flow rate.

The three regions could be clearly identified namely as the diffusion region, saturation or plateau region and unsaturation region. The region of the plot where the apparent vapor pressure remains constant with the flow rate was identified as saturation region (plateau region) and this flow rate cooresponding to the plateau region was selected for measurement. But one can see from the equation (2.21) that the apparent pressure is in inverse relationship with flow rate i.e. apparent pressure decreases with increase in flow rate but this decrease is higher at higher flow rate and nearly vanishing at low flow rate giving the impression that one had arrieved the saturation region [40] i.e. misinterpretation of the saturation region. In order to get a clear interpretation of the saturation region, a plot of $\dot{m}$ vs. $\dot{V}$ would be helpful [40, 41]. For $\dot{m}$ vs. $\dot{V}$ plot, $\dot{m}$ will increase linearly with increase in flow rate (equation 2.21), having three distinct regions namely the saturation or plateau region where the $\dot{m}$ varied linearly with $\dot{V}$ (the linear line when extended will pass through the origin), the diffusion region in which the $\dot{m}$ values were higher than the $\dot{m} = k\dot{V}$ linear line indicating that the carrier was super saturated with the vapor, and the under saturation region in which the

$\dot{m}$ values were lower than the $\dot{m} = k\dot{V}$ linear line indicating that the carrier was not fully saturated [40] with the vapor as shown in figure 2.5.

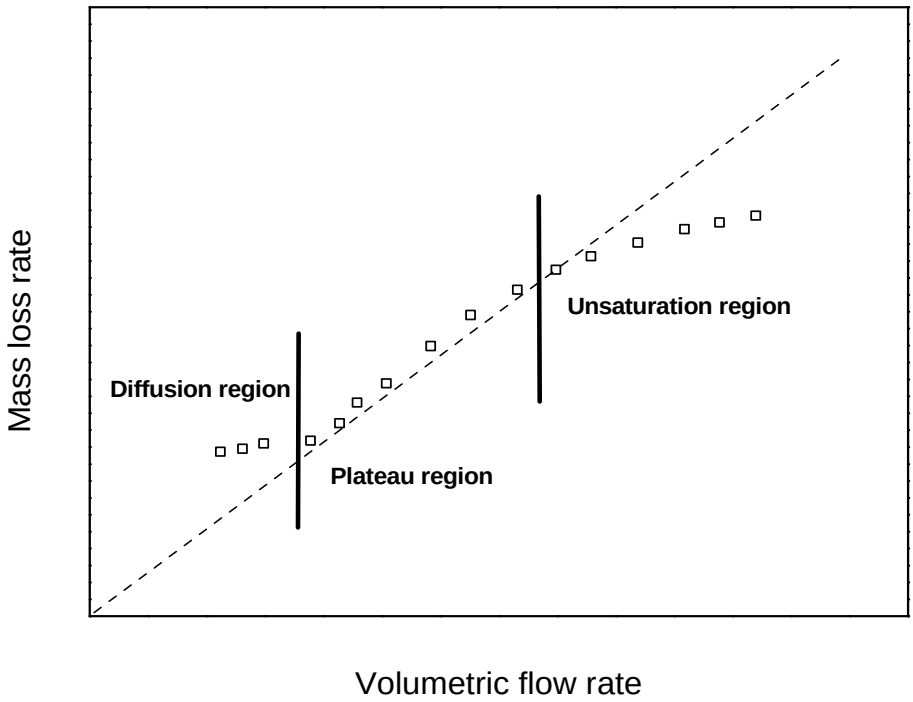

Figure 2.5: Variation of mass loss rate with volumetric flow rate.

However, one should ascertain consistency between P vs. $\dot{V}$ and $\dot{m}$ vs. $\dot{V}$ curves for every substance to be studied for the identification of the saturation region. In addition to above mentioned points it is also recommended that some validation experiment for the apparatus with substance with well established vapor pressure should be done before studying the unknown.Therefore, by careful consideration of these points, a commercial thermobalance could be successfully used for vapor pressure measurements.

2.3.3 Vapor pressure measurement using thermobalance

Langmuir considered the evaporation from an isolated solid surface into vacuum and presented the Langmuir equation shown below:

$$-\frac{dm}{dt} = p^{vap}\alpha\sqrt{\frac{M}{2\pi RT}} \qquad (2.22)$$

where *dm/dt* is mass loss rate, α is the vaporization coefficient of the compound, R is the gas constant, M is the molecular weight of the compound and T is the temperature in

K. This equation is applicable in the molecular flow regime (under high vacuum, K_n >1). Price and Hawkins [42] have formalized a procedure for estimating the vapor pressure of low-volatile substances from thermogravimetry data, which is obtained in the presence of an inert purge gas at atmospheric pressure using the Langmuir equation. In case of a substance volatilizing into a flowing gas stream at one atmosphere rather than a vacuum, α can no longer be assumed to be unity and has to be determined experimentally. The Langmuir equation can thus be rewritten as follows

$$P = kv \tag{2.23}$$

Where $v = \frac{dm}{dt}\sqrt{\frac{T}{M}}$ is the material dependent part of the Langmuir equation, and $k = \frac{\sqrt{2\pi R}}{\alpha}$ is the material independent part. Hence the value of k is determined for a particular set of experimental parameters, on a particular instrument using a calibiration substance whose vapor pressure is known.

Since the Langmuir equation is valid under molecular flow regime, which means under high vacuum and it was adopted for ambient pressures, the applied theory is not correct. However, through careful calibration with substances of comparable diffusion coefficient as the reference substances, some good results are reported in literature. An appropriate description of the method for using commercial thermobalances for vapor pressure measurement that in TGA experiments where crucibles are used to contain the substance and the inert gas flow rate has no effect on the vaporisation rate. At the surface of the substance, a saturated mixture is assumed as one boundary condition, while the mole fraction of the evaporating substance at the top of the crucible is assumed to be zero. Thus the height of the crucible above the substance may be taken as effective boundary layer thickness [43]. Under these conditions the vapor pressure of evaporating species is related to the weight loss under isothermal conditions as given by Nyman et al. [43]

$$p^{vap} = \frac{\Delta m}{\Delta t}\frac{R\,T\,d}{S\,M\,D_{AB}} \tag{2.24}$$

where, d is the length of the free space above the substance in the crucible (boundary layer thickness), *S* is the area of the substance evaporation surface, M is the molar mass of the substance and D_{AB} is the diffusion coefficient of substance A in the carrier gas B. It is clear from the relation of Nyman that the mass loss rate in a typical thermobalance depends upon the diffusion coefficient, and the height of the sample in the crucible. Dependence of the mass loss rate on these two factors has been pointed out recently [44-46] and this will be further elaborated in the diffusion coefficient section. Therefore, vapor pressure measurements are possibly irrelevant if diffusion effects dominate the transport rate.

2.3.4 Vapor pressure using gas chromatographic method

Gas chromatography (GC) is generally used to isolate specific substances from other similar compounds and to quantify each species individually. Separation of the compounds is accomplished by passing the sample through a column which "holds up" different chemical species for different amounts of time (retention time). The individual compounds elute to the detector as separate "peaks". The peaks are then identified by their retention time on the column.

A number of experimental methods for determining vapor pressure and vaporization enthalpies by using GC are based on measuring retention volume. Hamilton [47] gave the relationship between retention volume (V_r) and the vapor pressure for two substances run on a column under same conditions. For nonselective column (e.g. silicone SE-30) the relationship between the vapor pressure and retention volume is expressed as [47]

$$\frac{P_2}{P_1} = \frac{V_{r_1}}{V_{r_2}} \tag{2.25}$$

as the substance with higher vapor pressure will elute first. The retention volume can be calculated as product of retention time with carrier gas flow rate. The vapor pressure by gas chromatographic method for the two substances are related through the equation developed by Hamilton [47] as

$$\ln\left(\frac{V_{r_1}}{V_{r_2}}\right) = \left(1 - \frac{\Delta H_1}{\Delta H_2}\right)\ln P_2 - C \tag{2.26}$$

A plot of $\ln V_{r_1}/V_{r_2}$ versus $\ln P_2$ would give a straight line with slope $\left(1-\Delta H_1/\Delta H_2\right)$ and intercept of $-C$, where V_{r_1}/V_{r_2} is the relative retention volume at the temperature where the reference compound has vapor pressure P_2.

The vapor pressure P_1 of the unknown sample at any temperature can be calculated from the known vapor pressure of the reference compound at that temperature, and the constant of the linear equation using equation (2.26). The average precision of the GC methods, expressed as relative standard deviation was 9-36% as measured for some organic compound. Such a disappointing result has not extended use of the GC method in spite of the several advantages like its simplicity, speed, solute sample size as well as purity.

In another gas chromatographic method developed by Fuchs and Peacock [48] for liquid substances get the vaporization enthalpy. It is based on measuring the enthalpies of transfer from solution in a GC stationary phase to vapor to get the vaporization enthalpy using the relation

$$\Delta H\left(v \rightarrow S\right) = -R\frac{d\ln V_r}{d\left(1/T\right)} \tag{2.27}$$

where V_r is defined by the equation as

$$V_r = \frac{F_c J}{W_t}(t_r - t_a)\frac{273.15}{T_r P_o}(P_o - P_w) \tag{2.28}$$

where, F_c is the carrier gas flow rate

W_t is the weight of the stationary phase

t_r is the retention time of the sample

t_a is the retention time of the reference

T_r is the ambient temperature

P_o is the outlet pressure

P_w is the vapor pressure of water at ambient temperatures.

If these quantities are held constant, the retention volume equals to constant multiplied Δt and a plot $\ln \Delta t$ $(t_r - t_a)$ versus *1/T* will give a straight line and intercept of this plot differ from the plot of $\ln V_r$ versus *1/T* but the slope is unchanged. The slope of the curve multiplied by gas constant will give the enthalpies of transfer from solution, viz. the stationary phase of the GC column, to vapor. The heat of vaporization ΔH_v can be calculated by using relation

$$\Delta H_v = \Delta H_s - \Delta H(v \rightarrow S) \qquad (2.29)$$

where ΔH_s ,is the enthalpy of solution is measured calorimetrically. Chickos et al. [49] found that in the cases where compounds are properly selected with regard to molecular structure, a plot of $\Delta H(v \rightarrow S)$, which is the enthalpy of transfer from solution, viz. the stationary phase of the GC column, to vapor versus ΔH_v results in a straight line. The equation of this line can subsequently be used to evaluate the unknown vaporization enthalpy of any structurally related material provided that the unknown is analysed at the same time as the standard or reference compound. Also a plot of $\ln \Delta t$ versus *ln P* where *P* is the vapor pressure of a reference compound with well known and well established value of vapor pressure can be subsequently used to evaluate the unknown vapor pressure of any structurally related material provided that the unknown is studied at the same time as the standard or reference compound.

The GC correlation technique developed by Chickos et al.[49-51], proved to be an accurate means of determining vapor pressures and vaporization enthalpies of organic molecule. The GC methods as a rule require the use of one or several reference compound whose vapor pressure are known over the whole temperature range used by measuring chromatographic retention time. The only limitation of this method is the dependency on the choice of standards and the reliability of their vaporization enthalpies and vapor pressure [21].

2.3.5 Vapor pressure using the static method

In this method the sample is enclosed in a closed vessel. The temperature of the vessel is held constant for a certain period of time to permit thermal equilibrium between the condensed phase and the vapor phase. The sample is carefully degassed and vessel is

evacuated prior to beginning of the measurements. Working with corrosive sample or when measurement temperature is out of the range of the pressure gauge measurement is usually carried out by using the U tube manometer filled with mercury or using metal diaphagram in order to isolate the sample vapor from pressure gauge. When the DPI (differential pressure indicator) indicates that the pressures of an inert reference fluid and the sample are equal, the reference fluid pressure is measured using an appropriate pressure gauge.

If proper degassing of the sample is not done or some volatile impurities are still associated with the sample, the measured vapor pressure value is higher. In working above room temperature the condensation of vapor can take place in cooler parts of the apparatus, therefore, it is essential that all the parts of the apparatus must be at same temperature. Sometime adsorption on the wall of the apparatus can also be a possible source of error which can be avoided by using electrochemically polished tubings, keeping the internal surface of the setup as small as possible and using turbo molecular pump instead of using rotatory or diffusion pump, so as to avoid the deposition of oil films on the inner surface which enables the adsorption of vapors. Errors due to thermal transpiration could originate when the temperature of the vessel (T_1) is lower than the temperature of the pressure gauge (T_2), which could result in higher values of P_2 measured at T_2 than P_1 value at T_1 i.e.

$$\frac{P_2}{P_1} \neq 1 \qquad (2.30)$$

This ratio depends upon Knudsen number (see section 2.3.1.1.1), T_2/T_1 and tubing material. The ratio $P_2/P_1 = 1$ (hydrodynamic region; higher pressure) and for transitional regime the ratio P_2/P_1 comes to its limiting value. A detailed discussion about thermal transpiration can be found in the work of Ruzicka et al [52]. He found that there was no effect of thermal transpiration on the vapor measurement for Napthalene up to 473.15 K.

Using this method the vapor pressure was measured in the range 10^{-3} to 10MPa. The advantage of this method lies in allowing absolute calibrations and accurate temperature determination (±0.002K). The main drawback of this method is the time of measurement which is in days for low volatilitality samples.

Various other experimental method have been described in the literature for measuring the vapor pressure but no single method can be applied in the whole pressure range. The choice of method depends upon the temperature and pressure range of interest. The vapor pressure at low temperatures particularly near room temperature are desirable for environmentally relevant compound which could be effectively measured by using the transpiration method and gas chromatographic methods. Measurement at elevated temperature for volatile substances involves calorimetric, static and ebulliometric methods [21]. Measurements at high temperature for low volatility compounds can be done with high accuracy using effusion method and transpiration method. The choice of the method sometimes also depends upon the amount of the available sample. Static method generally requires sample in grams where as effusion and gas saturation method require only milligrams of the sample. Sometimes a wide variation in vapor pressure data reported by different authors for the same compound, the reasons for such are often unclear.

The Knudsen effusion method has long been employed for determining low vapor pressure. There are large numbers of references on determining vapor pressures of low volatility compounds based on the Knudsen effusion method.This method has been recommended as a standard technique for determination of vapor pressures [20,21]. In the present work, the Knudsen effusion method has been used for the determination of the vapor pressures of the organometallic compounds.

2.4 Temperature dependence of vapor pressure

2.4.1 Enthalpy of sublimation or vaporization

The vapor pressure of a solid / liquid, is constant at a given temperature increases continuously with increase in temperature up to the critical point of the solid / liquid. The solid / liquid no longer exists above the critical temperature and consequently the concept of a saturated vapor pressure is no longer valid. In terms of kinetic theory the increase in vapor pressure with temperature is easily understandable. As the temperature increases, a larger proportion of the molecules acquire sufficient energy to escape from the solid / liquid and consequently a higher pressure is necessary to establish equilibrium between vapor and solid.

Sublimation of a substance means the transition of the substance from the solid phase to the gas phase without the intermediate liquid phase. The enthalpy of sublimation is

defined as the heat of evaporation from solid phase to gas phase. It is known as the enthalpy required to transforming a given quantity of substance into gas. The enthalpy of sublimation can also be defined as the enthalpy required to overcome the intermolecular interactions in the solid material.

For any pure substance in a single phase, a change in Gibbs free energy is given by the following fundamental equation

$$dG = -SdT + VdP \tag{2.31}$$

To have equilibrium in the phase dG has to be zero at constants T and P. Since $dG = 0$ in the above equation when $dT = dP = 0$, the phase is in equilibrium when the pressure and the temperature are constant and uniform throughout the phase.

The transitions of a pure substance from one phase to another can be represented by the equation below:

$$G_1 = G_2 \tag{2.32}$$

for which ΔG is given by

$$\Delta G = G_2 - G_1 \tag{2.33}$$

where, G_2 = the molar free enthalpy of a substance in the final state

and, G_1 = the molar free enthalpy of a substance in the initial state

When $\Delta G = 0$ at constant temperature and pressure, all phase transformations will attain equilibrium. Imposing this condition on equation (2.33*)*, we see that $G_2 = G_1$ because all such transformation will be in equilibrium at constant temperature and pressure when the molar free enthalpies of the substance are identical in both phases. Suppose that we have two phases in equilibrium and that the pressure of the system is changed by dP. The temperature of the system will then have to change by dT in order to preserve the equilibrium. In such a situation dP and dT can be related as follows: Since $G_2 = G_1$, then we have also $dG_2 = dG_1$.

However, $$dG_2 = -S_2 dT + V_2 dP \tag{2.34}$$

and $$dG_1 = -S_1 dT + V_1 dP \quad (2.35)$$

By equating these expressions, we get

$$-S_2 dT + V_2 dP = -S_1 dT + V_1 dP \quad (2.36)$$

$$(V_2 - V_1)dP = (S_2 - S_1)dT \quad (2.37)$$

$$\frac{dP}{dT} = \frac{(S_2 - S_1)}{(V_2 - V_1)} = \frac{\Delta S}{\Delta V} \quad (2.38)$$

where, $\Delta S = S_2 - S_1$ is the change in molar entropy and $\Delta V = V_2 - V_1$ is the change in molar volume for the process. Further with the equation of Gibbs free energy at constant temperature and pressures $\Delta G = \Delta H - T\Delta S$, with $\Delta G = 0$ yields $\Delta S = \frac{\Delta H}{T}$, where ΔH is the change in molar enthalpy for the reversible transformation occurring at temperature T. Substituting this value of ΔS into equation (2.38), we obtain

$$\frac{dP}{dT} = \frac{\Delta H}{T\Delta V} = \frac{\Delta H_{sub/vap}}{T(V_v - V_s)} \quad (2.39)$$

where, $\Delta H = \Delta H_{sub/vap}$ = the heat of sublimation of solid

T = the temperature

$\Delta V = V_v - V_s$

V_v = the volume of the vapor

V_s = the volume of solid or liquid

Equation (2.39) is known as the Clapeyron equation and it relates the change in temperature which must accompany a change in pressure occurring in a system containing two phases of a pure substance in equilibrium. V_s is quite small if compared with V_v and it may be neglected. Further, if we assume that the vapor behaves as an ideal gas, then V_v per mole is given by:

$$V_v = \frac{RT}{P} \tag{2.40}$$

By substituting the value to equation (2.39), the following equation is obtained:

$$\frac{dP}{dT} = \frac{\Delta H_{sub/vap}}{TV_v} = \frac{\Delta H_{sub/vap} P}{RT^2} \tag{2.41}$$

$$\frac{1}{P}\frac{dP}{dT} = \frac{\Delta H_{sub/vap}}{RT^2} \tag{2.42}$$

$$\frac{d\ln P}{dT} = \frac{\Delta H_{sub/vap}}{RT^2} \tag{2.43}$$

This equation is known as Clausius-Clapeyron equation and the variation of vapor pressure with temperature can be expressed mathematically by this equation. The Clausius–Clapeyron equation can be easily integrated for the phase changes of solid to gas or liquid to gas by making following assumptions

1. The volume of vapor is much larger than condensed phase.
2. The vapor phase behaves as an ideal gas.
3. $\Delta H_{sub/vap}$ is constant over the temperature range involved.

The assumptions mentioned above are valid only over a limited temperature range and are far away from the critical point. As both $\Delta H_{sub/vap}$ and ΔV depend upon the temperature in similar form and both become zero at the critical point, as at critical temperature molar volume of both phases are equal so are all the physical properties and therefore, the distinction between two phases vanishes. Thus Clausius–Clapeyron equation is valid up to the critical point.

Based on these assumptions, integration equation (2.43) yields

$$\ln P = \frac{\Delta H_{sub}}{R}\int \frac{dT}{T^2} + B \tag{2.44}$$

$$\ln P = -\frac{\Delta H_{sub}}{R}\left(\frac{1}{T}\right) + B \tag{2.45}$$

where, B = the constant of integration. If we compare this equation with the equation of a straight line, which is written as

$$y = mx + c \tag{2.46}$$

Now if a graph ln P for any substance is plotted against $1/T$, then the plot should be a straight line with slope $m = -\frac{\Delta H_{sub/vap}}{R}$, and the intercept of y, $c = B$. By doing so, we can conclude that from the slopes of the lines, the enthalpies of sublimation or vaporization for the substances can be calculated from:

$$slope = m = -\frac{\Delta H_{sub/vap}}{R} \tag{2.47}$$

$$\Delta H_{sub/vap} = -Rm \tag{2.48}$$

Thus Clausius–Clapeyron equation allows one to calculate the pressure change dP which is necessary in order to maintain the phase equilibrium when there is temperature change dT.

The total differential of the heat of vaporization can be expressed as

$$d\Delta H = \left(\frac{\partial \Delta H}{\partial T}\right)_p dT + \left(\frac{\partial \Delta H}{\partial P}\right)_T \left(\frac{dP}{dT}\right) dT \tag{2.49}$$

where, $\left(\frac{\partial \Delta \mathrm{H}}{\partial \mathrm{P}}\right)_{\mathrm{T}} = \mathrm{V} - \mathrm{T}\left(\frac{\partial \mathrm{V}}{\partial \mathrm{T}}\right)_{\mathrm{P}}$ and $\left(\frac{\partial \Delta H}{\partial T}\right)_p = C_p$

and the dependence of enthalpy of vaporization on temperature can be expressed as

$$\left(\frac{\partial \Delta H}{\partial T}\right)_s = \Delta C_p + \left[\Delta V - T\left(\frac{\partial \Delta V}{\partial T}\right)_P\right]\left(\frac{dP}{\mathrm{dT}}\right) \tag{2.50}$$

where, $\Delta C_p = C_P^g - C_p^{cd}$

Thus the temperature dependence of the enthalpy of vaporization will depend upon the heat capacity difference between an ideal gas and the condensed phase. At low pressure where the behaviour of the vapor phase can be approximated by the ideal gas equation and the volume of the condensed phase can be neglected and the *PVT* behaviour (second term on right hand side of equation 2.50) are negligible compared to ΔC_p and the above equation can be written as

$$\left(\frac{\partial \Delta H}{\partial T}\right) = \Delta C_p \tag{2.51}$$

Integrating over an interval of temperatures T_1-T_2 gives

$$\int_{T_1}^{T_2} \Delta H = \int_{T_1}^{T_2} \Delta C_p \tag{2.52}$$

$$\Delta H(T_2) = \Delta H(T_1) + \int_{T_1}^{T_2} \Delta C_p dT \tag{2.53}$$

As the heat capacities of the substance involved in the transformation can be expressed in the form of power series

$$Cp = a + bT + cT^2 + ... \tag{2.54}$$

it follows

$$\Delta H(T_2) = \Delta H(T_1) + \Delta aT + \frac{\Delta b}{2} T^2 + \frac{\Delta c}{3} T^3 + ... \tag{2.55}$$

where all the term beyond the first on the right hand side of equation (2.55) arise from the change of heat capacities for vaporization / sublimation process. In absence of the reliable data on heat capacities for solids especially in case of organometallic substances change in heat capacity may be accepted to be taken as zero. If $\Delta C_p = 0$ then $\Delta H(T_2) = \Delta H(T_1)$.

A pure or single component substance can exist in three phases and the process by which one phase is transformed into another, include liquid-gas, solid-gas, solid-liquid and solid-solid. For solid-gas transition, when both phases are in equilibrium at constant temperature and pressure the change in free energy $\Delta G = 0$, meaning G_{cd} (condensed

phase) = G_g (gasesous phase). In general, the molar free energies are dependent upon both temperature and pressure. For the condensed phase, the dependence of G_{cd} of pressure is small but for $G_{g,}$ this is however significant. At constant temperature the free energy change is given by equation

$$\Delta G_g = V_g\, dP = RT\frac{dP}{P} \tag{2.56}$$

Integrating the above equation at constant temperature T from the hypothetical gas state at $P=P_{st}$ where $G_g = G_g^{\circ}$ to the actual vapor at $P=P_s$, the saturation pressure at temperature T yields

$$G_g = G_g^{\circ} + RT\ln\frac{P_s}{P_{st}} \tag{2.57}$$

Superscript ° denotes the reference or standard state at P_{st}. Equating $G_{con} = G_g$ we get

$$RT\ln\frac{P_s}{P_{st}} = -(G_g^{\circ} - G_{cd}) = -\Delta G_{Vap/Sub} = -(\Delta H_{Vap/Sub} - T\Delta S^{\circ}) \tag{2.58}$$

Assuming that the enthalpy of vaporization / sublimation is independent of temperature (in the small temperature range) the superscript ° can be dropped from this term and the equation representing the relationship between the enthalpy and entropy of vaporization / sublimation get a form of

$$\Delta S(T) = \frac{\Delta H}{T} + R\ln\frac{P_S}{P_{St}} \tag{2.59}$$

where P_s is measure vapor pressure at temperature T, P_{st} is the standard pressure (1atm, 760 Torr, 101.325 kPa), ΔH and ΔS (T) are enthalpy and entropy of vaporization / sublimation respectively at a definite fixed temperature (T)

2.5 Vapor pressure equations

The very earliest vapor pressure equation was given by Dalton who suggested that pressure increased in geometrical progression and temperature in arithmetic progression. Dalton equation can be represented as

$$\log P = b + a \cdot t \qquad (2.60)$$

where, b and a = constant

t = temperature in°C

This relation was quickly rejected when more accurate data were available. Most the equation used for representing vapor pressure data stems from the integration of Clausius-Clapeyron equation as

$$\ln P = -\frac{\Delta H_{sub}}{R}\left(\frac{1}{T}\right) + A = A - \frac{B}{T} \qquad (2.61)$$

It is a fairly good relation for approximating vapor pressure over a small temperature ranges. The application of this equation to accurate experimental data reveals that *1/T* does not give a true picture of vapor pressure relationship. There are deviations that exceed reasonable experimental errors and extrapolation over the measured temperature range is unwise even for a small temperature range.

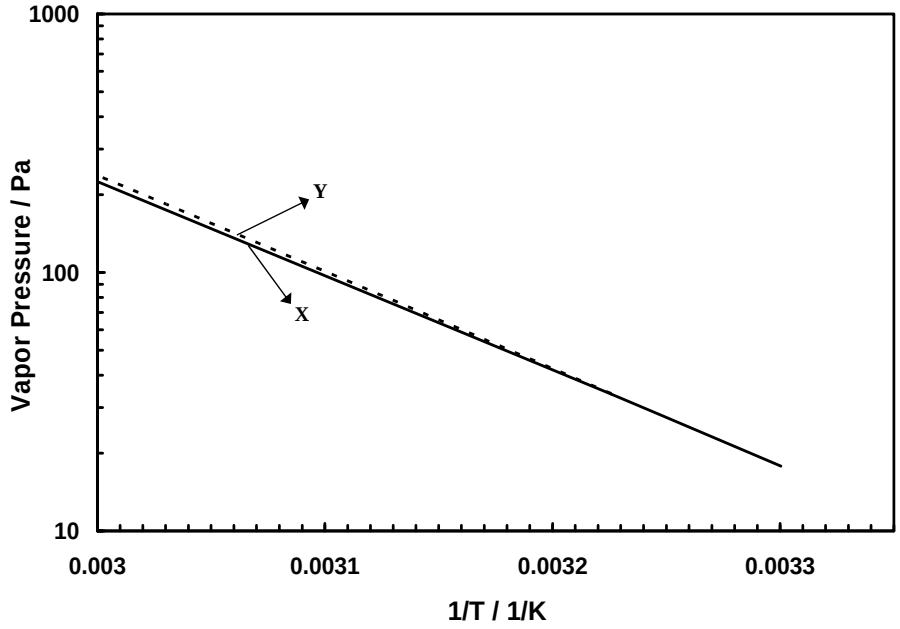

Figure 2.6: Vapor pressure of naphthalene for two temperature range.

Figure 2.6 shows a plot of napthalene vapor pressure against reciprocal of temperature with two lines (X and Y) for different temperature ranges, X is based on a higher temperature range (310-353 K) and Y is based on smaller temperature range (303-310 K). It can be easily seen that the extrapolation of the curve Y to higher temperrature will yield erroneous results. It is clearly desirable for the variation of vapor pressure with temperatures should be represented analytically, as if $log_{10}P$ is slightly curved and is incapable of representing accurate data over the whole range from boiling up to the critical point as shown in figure 2.7.

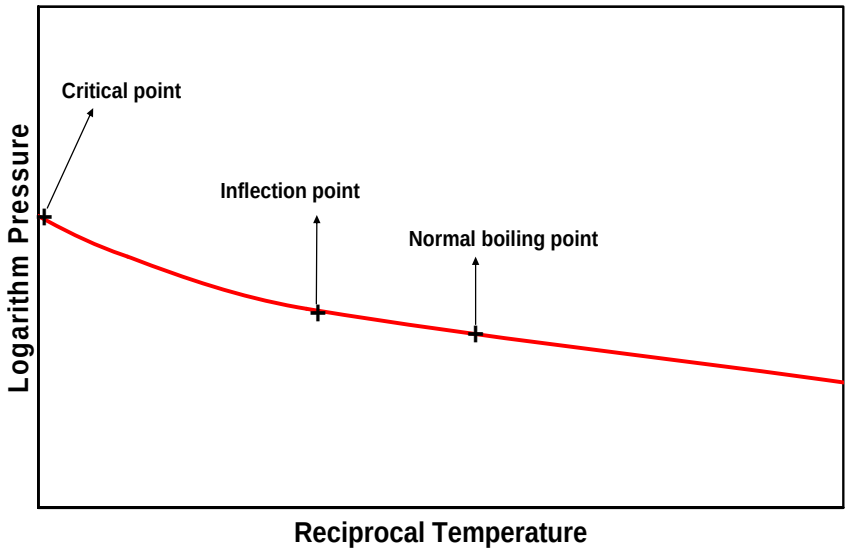

Figure 2.7: Variation of logarithmic vapor pressure with temperature.

The assumption that $\Delta H_{sub\ /\ vap}$ is constant was seen to be one of the chief contributing factor in the ability of *1/T* formula to represent the data within experimental error [53]. Another approach from above equation is to represent B in polynomial equation as

$$B = B_0 + B_1 T + B_2 T^2 + B_3 T^3 + ... \quad (2.62)$$

Substitution in equation (2.57) followed by integration leads to a expression

$$\ln P = A + \frac{B_0}{T} + B_1 \ln T + B_2 T + \frac{B_3}{2} T^2 + ... \quad (2.63)$$

With sufficient number of coefficients, this equation is valid over the entire temperature range up to the critical point. One of the simpler forms of the above equation is to assume that $B_2, B_3 ..... = 0$.This form of the equation is known as Kirchhoff equation which can be used for representation of results in the neighbourhood of boiling point and can be represented as

$$\ln P = A + \frac{B}{T} + C \ln\left(\frac{1}{T}\right) \quad (2.64)$$

Riedel [54] proposed a vapor pressure equation of the form

$$\ln P = A + \frac{B}{T_r} + C \ln\left(\frac{1}{T_r}\right) + DT_r^6 \quad (2.65)$$

The term T^6 (T_r is the reduced temperature) permits a depiction of the inflection point at high temperatures, however, the curve diverges at low pressures [55]. The Wagner equation [56] can be represented as the ratio of the logarithm of the vapor pressure and the critical pressure and is expressed as an expansion $\tau = (1 - T/T_c)$, where T_c is the critical temperature and is denoted as

$$ln\left(\frac{P}{P_c}\right)=\frac{T_c}{T}+\sum_{i=1}^{m}A_i\left(1-\frac{T}{T_c}\right)^{\alpha i} \tag{2.66}$$

Exponents have α_i have fixed values that are determined by statistical analysis method [56]. The Wagner types of equations have been very popular for fitting vapor pressure of liquids. Antoine proposed a simple modification of equation (2.61) which is widely used and gives a better representation of the temperature dependence of vapor pressure

$$\ln(P/Pa)=A_i-\frac{B_i}{(T/K+C_i)} \tag{2.67}$$

where, *Ai, Bi* and *Ci* are the substance specific constants ,T is the temperature in Kelvin. The Antoine equation is arguably the most popularly used vapor pressure correlation that provides a good representation of the vapor pressure–temperature relationship over a limited temperature below inflection point. Its extrapolation over very small temperature ranges generally yields reasonable results. It fits more accurately for every case than the 1/T form and reproduces the values closer than the other equations which are more complicated and are also difficult to use due to determining the empirical constants which is usually tedious work. According to Thompson [53] the equation is a appropriate three constant equation for interpolation purpose. But it cannot be extrapolated above a reduced temperature of about 0.85 without serious errors .This is the reason why different sets of constant are given for different temperature range. The advantages of using the Antoine equation are as

1. It requires only three constant.
2. It is quite similar to Clausius-Clapeyron equation which has an accepted theoretical basis.
3. Temperature may be made a dependent variable as 1/T.
4. It is the most widely used equation for fitting of vapor pressure data, so dependability of the equation is almost certain.
5. Extrapolation and interpolation with Antoine equation is strikingly more trustworthy than most other equations.
6. It can be effortlessly transformed into a simple linear equation.

Various other equations for describing dependence of vapor pressure on temperature have been discussed in detail by Thompson [53] and Wisniak [57]. In this study

experimental vapor pressure data are fitted to Antoine equation due to its ease of applicability and reliability and also due to the fact that other equation like Kirchhoff equation has no reliability and equation of Riedel and Wagner are defined using the critical data, which are generally unknown for organometallic compounds.

2.5.1 Curve fitting for calculating Antoine constants

Non linear regression analysis is a useful tool for curve fitting purposes. The method of least squares yields the parameters which minimizes the sum of squares of the residuals (the deviation of each measurements of the dependent variable from its calculated value)

$$SS_{resid} = \sum_{n=1}^{N} \left(X_{Exp} - X_{Calc} \right)^2 \qquad (2.68)$$

where X_{Exp} is the experimental value and X_{Cal} is the calculated value from the equation. The best fit of the curve is considered to be found when the sum of the squares of the deviations or residuals of the data points from the calculated curve is a minimum.

Least square method is based on the following assumptions

1. The given type of equation is a true representation of the observation.
2. The observations differ by from the true values only by random errors.
3. The errors are normally distributed.

Thus least square method gives most reliable values of empirical constants regardless of the form in which the equation is handled [56]. The empirical Antoine constants for each compound can be effectively determined by the least square curve fit method where the vapor pressure plot for each compound is fitted to Antoine equation.

2.6 Molecular gaseous diffusion coefficient

2.6.1 Basic concept and definition

Molecular diffusion or the diffusion of the molecules of one gas through those of another is a phenomenon dependent on the concentration gradient. Thus diffusion can be defined as the process by which molecules mix spontaneously moving from the regions of relatively high concentration into the regions of lower concentration. Diffusion coefficient is a factor of proportionality representing the amount of substance diffusing across a unit area through a unit concentration in unit time.

Diffusion coefficient for binary mixture of gases A and B is defined by

$$J_A^M = -cD_{AB}\frac{dx_A}{dz} = -D_{AB}\frac{dc_A}{dz} \quad (2.69)$$

$$J_B^M = -cD_{BA}\frac{dx_B}{dz} = -D_{BA}\frac{dc_B}{dz} \quad (2.70)$$

where c is the total molar concentration (V^{-1}), J_A^M and J_B^M represents molar flux of A and B in a mixture of A and B and diffusion is taking place in the "z" direction. Since $D_{AB} = D_{BA}$, therefore, the diffusion coefficient then represents the proportionality between the flux of A relative to a plane of no net molar flow and the gradient.

The knowledge of molecular diffusivities for example is needed for the calculation of Sherwood and Lewis number used to describe mass transfer process. In environmental science molecular diffusivities are essential for calculation of chemical fluxes of various compounds that are present in the environment across air interphase. The importance of gaseous diffusion coefficient is well recognised as the availability of the experimental data is limited and desired values are usually obtained from various correlations that have been developed exclusively for organic compounds only. No such experimental data or either correlation for estimation of diffusion coefficient for organometallic compounds are available which are typically important substances from the environmental point of view and also they are used in many industrial processes which would help to describe its mass transfer process.

2.6.2 Empirical correlations for estimation of binary gas diffusion coefficient

In elementary hard sphere model assumption is made that all molecules are non attracting rigid spheres of diameter (σ) moving randomly with a mean velocity "*V*". The moving molecules undergo collision with each other and with molecules of other species and thus these molecular collision play important role in controlling the overall the rate at which transport occurs. The speeds of the molecules of gasses are very high (10^4 cm/s) when compared to the actual diffusion velocities which are around 1cm/s [58]. The molecular collision is governed by the forces of interaction between molecules.

From the knowledge of fundamental intermolecular forces, kinetic theory of gases can be used to determine the gaseous diffusion coefficient.

The diffusion process can be explained as the molecules velocity changes due to collision, however a large fraction of molecules within a particular velocity range is nearly constant and this fraction is specified as Maxwell distribution. The diffusion coefficient can be calculated from a flux derived from a molecular concept- the integral of molecular velocity over nonequllibrium velocity distribution function [58]. The changes in velocity distribution must satisfy the Boltzmann equation [58, 59], which is applied to study the nonequilibrium behaviour of gaseous molecules. The Boltzmann equation applies to a quantity known as distribution function, which describes this nonequilibrium state mathematically and specifies how quickly and in what manner the state of the gases changes when the disturbing forces are varied. A solution to Botlzmaan equation was obtained both by Chapman and Enskog [59] independently giving the relation

$$D_{AB} = \frac{0.00146 T^{3/2} M_{AB}^{1/2}}{p\ \sigma_{AB}^2} \qquad (2.71)$$

where T is the temperature in K, p is the pressure in bar , σ_{AB} is the characteristic diameter given by $\sigma_{AB} = \frac{\sigma_A + \sigma_B}{2}$ and $M_{AB} = \frac{2}{(1/M_A + 1/M_B)}$ (M_A and M_B is the molecular mass of the substances A and B).

The Chapman and Enskog theory gives the expression for the transport properties in terms of intermolecular potential $\phi(r)$, where r is the distance between a pair of molecules undergoing collision. The intermolecular force is then given by $F(r) = -d\phi / dr$ and the intermolecular potential ϕ is then given by using empirical expression Lennard Jones (6-12) potential given by the expression

$$\phi(r) = 4\varepsilon \left[\left(\frac{\sigma}{r} \right)^{12} - \left(\frac{\sigma}{r} \right)^{6} \right] \qquad (2.72)$$

in which σ is a characteristic diameter of the molecule, often called the collision diameter and ε is a characteristic energy, the maximum energy of attraction between a

pair of molecules. The equation (2.71) gives a temperature dependence of $T^{3/2}$ though the experimental evidence shows this is to be low. The observed temperature dependence varies between 1.7-1.8 [60-62]. The correlation provided good results within the temperature range used for calculating σ_{AB} but the scarcity of experimental data for σ_{AB} was one of the major drawback in using this correlation for variety of other organic compounds. To overcome the drawback of absence of σ_{AB} value, Gilliland [63] correlated σ_{AB} as the cube root of the sum of LeBas [64] atomic volume parameter to overcome the problem of scarcity of values σ_{AB} and finally arrived at the relation having the same temperature dependence

$$D_{AB} = \frac{0.0043\, T^{3/2}\left(1/M_A + 1/M_B\right)^{1/2}}{P\left(V_A^{1/3} + V_B^{1/3}\right)^2} \tag{2.73}$$

An equation similar to that Gilliland was given by Arnold [65] who tried to overcome the limitation of Chapman and Enskog relation by introducing Sutherland [66] temperature correction C_{AB}, to account for the deviation from hard sphere model and getting better temperature dependence in form of the relation given as

$$D_{AB} = \frac{0.00837 T^{3/2}\left(1/M_A + 1/M_B\right)^{1/2}}{P\left(V_A^{1/3} + V_B^{1/3}\right)^2\left(1 + C_{AB}/T\right)} \tag{2.74}$$

where, C_{AB} (Sutherland constant for mixture in K) = $F\left(C_A C_B\right)^{1/2}$

C_A and C_B are estimated from relation $C = 1.47 T_b$

$$F = \left[2\left(V_{A'}^{1/3} + V_{B'}^{1/3} \right)^{1/2} / \left(V_{A'}^{1/3} + V_{B'}^{1/3} \right) \right]^3$$

Introduction of term $\left(1 + C_{AB}/T\right)$ gives rise to a rather complicated temperature dependence of 2.5 at low temperatures to 1.5 at higher temperatures [60]. An improved temperature dependence of 1.78 which agrees quite well with the experimental data was given in Andrussow [67] equation

$$D_{AB} = \frac{0.606T^{1.78}\left\{\left(\frac{1}{M_A}+\frac{1}{M_B}\right)^{1/2}+\frac{1}{(M_A M_B)^{1/2}}\right\}}{P\left(V_A^{1/3}+V_B^{1/3}\right)^2} \qquad (2.75)$$

Hirschfedler Bird and Spotz [68, 69] used the Chapman-Enskog approach and calculated collision integral which is a complicated function of reduced temperature and can be regarded as a correction factor for the deviation from hard sphere model taking into account the potential field surrounding the molecule. It accounts for the details of path that molecule take up during a binary collision. If the gas were made up of rigid spheres of diameter σ (instead of a real gas molecule with attractive and repulsive forces) then the collision integral would be exactly unity and therefore, it can be interpreted as describing the deviation from the rigid sphere behaviour. The collision integral can be calculated using the Neufeld [70] equation which is represented as

$$\Omega = \frac{A}{(T^*)^B}+\frac{C}{\exp(DT^*)}+\frac{E}{\exp(FT^*)}+\frac{G}{\exp(HT^*)} \qquad (2.76)$$

$$T^* = \left(KT/\varepsilon\right)_{AB} \qquad (2.77)$$

A =1.066036	B =0.15610	C =0.19300	D =0.47635
E =1.03587	F =1.52996	G =1.76474	H =3.89411

The resulting equation of Hirschfedler Bird and Spotz is given as

$$D_{AB} = \frac{0.001858T^{3/2}\left(1/M_A+1/M_B\right)^{1/2}}{P\sigma_{AB}^{\,2}\Omega} \qquad (2.78)$$

Introduction of Ω gives a temperature dependence of approximately 2.0 at low temperatures upto 1.65 at high temperature and this corresponds very well to a number of systems [60]. Based on critical properties several methods were proposed for the calculation of $\left(\varepsilon/K\right)$ and σ and following relationship were given for calculation of Ω

$\left(\varepsilon/K\right) = 0.77T_C$ and $\sigma = 0.833V_c^{1/3}$ by Hirschfedler Bird and Spotz

$\left(\varepsilon/K\right) = 1.267T_C^{0.906}$ and $\sigma = 1.18\,V_C^{0.4006}$ by Chen and Othmer [71]

$\left(\varepsilon/K\right) = 1.267T_C^{0.906}$ $\sigma = 1.18V^{1/3}$ by Wilkee and Lee [72] (V from LeBas volume)

The best results were obtained from viscosity data as observed by Reid and Sherwood with an average error of 6% [64]. In using the relationship, it is important to use the same set of relations to obtain the value of σ and ε from a single source. Wilke and Lee [72] proposed a modification to Hirschfelder, Bird and Spotz based on experimental observations giving equation.

$$D_{AB} = \frac{0.00214 - 0.000492T^{3/2}\left[\frac{1}{M_A} + \frac{1}{M_B}\right]^{1/2}}{P\sigma_{AB}^2\Omega} \tag{2.79}$$

Chen and Othmer [71] also developed a correlation based on critical properties of the substances which is given by the equation

$$D_{AB} = \frac{0.43\left(\frac{T}{100}\right)^{3/2}\left(\frac{1}{M_A} + \frac{1}{M_B}\right)^{1/2}}{P\left(\frac{T_{cA}T_{cB}}{10000}\right)^{0.1405}\left(\frac{V_{cA}^{0.4}}{1000} + \frac{V_{cB}^{0.4}}{1000}\right)^2} \tag{2.80}$$

An empirical correlation based on about 350 data points for 153 different binary system was developed by Fuller, Schettler and Giddings [74]. Their correlation is given by the equation

$$D_{AB} = \frac{0.001T^{1.75}\left(1/M_A + 1/M_B\right)^{1/2}}{P\left(V_A^{1/3} + V_B^{1/3}\right)^2} \tag{2.81}$$

where $V_A, V_B = \sum_i V_i$ where V_i are special volume increments. The atomic parameters were determined by a regression analysis of experimental data points. This equation gives a better agreement with experimental data due to improved temperature

dependence of 1.75 and determination of effective σ_{AB} based on actual diffusion measurements.

The correlation for diffusion coefficient can be broadly classified into two categories. The first category includes all those which require molecular properties such as viscosity, σ etc. In the second category parameters are obtained from atomic and simple group constants such as atomic weight and size. Therefore, category two has more practical application as these data are easily available. But to say that which one of the categories could provide us with good values of diffusion coefficient is difficult to say.

The diffusion coefficients are difficult to measure due to experimental complexities like compositional analysis of the diffusing substance. Whatever experimental data are available a fair amount of difference in the values are observed even for organic compounds for which fair amount studies were undertaken. So the amount of error or the uncertainties on comparison of experimental values with values obtained from correlation are difficult to access. For organometallic compounds no correlation are available for the estimation of gaseous diffusion coefficient.

In general correlation Hirschfedler Bird and Spotz could give good result provided that the viscosity data are available for the system under study. But the correlation of Fuller et al. yielded smallest average error [64] and therefore, this method is recommended [64] for use. The most important drawback of all the correlations is that they are applicable with precision only for organic compounds. Since all the correlations for estimation are based either on physical quantities like critical temperature and volume or on atomic sizes. Various correlations and experimental data for these physical constants are available only for organic compounds but no such data are available for organometallic compounds.

2.6.3 Experimental determination of molecular gaseous diffusion coefficient

2.6.3.1 Closed tube method

This method was developed by Loschmidt in 1870. The apparatus consists of a long closed vertical tube which is divided into two portions with the help of partition. Each half of the tube is filled with a different gas and both the halves are maintained at constant temperature and pressure. The partion is then removed and diffusion of one gas takes place into the other gas for a measured time *"t"*, after which the partition is reinserted and the content of the two sections are analysed to determine the change in composition. The diffusion coefficient is determined using the relation

$$D_{AB} = \frac{l^2}{\pi^2 t} \log\left(\frac{\sqrt{3}/\pi}{C_1(t) - 1/2} \right) \tag{2.82}$$

where l is the length of the tube, t is the diffusion time , C_1 is the concentration of the gas 1. Gaseous D_{AB} for various systems were determined with this method in the temperature range 195-478 K with accuracy of 1-3% [58].

2.6.3.2 Two bulb method

The two bulb method was developed by Ney and Armstead [75] in order to determine the self diffusion coefficient of UF_6. The apparatus consists of two bulbs or chamber connected together by a narrow tube through which the diffusion occurs with an assumption of quasi stationary state i.e. the flux of the component is constant along the connecting tube. The material from one bulb is drawn into another bulb and the composition in the bulb varies exponentially with time as

$$\Delta x(t) = \Delta x(0) \exp(-t/\tau) \tag{2.83}$$

and D_{AB} can be obtained from the relation

$$\tau = \frac{D_{AB} A}{K l} \left[\frac{V_1 + V_2}{V_1 V_2} \right] \tag{2.84}$$

$$K = 1 + \frac{A\,l}{3V_1}\left[\frac{1 - V_1/V_2 + \left(V_1/V_2\right)^2}{1 + V_1/V_2}\right] \tag{2.85}$$

where V_1 and V_2 are the volume of two bulbs.

2.6.3.3 Gas chromatographic method

This method involves introduction of the trace amounts of gas as a pulse into a carrier gas flowing through a long hollow tube or packed column was developed by Giddings and Seager [76]. Considering the case where the long hollow tube is used, theoretical plate height, H (distance a solute moves while under going one partition, and is numerically equal to the column length divided by the number of theoretical plates in the column) in a typical gas chromatographic column is given by the relation

$$H = \frac{1}{\left(1/2\lambda D_p + 1/C_g V\right)} + \frac{2\gamma D_{AB}}{V} + C_l V + C_k V \tag{2.86}$$

where D_{AB} is the binary diffusion coefficient for the sample and carrier gas and D_p average diameter of the packing material.

The theoretical plate height, H can be determined from the relation

$$H = \frac{L\tau^2}{t^2} \tag{2.87}$$

where L is the length of the column, τ is the peak variance in time units, t is the retention time and C_g C_k, and C_l are non equilibrium term (representing gaseous diffusion, adsorption processes and liquid diffusion) originated from non uniform flow velocity existing in the tube crossection. For an empty tube of circular crossection, it is assumed that the adsorption at the wall is negligible, so that the term $C_k = 0$. Since there is no liquid inside the tube, therefore, $C_l = 0$ and the term $2\lambda D_p$ goes to infinity because there is no mixing stages (no packed column) and γ being an obstruction factor having

value close to unity for such capillary column and replacing value of C_g ($C_g = \frac{r_o^2}{24D_{AB}}$) in the above equation we get

$$H = \frac{2D_{AB}}{V} + \frac{r_o^2 V}{24D_{AB}} \qquad (2.88)$$

r_0 = tube radius, and V is the velocity of carrier gas averaged over the tube cross section.

The binary diffusion coefficient in the gas phase can be obtained in terms of experimentally determined value of H and equation (2.84) can be written as

$$D_{AB} = \frac{\overline{V}}{4}\left(H \pm \sqrt{H^2 - r_o^2/3}\right) \qquad (2.89)$$

The positive root of the equation is valid upto a certain critical velocity, $\overline{V}_c$. In practice the proper choice of the root posses no serious problem since one can make a reasonable estimate of $\overline{V}_c$ by calculating before hand. This could be done by choosing some arbitrary value of D_{AB}, calculating H at various velocities from equation 2.85 and then ploting the two D_{AB} values (obtained from various H) using both positive and negative root from equation 2.86, w.r.t velocity of the carrier gas. From this graph the value of D_{AB} is chosen where the plot of positive and negative root intersects. $\overline{V}_c$ can be obtained using the relation

$$\overline{V_c} = \sqrt{48}\left(D_{AB}/r_o\right) \qquad (2.90)$$

Positive root should be taken when $\overline{V} < \overline{V}_c$ and negative root when $\overline{V} > \overline{V}_c$.The inaccuracies in D_{AB} determination using GC method have been reported to be 1-2 %.

2.6.3.4 Evaporation tube method

In 1873 Stefan developed an evaporation tube method for the determination of D_{AB}. The method involves volatilization of substances placed in a vertical tube and a carrier gas

flows over it. The evaporation rate of the substance which partially fills the tube is controlled by diffusion through a stagnant gas which fills the rest of the tube. From the gas substance interface vapor diffuses through the gas to the mouth of the tube. At the interphase the mixture composition depend upon the vapor pressure of the substance. Across the tube outlet carrier gas flows and carries the vapor away.

The following assumptions were made

1. Quasi steady state approximation- a constant concentration of the substance is fixed at slowly moving surface of the substance which is slowly moving.
2. The vapor concentration at the top of the tube is zero i.e. carrier gas carries all the vapor of the substance from the outlet.
3. Gasses and vapors behave ideally so that the composition may be expressed in terms of partial pressure.
4. The gas does not dissolve or adsorb on to the substance surface.

Under these assumptions, the expression for D_{AB} is given as

$$D_{AB} = \frac{\Delta Z^2 RT\rho}{2\Delta tPM}\left(\frac{\ln P - P_s}{P}\right) \qquad (2.91)$$

where ΔZ is the change in height of the sample in the tube in time Δt, P_s is the vapor pressure and P is the total pressure. The evaluation of the term $\left[\frac{\ln P - P_s}{P}\right]$ indicates that the small changes in pressure and temperature can cause large uncertainties in measured values of D_{AB} [77]. This means that a significant variation in atmospheric pressure or the temperature may lead to inaccurate values. Secondly if a very high volatile substance is studied, a non equilibrium condition may exist due to the fast evaporation of substance leading to cooling effect at the surface. Correct determination of diffusion length is also important, errors could occur due to the surface tension at the gas liquid interface. Inaccuracies sometimes amount to several percents [76, 78].

2.6.3.5 Diffusion coefficient using point source method

Walker and Westenberg [79] first used this method to determine the gaseous diffusion coefficient N_2-CO_2 system. This method involves the introduction of a tracer gas through a fine tube into a slow uniform and laminar flow of carrier gas flowing in the

same direction. Measurement of the trace gas concentration *C* downstream of the source by means of precise gas sampling permits the determination of D_{AB} using the relation

$$C = \left(\frac{\dot{Q}}{4\pi R D_{AB}} \right) \exp\left[-(R - Z)U/2D_{AB} \right] \qquad (2.92)$$

where

$\dot{Q}$ = Volumetric flow rate of carrier gas.

R = radial distance measured from the source.

Z = axial distance from the point of injection.

U = velocity of the carrier gas.

A plot of *lnCR* versus (*R-Z*) gives a slope of $-U/2D_{AB}$, if U is known, D_{AB} can be obtained. The other method is to use the maximum value of C at the point on X axis where *Z*=*R* then $C_{MAX} = \dot{Q}/4\pi D_{AB}$ and if $\dot{Q}$ is known then D_{AB} can be obtained. The author reported a accuracy of ± 1% but in general this method can give result within accuracy of 5% [58].

2.6.3.6 Diffusion coefficient using QCM method

Recently a new method was developed by Chen et al. [80] who used quartz crystal microbalance (QCM) for the determination of D_{AB} of naphthalene in air. The conventional digital balance is replaced by a QCM having a high mass resolution. The QCM is placed onto the top of a closed Stefan tube and its active surface is covered with a thin layer of the substance of interest by depositing its vapor. At the end of the Stefan tube some adsorbent material is placed to adsorb the vaporizing material. The theory originates from Sauerbrey [81] equation which relates the mass change per unit area at the QCM surface to observed change in oscillating frequency of the crystal that can be expressed as

$$\Delta f = C_f \Delta m \tag{2.93}$$

where C_f is the sensitivity factor for the crystal (e.g 56.6 Hz μg^{-1} cm² for 5 MHz AT cut quartz crystal at room temperature) and $\triangle m$ is the mass change per unit area.When the active surface of QCM is coated with the thin film, its apparent frequency will decrease from the initial frequency f (without coating) to f_c (with coating) due to increase in mass of the QCM. An increase in frequency of the QCM will be observed when the deposited layer of the substance evaporates. The change in frequency is determined by

$$\Delta f = f - f_c \tag{2.94}$$

The mass flux can be determined as

$$\dot{m} = \frac{(\Delta f - \Delta f_o)}{C_f (t - t_o)} \tag{2.95}$$

C_f is the mass sensitivity of QCM and Δf_o denotes the frequency shift of QCM at the time constant t_o. The diffusion coefficient is based on Fick`s diffusion law and is given as

$$D_{AB} = \frac{\dot{m} X}{\rho_D - \rho_{D,o}} = \frac{(\Delta f - \Delta f_o)}{C_f (t - t_o) \rho_D} \tag{2.96}$$

where ρ_D and $\rho_{D,o}$ denotes the mass concentration of the sample vapor on the deposited surface and on the adsorbent material and X is the diffusion length.

The above equation is based on the following assumptions:

1. Both the examined substance and air behaves as ideal gas.
2. The diffusion process in the diffusion tube is one dimensional and steady.
3. The air is not adsorbed by adsorbent, only the substance is adsorbed.
4. The gas mixture within the diffusion tube consists only of air and vapor of the substance without the presence of temperature and pressure gradient, external forces and chemical reactions.
5. The mass concentration of the examined substance vapor at the surface of the QCM and air is constant value and is zero on the surface of the activated adsorbent.

Chen et al. [80] reported a maximum of 3-12% variation of the measured value for gaseous diffusion coefficient of napthalene from the value predicted by empirical correlation of Fuller et al. [74]. The accuracy of this method depends upon how well one can do the compositional analysis of the diffusing substance. For accurate measurements the mass of the evaporating substance must be sufficiently small when compared to the mass of QCM and Δf should be a value below 2% of f . Therefore, to meet these requirements one should deposit a very thin and uniform layer of the substance on the active surface of the QCM, which is rather difficult to achieve by just letting the vapors of the substances to condense on the QCM. The main advantage of this method that measurements can be done at relatively at low temperatures in a short span of time but air sensitive substances cannot be examined with this technique.

2.6.3.7 Diffusion coefficient from volatization of solid sphere

Delgado et al. [82] developed a method based on mass transfer theory to determine D_{AB} . The process is based on mass transfer from a volatile solid sphere of the substance buried in a packed bed of inert particles (sand), through which air is forced to flow continuously at very low velocities, the rates of mass transfer are strongly determined by molecular diffusion. The equation for the calculation of D_{AB} can be obtained using the relation [83]

$$\frac{Sh}{\xi} = \left[4 + \frac{4}{5}(Pe\frac{d_1}{d})^{2/3} + \frac{4}{\pi}(Pe\frac{d_1}{d}) \right]^{1/2} \quad (2.97)$$

$$Sh = \frac{Kd_1}{D'_{AB}} \text{ = Sherwood number} \quad (2.98)$$

$$Pe = \frac{\mu_0 d}{D'_{AB}} \text{ = Peclet number} \quad (2.99)$$

where d_1 is the diameter of the sphere, d is the diameter of the inert particle and μ_0 is the interstitial velocity. Substituting the value of Sherwood and Peclet number in the equation one gets the relationship given as

$$\frac{Kd_1}{\xi} = D'_{AB}\left[4 + \frac{4}{5}(\frac{\mu_o d_1}{D'_{AB}})^{2/3} + \frac{4}{\pi}(\frac{\mu_o d_1}{D'_{AB}}) \right]^{1/2} \quad (2.100)$$

$$D'_{AB} = D_{AB}/\varsigma \quad (2.101)$$

where ς = Tortuocity factor having a value of $\sqrt{2}$ for packed bed of granular material.

ξ = Bed voidage.

The above equation is valid for molecular diffusion under the condition when Peclet number $\cong 1$ (which is based on the diameter of the inert particle making up the bed), above this value the convective dispersion rather than molecular diffusion would be then the relevant mechanism of mass transfer. The experimental value of mass transport coefficient can be calculated using the relation

$$K = \frac{\Delta m\, R\, T}{\Delta t\, M\, \pi\, d_1^2\, P} \quad (2.102)$$

The author reported that u under the given condition of Peclet number $\cong 1$, the equation reproducibility of the obtained values for D_{AB} was within 10%.

2.6.3.8 Diffusion coefficient using thermogravimetric analyser

This method has been recently developed by Siddiqi and Atakan [44] and is similar to the Stefan tube method. In a typical TG/DTA apparatus the sample crucible and a reference crucible are placed on a sample holder in a tube furnace in a gas stream. The sample crucible is filled to some amount with the substance to be investigated. This amount is changing with time due to evaporation. If the vapor pressure of the sample is low (below 10 mbar at a total pressure of 1000 mbar) the deviation of the mole fraction of the inert gas from unity can be neglected. According to the theory of diffusion processes the crucible may be approximated as a one dimensional quasi-stationary system where a constant concentration of the substance is fixed at the (slowly moving) surface of the substance due to the loss of the substance from the crucible, while at the upper edge of the crucible the concentration of the substance is negligible. The mass change rate is determined by the diffusion rate out of the crucible. The derivation is adapted from the textbook by Bird et al. [84].

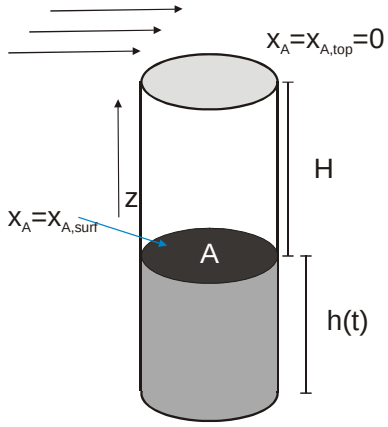

Figure 2.8: Diffusion of A through nondiffusing B.

The starting point is the mass balance, which basically states that the molar evaporation rate of the sample is equal to the molar diffusion rate out of the sample in the gas phase

$$S\frac{\rho_A}{M_A}\frac{dh(t)}{dt}=\frac{c\,D_{AB}}{H+h(t)}(x_{A,surf}-x_{A,top})\,S \qquad (2.103)$$

Here ρ_A is the apparent density of the evaporating substance A and M_A is its molecular mass. H is the initial distance between the surface of the substance and the top of the

cylinder, S is the surface area of the evaporating substance, $h(t)$ is the time dependent height of the sample evaporated, being zero initially and getting positive at longer times; c is the molar density of the gas ($c = p/RT$; p being the total pressure); $x_{A,surf}$ is the mole fraction of A at the surface and $x_{A,Top}$ is its mole fraction at the top. Since the change in height is quite slow the steady state evaporation rate at any time t has been used on the right hand side of equation (2.103).

The mole fraction of the vapor at the top of the cylinder can be neglected if the buffer gas flow rate is high enough (i.e. $x_{A,Top} \approx 0$). The ideal gas law ($p = cRT$) and Dalton's law ($p_A = x_{A,surf} P$) are used to integrate between the starting time and a given time, t:

$$\int_0^h [H + h(t)]dh = \frac{p_A^{vap} D_{AB} M_A}{RT \rho_A} \int_0^t dt \qquad (2.104)$$

The solution of the integration

$$h = \sqrt{H^2 + \frac{2 p_A^{vap} D_{AB} M_A}{RT \rho_A} t} - H \qquad (2.105)$$

is then used to derive an expression between the mass loss and the evaporation time, or for the product of vapor pressure and the binary diffusion coefficient

$$p_A^{vap} D_{AB} = \left\{(h + H)^2 - H^2\right\} \frac{RT \rho_A}{2Mt} = \left\{ \left(\frac{\Delta m}{S \rho_A} + H\right)^2 - H^2 \right\} \frac{RT \rho_A}{2M t} \qquad (2.106)$$

Experimental vapor (sublimation) pressures obtained from Knudsen cell measurements together with the measurements of the TG/DTA apparatus were then used to evaluate the diffusion coefficients.

The determination of D_{AB} requires the measurement of temperature, pressure, geometrical factors such as diffusion length, and composition. Measurement of pressure and temperature can be done with ease and are less prone to errors but sometimes the use of poor methods of compositional analysis of the sample, errors may lead to

inaccuracies in the measurements. Measurements are considered to be good when the associated uncertainties are within 2% [58] which is rather difficult to achieve. Values of D_{AB} estimated from various correlation agree within 5-10% of the experimental value although discrepancies of more than 20% are possible [64]. Marrero et al. [58] in his review paper for gaseous diffusion coefficient had given a very excellent and detailed review of various experimental techniques used in the determination of D_{AB}. During the literature survey for experimental gaseous diffusion coefficient it had been found that recent works were mainly based on gas chromatography or Stephan tube method for organic compounds or gas-gas system. Some of the recent work on D_{AB} includes the work of Delagado et al. [82] for napthalene-air system, Caldwell [85] for napthalene- air/ H_2 system, Cho et al [86] for napthalene-air system, Gustafson et al. [87] for various PAH –air system, Tashiro et al [88] for NaI –argon system, Gardner et al. [89] for SnBr and SnI –argon system, Battino et al. [90] for aromatics-SF_6 system and. All these method were based on Stefan tube method except the work of Gustafson which was based on GC and Delgado who had used the mass transfer approach. No diffusion coefficient data were available for organometallic compounds.

2.6.4 Temperature dependence of diffusion coefficient

The observed temperature dependence varies from system to system with typical values lying between 1.5- 2. Seager et al. [61] gave a value of 1.7 for all gasses and vapors. The correlation of Chapman and Enskog gave a temperature dependence of 1.5 which is too low when experimental evidences are considered. This is due to fact that σ_{AB} tends to decrease with increase in temperature as molecules tends to move faster at higher temperatures and approach each other more closely in encounters or collisions and the effective diameter is reduced i.e. failure of rigid sphere model which assumes that molecules are non attaracting. The HSB [68,69] correlation based on Chapman and Enskog approach and used collision integral Ω which gives the deviation of a gas of rigid or hard elastic spheres or as correction factor for deviation the from hard sphere model. The values of the collision integral depend on the potential energy profile obtained from Lennard Jones (6-12) potential. The entire temperature dependence can be given by the equation

$$D_{AB} \propto \left(\frac{T^{3/2}}{\Omega(T)} \right) \tag{2.107}$$

According to Marrero et al. [58] the term $\frac{d \ln \Omega_D}{d \ln T}$ varies from 0 to -1/2, thus D_{AB} varies as $T^{3/2}$ to T^2 which is quite reasonable value when Fuller et al. correlation which gave the least errors is considered as $D_{AB} \propto T^{1.75}$ and this was also found experimentally. The temperature exponent first increases and then decreases [61, 73] indicates that the correlation with constant exponent would be limited in the range of applicability or in other words estimation using correlation should be done in the temperature range near to those used in experimental determination of collision integral.

2.6.5 Pressure dependence of diffusion coefficient

D_{AB} should vary inversely with pressure as shown by equation (2.78). The product D_{AB} P in low pressure region is nearly constant as density "n" is directly proportional to pressure in low pressure region [64]. Since molecular collision governs the rate of mass transport. For gasses under ordinary condition of moderate temperature and pressure only binary collision are important and molecular flux is independent of pressure for binary collision as molecular flux is directly proportional to concentration / number density (number of molecules / volume) and number of molecules that retard the flux by collision is also proportional to number density. Thus the two effects counter each other. But at high pressure the product of D_{AB} P or D_{AB} ρ is no longer constant but decrease with increase in pressure because of gas non idealities with their associated effect on system comes into play.

2.6.5 Dependence of diffusion coefficient on nature of carrier gas

The diffusion coefficient depends upon on the intermolecular forces. Therefore, the diffusion coefficients of the substance should not be same in the two different gases. In general the diffusion coefficient should increase with decreasing molecular weight of the carrier gas. The diffusion coefficient of a substance into argon, oxygen, nitrogen and hydrogen increases in the same order [86]. But it has been observed that the diffusion coefficient of the substances in air, nitrogen and oxygen is nearly same. For air and N_2,

the binary gaseous diffiusion coefficient is almost the same as air consist of about 80% N_2 and rest oxygen and the molecular weight of O_2 and N_2 donot differ much. It is found to vary within 2.5% of the observed value [73,76,91] and thus the reduced molecular weight M_{AB} plays a vital role in the determination of diffusion coefficient along with the intermolecular forces.

CHAPTER 3

EXPERIMENTAL MATERIAL AND METHOD

3.1 Experimental material

In this study three categories of substances were studied for their thermal stability, vapor pressure and diffusion coefficient measurements.

3.1.1 Commercially available precursors

The first category includes commercially available substances which are

1. Metal β-diketonates – metal acetylacetonates [$M(acac)_n$] and Metal 2,2,6,6-tetramethyl-3,5-heptandionate [$M(tmhd)_n$].
2. Metal cyclopentadienyl compounds [$M(cp)_n$].

Substances under this category were obtained from different companies with a minimum purity of 99 %, and were in general used as such without further purification but in some of the cases the substance were purified by sublimation and then used further. A list of commercially available substances which were studied is given in table 1.

Substance	**Chemical formula**	**Company**	**Purity**	**Molecular weight**
Metal acetylacetonate / Metal 2,4-pentanedionato/[M ($C_5H_70_2$)$_n$]				
1. Aluminium (III) acetylacetonate	[Al $(acac)_3$]	ABCR GmBH.	99%	324.30
2. Chromium (III) acetylacetonate	[$Cr(acac)_3$]	Merck	>98%	349.32
3. Iron (III) acetylacetonate	[$Fe(acac)_3$]	Merck	99%	353.17
4. Thulium (III) acetylacetonate	[$Tm(acac)_3$]	Alfa Aesar	99.99%	426.42
5. Manganese(III) acetylacetonate	[$Mn(acac)_3$]	Alfa Aesar	99%	352.26

6. Ruthenium (III) acetylacetonate	$[Ru(acac)_3]$	ABCR GmBH.	99%	398.39
7. Vanadium(III) acetylacetonate	$[V(acac)_3]$	Alfa Aesar	97%	348.26
8. Dysprosium(III) acetylacetonate	$[Dy(acac)_3]$	Alfa Aesar	99.9%	459.82
9. Zinc (II) acetylacetonate	$[Zn(acac)_2]$	ABCR GmBH	98%	281.61
10. Copper (II) acetylacetonate	$[Cu(acac)_2]$	Aldrich	99.99%	261.76
11. Nickel (II) acetylacetonate	$[Ni(acac)_2]$	Merck	>98%	256.90
Metal 2,2,6,6-tetramethyl-3,5-heptandionate / Metal dipivaloylmethane/$[M(C_{11}H_{19}0_2)_n]$				
1. Iron (III) 2,2,6,6-tetramethyl-3,5-heptandionate	$[Fe(tmhd)_3]$	ABCR GmBH	99%	605.66
2. Manganese (III) 2,2,6,6-tetramethyl-3,5-heptandionate	$[Mn(tmhd)_3]$	ABCR GmBH	99%	604.74
3. Aluminium (III) 2,2,6,6-tetramethyl-3,5-heptandionate	$[Al(tmhd)_3]$	Strem	99%	576.80
4.Chromium (III) 2,2,6,6-tetramethyl-3,5-heptandionate	$[Cr(tmhd)_3]$	Strem	99%	601.82
5. Europium (III) 2,2,6,6-tetramethyl-3,5-heptandionate	$[Eu(tmhd)_3]$	ABCR GmBH	99.99%	701.78
6. Nickel (II) 2,2,6,6-tetramethyl-3,5-heptandionate	$[Ni(tmhd)_2]$	ABCR GmBH	98%	425.13

7. Copper (II) 2,2,6,6-tetramethyl-3,5-heptandionate	$[Cu(tmhd)_2]$	Strem	99%	430.05
Metal Cyclopentadienyl/ $[M(C_5H_5)_n]$				
1. Nickelocene	$[Ni(cp)_2]$	ABCR GmBH	99%	188.90
2. Ruthenocene	$[Ru(cp)_2]$	Lab synthesized		231.26

Table 3.1: **Commercially available precursors.**

3.1.2 Non Commercial or lab synthesized precursors

The second category includes the precursors which were synthesized by different research groups in their laboratory and have been used as CVD precursors for the deposition process [92-97]. These are classified as

1. **Hafnium (Hf) and Zirconium (Zr) precursors:** These new precursors were synthesized by the research group of **Prof. Dr. Anjana Devi (**Ruhr-Universität Bochum). These precursors find their use in the manufacture of complementary metal oxide semiconductor devices. HfO_2 and ZrO_2 due to their high dielectric constant are considered to be ideal candidates for replacing SiO_2 which had the disadvantage of high leakage currents. These new precursors were needed due to some drawbacks associated with the existing classes of precursors (halides, alkoxides, amides and metal β-diketonates) such as high deposition temperature, decomposition during evaporation, corrosive by-products and high air and moisture sensitivity.
2. **Precursors for Gallium antimonide (GaSb) films:** The single source precursor for GaSb film has been developed by the research group of **Prof. Dr. Stephan Schulz (**Universität Paderborn). GaSb films find applications in thermovolatic and optoelectronic devices operating in infrared regime. For depositing GaSb films using MOCVD process GaR_3 (R = CH_3 or C_2H_6) and SbH_3 are used as precursors. Problems of high decomposition temperature of the precursors and maintaining

optimum V/III molar ratio for good quality films are encountered on using these precursors. These problems can be resolved by using single source precursors.

3. **Ruthenium (Ru) precursors:** These new precursors were synthesized by the research groups of **Prof. Dr. Ulrich Zenneck** (Universität Erlangen-Nürnberg) and **Prof. Dr. Heinrich Lang** (Technische Universität Chemnitz). Ruthenium thin films found use as a catalyst for various hydrogenation reactions in the industrial chemistry and in the production of fine chemicals. Apart from their use as a catalyst, they also find application in the manufacture of integrated circuits. Several ruthenium precursors like $[Ru(cp)_2]$, $[Ru(acac)_3$ and $[Ru(tmhd)_3]$ have been successfully used for depositing Ru and RuO_2 thin films. The main disadvantage associated with these classes of compound is high carbon contamination of the film which is not desirable both for microelectronic applications and catalysis. The new lab synthesized Ru precursors intended to serve as a source for producing ruthenium films with minimal carbon contamination at moderate temperatures.
4. **Tungsten (W) precursors:** These new precursors were synthesized by the research group of **Prof. Dr. Ulrich Zenneck** (Universität Erlangen-Nürnberg) to over come the problem purity of the film and high deposition temperature associated with other organometallic tungsten precursors.
5. **Zinc (Zn) precursor:** Thin films of zinc oxide (ZnO) have a number of applications as solar cell, gas sensor and semiconductor material. Unfortunately, there are some drawbacks with the existing precursors (halides, alkoxides, and metal β-diketonates) such as high evaporation and deposition temperature, decomposition during evaporation, and high air and moisture sensitivity. This precursor was synthesized by the research group of **Prof. Dr. Matthias Driess** (Technische Universität Berlin) has the advantages of being accessebile in multigram scale and can be handled in air.
6. **Copper (Cu) precursor:** Copper precursor was synthesized by the research group of **Prof. Dr. Heinrich Lang** (Technische Universität Chemnitz) for deposition of thin copper films at low deposition temperatures.

A list of lab synthesized precursors which were studied is given in table 3.

Research Group	Precursor
1**. Prof . Dr. Anjana Devi** AG Chemie Anorganischer Materialien, Lehrstuhl für Anorganische Chemie II, Ruhr-Universität Bochum, Bochum , Germany.	1. $Zr(NEt_2)_2$ (di-*ter*-butylmalonate) $_2$ $[Zr(N(C_2H_5)_2)_2$ $((C_4H_9)_2(C_3H_2O_4))]$ 2. $Hf(NEt_2)_2$ (di-*ter*-butylmalonate) $_2$ $[Zr(N(C_2H_5)_2)_2$ $((C_4H_9)_2(C_3H_2O_4))]$ 3. $Hf(NEt_2)_2$ (deguan) $_2$ $[Hf\{\eta^2\text{-}(^iPrN)_2CN(C_2H_5)_2\}_2(N(C_2H_5)_2)_2]$
2**. Prof. Dr. Stephan Schulz** Department Chemie, Universität Paderborn, Paderborn, Germany (Presently at Universität Duisburg-Essen)	1. $[t\text{-}(C_4H_9)_2GaSb(C_2H_5)_2]_2$ 2. $[t\text{-}(C_4H_9)_2GaSb(C_3H_7)_2]_2$ 3. $[t\text{-}(CH_3)_2GaSb(CH_3)_2]_2$ 4. $[t\text{-}(C_4H_9)_2GaSb(CH_3)_2]_2$
3. **Prof. Dr. Ulrich Zenneck** Institut für Anorganische Chemie Universität Erlangen-Nürnberg Erlangen, Germany	1. [Ru (Benzene) (Isoprene)] $[Ru\ (C_6H_6)\ (C_5H_8)]$ 2. [Ru (Benzene) (2, 3-dimethyl butadiene)] $[Ru\ (C_6H_6)\ (C_6H_{10})]$ 3. [Ru (Benzene) (1, 3-Cyclohexadiene)] $[Ru\ (C_6H_6)\ (C_6H_8)]$ 4. [Ru (Toluene) (1, 3-Cyclohexadiene)] $[Ru\ (C_7H_8)\ (C_6H_8)]$ 5. [Ru (Toluene) (2,3-dimethyl1,3 butadiene)] $[Ru\ (C_7H_8)\ (C_6H_{10})]$ 6. Cis [W (1, 3 Cyclohexadiene) $_2(CO)_2$] $[W\ (C_6H_8)_2(CO)_2]$ 7. Cis& trans [W (1, 3 Cyclohexadiene)$_2(CO)_2$]
4. **Prof. Dr. Heinrich Lang** Insitut für Chemie, Lehrstuhl für Anorganische Chemie, Technische Universität Chemnitz, Chemnitz , Germany	1. $[(n\text{-}C_4H_9)_3P)_2Cu(acac)]$ 2. Bis(dimethylpentadienyl)ruthenium(II) $[Ru\ (C_7H_{11})_2]$ 3. (Cyclopentadienyl)- (3-((dimethylamino)methyl)cyclopenta-1,4-dienyl)ruthenium(II) $[Ru(cp)(cpCH_2N(CH_3)_2)]$ 4. Bis((methyloxopentenyl)ruthenium(II) $[Ru(0C_6H_9)_2]$

5. **Prof. Dr. Matthias Driess** Institut für Chemie, Technische Universität Berlin, Berlin, Germany.	1. Methylzinc isopropoxide $[(CH_3)Zn(OCH(CH_3)_2)]$

Table 3.2: Lab synthesized compounds.

3.1.3 Polyaromatic hydrocarbons

The third category includes polyaromatic hydrocarbons. These were obtained from different companies with a minimum purity of 99 %, and were in general used as such without further purification. These compounds are also recommended as a reference compound for vapor pressure measurements. These are given in table 4.

Polyaromatic organic compound				
1. Anthracene	$C_{14}H_{10}$	Alfa Aesar	99%	178.23
2. Pyrene	$C_{16}H_{10}$	Alfa Aesar	99%	202.25

Table 3.3: Polyaromatic hydrocarbon.

Since most of the studied substances were sensitive to atmospheric air and moisture and tends to degrade when left open to atmosphere. This typical problem was not paid attention in most of the previous studies resulting in discrepancies within the published results. To overcome this problem an arrangement was made to keep the TGA apparatus in the glove box so as to avoid the exposure of the substance during measurements and also for storing the substances. The Knudsen cell for vapor pressure measurements was also filled in a glove box.

3.2 Experimental setup and procedure

3.2.1 Vapor pressure measurement

The vapor pressure measurements were done using the Knudsen effusion method. The experimental setup includes a Knudsen cell (shown in figure 3.1), two Pt100 thermometers, a heating chamber, a cooling trap, a diffusion pump, a pre-vacuum pump, a pressure sensor and the display and operating unit.

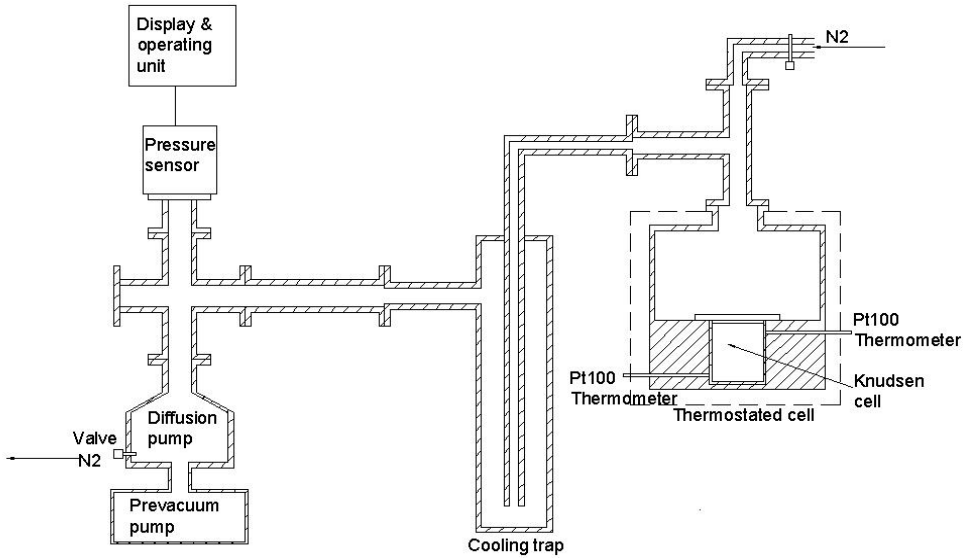

Figure 3.1: Experimental setup for measuring the vapor pressure.

The Knudsen cell is home built from stainless steel having a diameter 12 mm and height 28 mm. The upper lid of the Knudsen cell has a central hole with diameter 9 mm. The upper lid is covered with a thin aluminium foil and a small circular effusion hole was drilled on the foil. The lid together with the foil was well tightened with screws, so that the system remains vacuum tight.

The Knudsen cell is situated in a stainless steel vessel, also known as a heating and vacuum chamber, with good thermal contact around the cell. The heating wires were wrapped around up to the top of the heating chamber which acts as a thermal reservoir. The heating chamber was well insulated by using the glass wool and insulating bands. The temperature was measured using two pre-calibrated Pt100 thermometers inside the heating chamber around the area where the Knudsen cell was placed. The temperature difference between the two thermometers was found to be ±0.02K. This value is acceptable within the experimental error limits. Temperature inside the Knudsen cell was measured in order

to determine the temperature at which the vapor effuses out from the orifice and it was taken as the measurement temperature. This was necessary as there was always a difference between the temperature inside Knudsen cell and heating cell.

The Knudsen cell is evacuated with the help of a vacuum system consisting of a turbo molecular pump (Pfeifer TMH 071P), a pre vacuum pump (diaphragm backing pump, Pfeifer MVP 055-3) and a pressure gauge (Pfeifer TPG 261). The experimental setup is shown in figure 3.1. The pressure in the system was always below 10^{-5} mbar during each experimental run. A well defined amount of the substance (depending upon the temperature of the measurement and the substance) was weighed (accuracy: 0.05mg) into the cell. The cell was then tightened and put into the vacuum chamber. The inlet and outlet for the nitrogen gas were opened during the heating to allow its circulation in the heating chamber. The nitrogen supply was turned off and the inlet and the outlet valves were closed before the evacuation of the heating chamber.

Enough time (at least 60 minutes) was allowed for the attainment of a constant temperature which was recorded with the help of a calibrated Pt-100 thermometer. After evacuating the vacuum chamber the time was measured between the time when the vacuum reached the pressure of around 10^{-3} mbar and the time when the high vacuum pump was turned off and the pressure was above 10^{-3} mbar. Typical times were 1-5 hours, sometimes even longer depending upon the vapor pressure of the substance (in this time the weight losses were between 4 and 100 mg depending on the size of the hole, the temperature and the substance). The cell was then brought to room temperature in a desiccator and weighed again. The uncertainties in the evaporation time and in the mass loss are estimated to be 0.5 minutes and 0.05 mg, respectively. In the evaluation of the data, no additional calibration was performed. The vapor pressure was measured with Knudsen cell in the range of 0.01-25 Pa. The maximum overall uncertainty in vapor pressure measurements was estimated to be ± 0.1 to ± 0.5 Pa in the pressure range 10-25 Pa and ± 0.002 to ± 0.1 Pa in the pressure range 0.01-10 Pa.

A cooling trap was introduced between the heating chamber and the vacuum system to ensure that whatever substance evaporates during the experiment condenses inside the cooling trap, which would help in maintaining high level of vacuum during the experiment and preventing degradation of the vacuum pump.

An arrangement for circulating the nitrogen gas was made in the experimental setup. This was done in order to prevent the degradation of substances by atmospheric air and

moisture during the heating period. This was done by making an inlet at the top of heating cell for introducing the nitrogen into the experimental setup and outlet through a valve in the diffusion pump. Thus circulation of nitrogen was ensured during the heating period. To account for the amount of the substance which might have evaporated through the orifice during the heating period, the substance was kept inside the Knudsen cell and heated for 1 hour and the cooled to room temperature. This procedure was repeated for different temperature and every time it was found that whatever mass loss occurred was within the error limit of the weighing balance (0.05 mg).

Before using the foil, the diameter of the orifice was measured with the help a microscope.The photograph of a typical foil orifice is shown in figure 3.2. Five different orifice sizes were used throughout the experiment. The diameters of the orifice in aluminium foils were 0.4mm, 0.5mm, 0.6mm, 0.7mm, and 0.8mm.

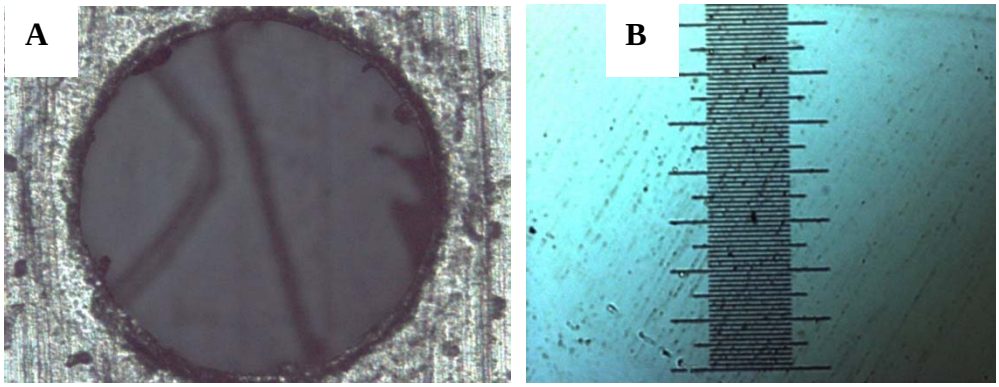

Figure 3.2: Microscopic photograph of one effusion hole (A) and scale (B).

The reason for using the foils with different orifice diameters for the experiments is to control the mass loss of the substance through the orifice. Smaller orifice limits the mass loss of the substance. This is useful when a substance with high vapor pressure especially at high temperature shall be studied. Larger orifice allow more mass loss through the orifice and are useful for substances with low vapor pressure or when measuring at low temperature. The thickness of the foil was 70µm. From the ratio of the diameter of the orifice to the thickness of the aluminium foil, the Clausing factor for the four aluminium foils was calculated with equation (3.1) as

$$K = 1 - 0.5\left(\frac{l}{r}\right) + 0.2\left(\frac{l}{r}\right)^2 \qquad (3.1)$$

The values for Clausing correction factor are given in Appendix A (Table A1). The system was first checked by measuring the vapor pressure of two reference substances, anthracene and pyrene. For this the mass of the substances evaporated in a definite time was measured and the vapor pressures were calculated using equation (2.10). For anthracene, the measurements were performed in the temperature range 339 K-399 K and for pyrene in the temperature range 341 K-418 K. The details of the measurement are given in Appendix A (Table A2 – A3) and the results are compared with the available literature values (discussed in the result and disscussion section). It is found that the measured values for both of these reference substances agree very well with the literature values throughout the temperature range studied. The setup provides reliable vapor pressure values and is therefore, used for measuring the vapor pressure of other substances. The experimental vapor pressures along with the experimental parameters for other substances are given in Appendix A (Table A4-A21).

The vapor pressure values at different temperatures were fitted to an Antoine type expression, with pressures *P* in *kPa* and temperature *T* in *K*:

$$\log(P/kPa) = A - \frac{B}{(T/K)} \qquad (3.2)$$

where, A, and B are the Antoine constants. The two coefficients A and B were found to represent the vapor pressure data within the experimental accuracy. The coefficients A and B along with the uncertainites are enlisted in Appendix B (Table B1).Some literature values for the enthaply of sublimation for the studied substances are also given in Appendix B (Table B1). For the laboratory synthesized precursor the uncertainites associated with the coefficients A and B are large due to less number of the experimental data points. The molar enthalpy of sublimation was calculated by plotting ln P (P in Pa) against $1/T$ (T in K) and determining the best fit slope $-\frac{\Delta H_{sub}}{R}$. On rearranging the equation (3.2), the enthalpy of sublimation (kJ · mol^{-1}) can be calculated using the relation

$$\Delta H_{Vap/Sub} = 2.303 \times R \times B \qquad (3.3)$$

where R is the universal gas constant (kJ·K^{-1}·mol^{-1}) and B is the Antoine equation constant.

3.2.2 Thermogravimetry

A commercial TGA/DTA (Bähr STA 503) was used to perform the thermogravimetric experiments. The atmosphere was nitrogen or helium. The flow rate of 100cm^3/min (for nitrogen) was controlled by a calibrated mass flow controller. This flow rate was found to be sufficient to ensure that the concentration of substance at the top of the crucible remains nearly zero throughout the measurement as proved experimentally: a change in flow rate did not change the mass loss rate measurably [41]. The pressure was throughout atmospheric. Open alumina crucibles were used in all experiments; the inner diameter being 5.35 mm, the inner height is 7.2 mm. The temperature sensor was calibrated by measuring the melting points of reference substances (4-nitrotoluene, naphthalene, indium and potassium perchlorate) which cover the whole temperature range for the measurements. The samples were filled inside the crucible, for diffusion coefficient experiments the initial height of the sample inside the crucible was between 3.0 and 5.0 mm. From the initial height, which was measured in the beginning of each experiment with an estimated accuracy of ± 0.2 mm, the volume of the sample was calculated. Using the initial mass the apparent density of the sample was derived. The gaseous diffusion coefficient in helium and nitrogen atmosphere was calculated using the equation (2.106). The uncertainty in mass loss rate was estimated to be ± 5% and ± 10% for the apparent density and for the diffusion coefficient ± 0.005 to ± 0.05cm$^2 \cdot$ s^{-1} depending on the system and arising mainly from the uncertainties in the initial distance between the sample surface and the top of the crucible. The mean of the measured value of gaseous diffusion coefficient of at least three experiments are given in Appendix A (Table A23-A26). The gasesous diffusion coefficient values at different temperatures were fitted to an expression represented as

$$D_{AB}(cm^2 s^{-1}) = A \times T^n \qquad (3.4)$$

where T is the temperature in Kelvin. The constants A and n are listed in Appendix B (Table B2).

3.2.2.1 Temperature programme

The types of temperature programme used in thermogravimetric experiment are shown in figure 3.3

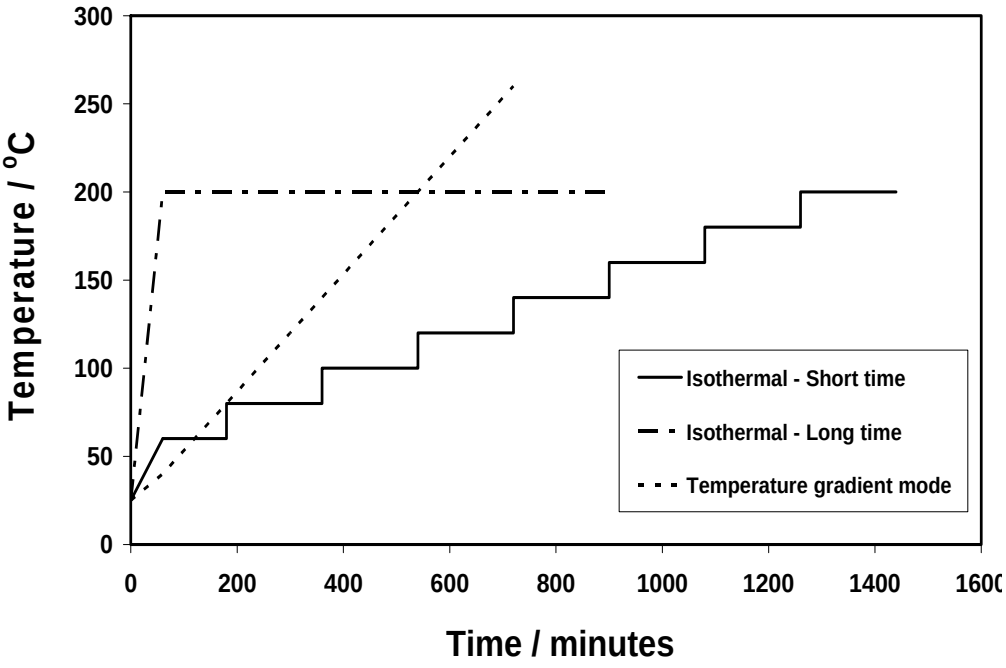

Figure 3.3: Types of temperature programme used in TGA.

For thermal stability measurements the experiments were performed using two types of temperature programme. In the beginning the experiments were performed using non isothermal temperature programme in which the temperature was raised linearly with a heating rate of 2K/ minute up to 500°C, and the mass loss of the substance with time and temperature was observed along with the DTA signal. This temperature programme provides the information regarding the sublimation temperature (defining the lower limit for its CVD application), melting point and first hand information regarding thermal stability. If the mass loss with time is not constant i.e. evaporation proceeds in multi steps and also when the substance leaves a considerable amount of residue, then it means that the evaporation might be accompanying with the decomposition of the substance. Generally a sharp endothermic peak from the DTA signal is the indication of melting point of the sample where as exothermic/ endothermic peaks corresponds to the decomposition of the substance. The experiment in non isothermal mode cannot provide reliable data regarding long time thermal stability as the temperature is raised at a linear rate and hence fails to detect decomposition process which is both time and temperature dependent. If the substance is not found to be stable i.e. mass loss occurrs in several / more than one steps,

no further experiments were performed but if it is stable, then it is subjected to a isothermal temperature programme in which the substance is held isothermally for long periods of time, in some experiments until all the sample was evaporated in order to determine its long time thermal stability. Again here the attention is being paid to amount of residue and linear curves. If the linear curves is obtained for mass loss versus time plot and substance evaporates without leaving any residue, (or if some residue is found, then it should be below 5%) it is then considered to be a thermally stable substance and used further for vapor pressure and diffusion coefficient measurements.

For diffusion coefficient measurement short time isothermal temperature program was used in which the temperature was changed after 2 hours to the next temperature, so that several temperatures could be investigated within one run.

CHAPTER 4

RESULT AND DISCUSSUIONS

4.1 Thermal stability using thermogravimetry

4.1.1 Metal acetylacetonates [$M(acac)_n$]

Thermograms in non isothermal and isothermal mode were used to study the thermal stability of acetylacetonetes of aluminium, chromium, iron, thulium, manganese, ruthenium, vanadium, dysprosium, zinc, copper and nickel. The thermograms in non isothermal mode are shown in figure 4.1 and 4.2. Figure 4.1 represent the thermograms for [$Al(acac)_3$], [$Cr(acac)_3$], [$Ru(acac)_3$], and [$Cu(acac)_2$] which were found to evaporate in a single step process without leaving any residue. Similar observation for [$Al(acac)_3$], [$Cr(acac)_3$], was also made by Beech and Lintonbon [98], for [$Cu(acac)_2$] Beech and Lintonbon [98] reported a residue of 10 % where as a residue less than 5 % was reported by Pauleau and Fasasi [99]. Lashdaf et al. [100] found [$Ru(acac)_3$] evaporating in multi steps and leaving a residue of 65% in inert nitrogen atmosphere, this discrepancy could be attributed to the impure sample as sample was synthesized in the lab, having some water content which was removed prior to mass spectrometric measurement. Presence of water was confirmed by multi steps evaporation process in their TG experiment and the sample purity was also not mentioned.

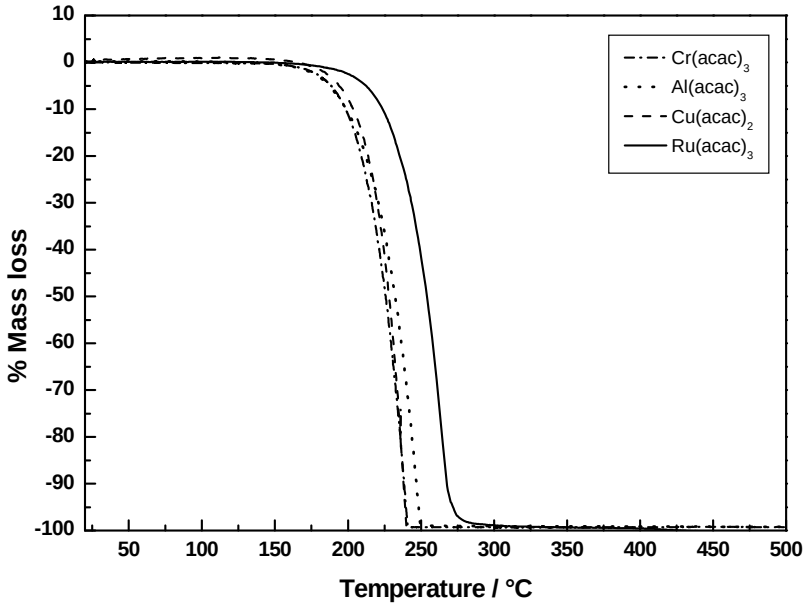

Figure 4.1: TG curve in non isothermal mode for [Cr(acac)$_3$], [Al(acac)$_3$], [Ru(acac)$_3$], & [Cu(acac)$_2$].

Figure 4.2 shows the thermograms for [Tm(acac)$_3$], [Zn(acac)$_2$], [Mn(acac)$_3$], [Ni(acac)$_2$], [Fe(acac)$_3$], and [Dy(acac)$_3$] which were found to evaporate in a multi step except for Fe(acac)$_3$ and leaving a considerable amount of residue in each case. From the findings it is concluded that these substances are not thermally stable.

For [Fe(acac)$_3$] our experiment showed a single step evaporation process with a residual of around 8 %. The presence of residual indicates that the evaporation is accompanied by a decomposition process. Beech and Lintonbon [98] found about 8.8% residual mass even at temperatures below 261°C. Varnek et al. [101] analysed the nature of volatility of iron compounds from Mössbauer data and reported only about 90% mass loss for [Fe(acac)$_3$]. Around 20% residual mass was obtained in the study of Li et al. [102].

For [Mn(acac)$_3$] Beech and Lintonbon [98] found about 77 % residual mass on heating upto the temperature of 177°C. Similarly Li et al. [102] reported 55% residual mass and around 36% residual mass was found in this study on heating upto the temperature of 500°C for [Mn(acac)$_3$]. Decomposition of [Mn(acac)$_3$] was also reported by Murray and Hill [103].

[Ni(acac)$_2$] also shows decomposition indicated by multi step evaporation with residual mass around 24%. Li et al. [102] also reported decomposition for [Ni(acac)$_2$] with residual mass around 30%. Thermogram of [Zn(acac)$_2$] shows a two step evaporation process the first step indicates the removal of chemically associated water or

dehydration step and the second step indicates the evaporation of dehydrated [$Zn(acac)_2$]. The total mass loss reaches a value of 97% at the temperature of 500°C. Similar observation was also made by Arii and Kishi [104] for [$Zn(acac)_2$]. Both [$Tm(acac)_3$] and [$Dy(acac)_3$] leave more than 75% residue which is an indication of decomposition.

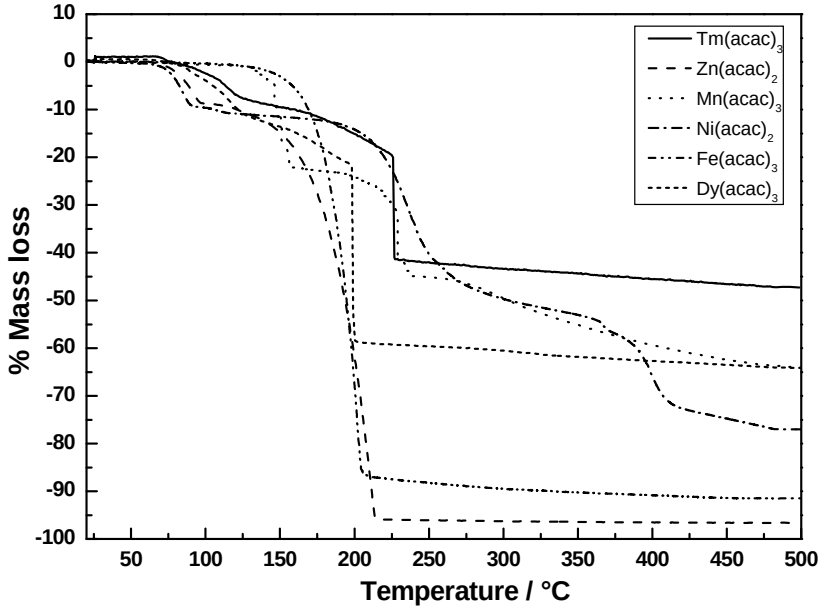

Figure 4.2: TG curve in non isothermal mode for [$Tm(acca)_3$], [$Zn(acca)_2$], [$Mn(acca)_3$], [$Ni(acac)_2$], [$Fe(acca)_3$] & [$Dy(acca)_3$].

As discussed earlier, investigation of thermal stability in non isothermal mode would not be useful especially in the case where evaporation proceeds in a single step but leaves behind some residue. Under this situation residue could be due to the decomposition of substance at higher temperatures. Therefore, for a more complete picture regarding thermal stability one should hold the substance isothermally for a long period of time at some desired temperature.

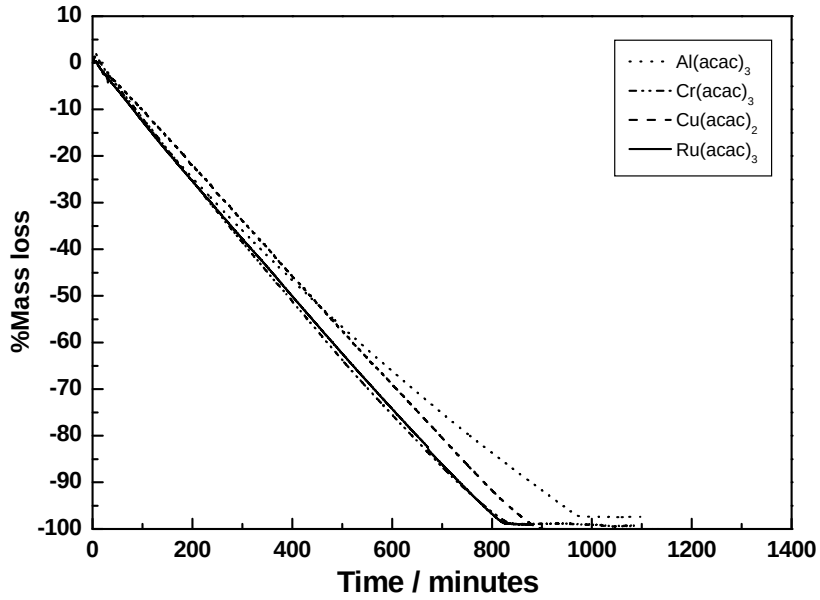

Figure 4.3: TG curve in isothermal mode for [Al(acac)$_3$], [Cr(acac)$_3$], [Cu(acac)$_2$] at 155°C & [Ru(acac)$_3$] at 174°C.

Figure 4.3 shows nearly linear curve for mass loss versus time plot isothermal curve for [Al(acac)$_3$], [Cr(acac)$_3$], [Cu(acac)$_2$] at the temperature of 155°C and for [Ru(acac)$_3$], the temperature was 174°C . All these acetylacetonates evaporate completely without leaving any residue indicating pure evaporation process.

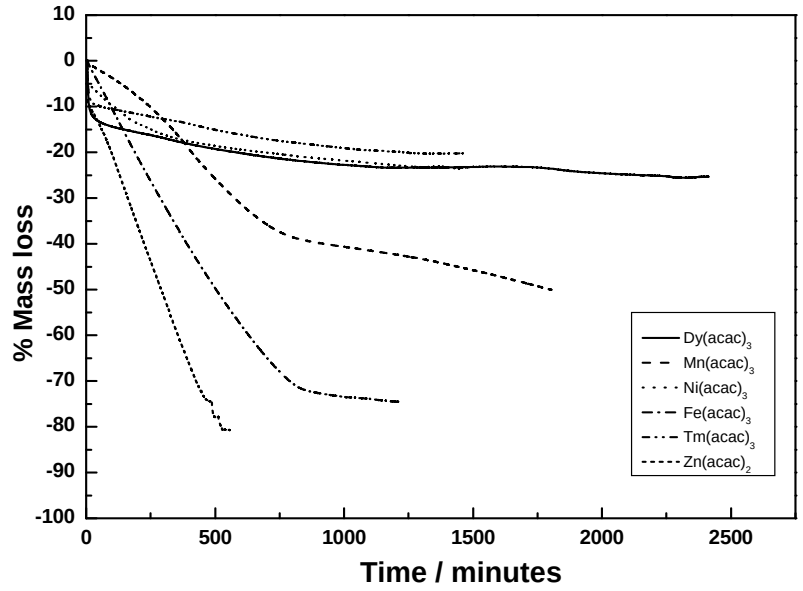

Figure 4.4: TG curve in isothermal mode for [Zn(acac)$_2$] at 95°C, [Mn(acac)$_3$] at 114.6°C, [Ni(acac)$_2$] at 175°C, [Fe (acac)$_3$] at 154°, [Tm(acac)$_3$] & [Dy(acac)$_3$] at 117°C.

The curves as shown in figure 4.4 for [Tm(acac)$_3$], [Zn(acac)$_3$], [Mn(acac)$_3$], [Fe(acac)$_3$], [V(acac)$_3$], [Ni(acac)$_2$], and [Dy(acac)$_3$] show a non linear mass loss curve, leaving behind a large amount of residue. For [Fe(acac)$_3$] at constant temperatures of 134.2°C and 154°C, residual masses of 32.3% and 25.5%, respectively, were observed, which indicate that the evaporation was accompanied by decomposition. This is shown in figure 4.4 for one temperature, 154°C. On the contrary Barron et al. reported that the [Fe(acac)$_3$] evaporated without leaving any residue and used it as a reference compound for determination of vapor pressure for various metal β-diketonates using TG method. The possible reason for the thermal instability of [Fe(acac)$_3$] may be that it is in polymerized form in the condensed phase, as no evidence of hydrolytic dissociation can be inferred from the TG curves both in isothermal and non isothermal mode which show no indication for the removal of some associated water. These polymerised compounds tend to decompose on heating [105]. The presence of residue in thermogravimetric measurement for [Fe(acac)$_3$] was also reported by many workers [98, 101, 102].

One can also see from the curves for [Ni(acac)$_2$], and [Mn(acac)$_3$], that even in the beginning the mass loss is not linear which indicates that the process is not exclusive evaporation of the precursor even at low temperatures. For [Mn(acac)$_3$] residual masses of 37.8%, 47.8% and 66.3% constant temperatures of 95.2°C, 114.6°C and 134.2°C were found. Hoene et al. [106] reported its decomposition around 170°C and Beech et al. [98] reported 41% residual mass in the temperature range 179°C – 262°C K. A typical evaporation curve, at 114.6°C is shown in Figure 1. Hosono et al. [107] studied the thermal decomposition behaviour of some zinc compounds and reported the decomposition of [Zn(acac)$_2$] below 200°C and our experimental results shows that it leaves about 20% residue on isothermal evaporation at 95 °C.

Self association in the condensed form is reported for [Ni(acac)$_2$] and [Zn(acac)$_2$] [108, 109]. These polymeric compounds have low volatility and are thermally dissociated when heated [105]. [Tm(acac)$_3$] and [Dy(acac)$_3$] leave more than 85% residue on isothermal evaporation at 117 °C. It seems that for both the compounds hydrolytic dissociation occurs as it is clear from the isotherms a rapid mass loss around 10-15 % within a short span of time is due to removal of some hygroscopic water. These hydrated compounds undergo hydrolytic dissociation on heating with the formation of involatile hydroxyl compounds [105].

4.1.2 Metal 2,2,6,6-tetramethyl-3,5-heptandionate [M(tmhd)$_n$]

TMHD of iron, manganese, aluminium, chromium, europium, nickel, and copper were studied for their thermal stability. These compounds were studied in isothermal mode and for all the compounds the mass loss versus time curve was found to be linear and substances evaporate completely without leaving any residue indicating exclusively evaporation process taking place as shown in figure 4.5 except for [Eu(tmhd)$_3$] which shows a residual mass of 30%. This indicate that for [Eu(tmhd)$_3$] evapoaration is accopained by the decomposition of the compound. The isothermal temperature for [Fe(tmhd)$_3$] and [Ni(tmhd)$_2$] was 155°C and for [Mn(tmhd)$_2$], [Al(tmhd)$_3$], [Eu(tmhd)$_3$] [Cr(tmhd)$_3$] and [Cu(tmhd)$_2$] was 174°C. Metal 2,2,6,6-tetramethyl-3,5-heptandionates show in general a better thermal stability than the corresponding metal acetylacetonates. It is likely that the replacement of end CH_3 in the acetylacetonates with a bulky tertiary butyl hydrocarbon group produces decrease in volatility due to the weakening of the intermolecular of van der Waals intereaction. It is also less susceptible to hydration and polymerization [105,110] possibly due to the steric hinderance generated by bulky subsituent groups.

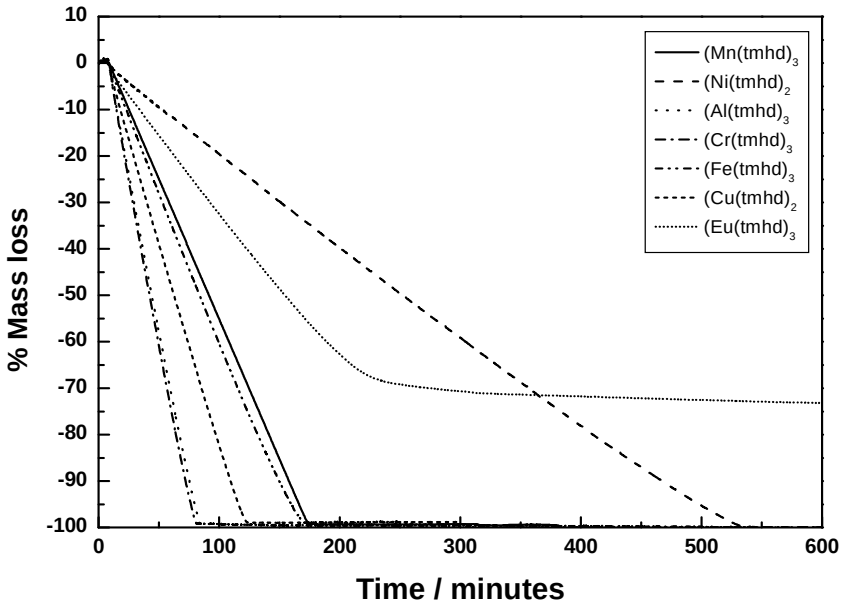

Figure 4.5: TG curve in isothermal mode for [Mn(tmhd)$_3$], [Al(tmhd)$_3$], [Cu(tmhd)$_2$], [Eu(tmhd)$_3$] & [Cr(tmhd)$_3$] at 174°C, [Fe(tmhd)$_3$] & [Ni(tmhd)$_2$] at 155°C.

4.1.3 Metallocene

Metallocene of nickel and ruthenium were investigated for their thermal stability by isothermal thermogravimetry. Thermograms from TGA are summarized in figure 4.6. Kang and Rhee [111] reported that no appreciable decomposition of $[Ni(cp)_2]$ occurs at 120 °C by holding $[Ni(cp)_2]$ isothermally in a sublimator and examining its gas phase IR spectra using a heated gas cell. Gas phase spectra at various temperatures were taken but the time factor was not taken into account. As decomposition is also a time dependent process, therefore, one should wait isothermally for some period of time after that one can only confirm whether decomposition is taking place or not. It is observed that the decomposition of $[Ni(cp)_2]$ can be detected at low temperature of 77°C as indicated by 18% residual mass and from the isothermal evaporation at 194 °C about 14% residue was found.

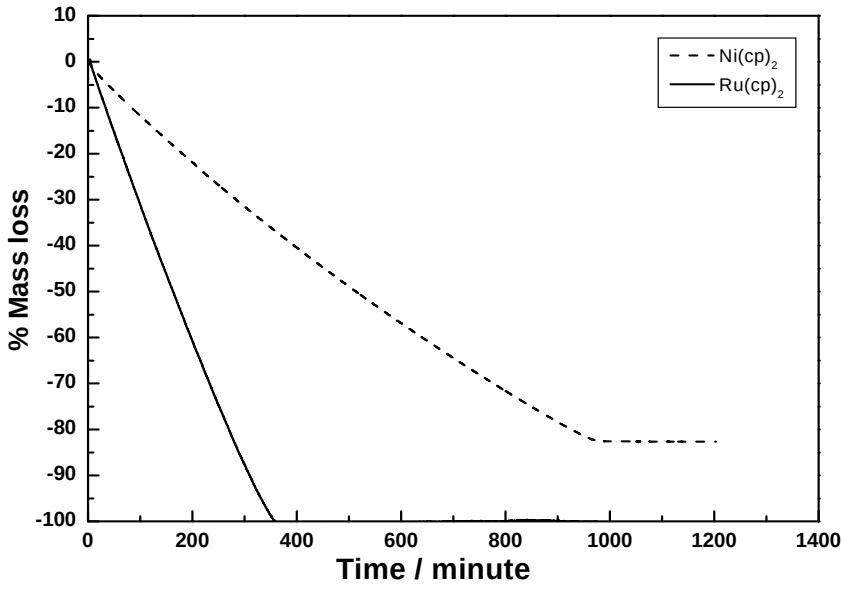

Figure 4.6: TG curve in isothermal mode for $[Ni(cp)_2]$ at 77°C and $[Ru(cp)_2]$ at 95°C.

If the isothermal experiments were for a short period of time, one could easily infer that it's a pure evaporation process (figure 4.7) where almost linear curve was obtained for short period of time i.e. 2 hours, however, the decomposition becomes only visible when the mass loss becomes constant after reaching a value 82 % after very long time which is around 15 hours at temperature of 77°C (see figure 4.6). On the other hand $[Ru(cp)_2]$ evaporate without leaving residuals indicating the pure evaporation of the compound without any decomposition.

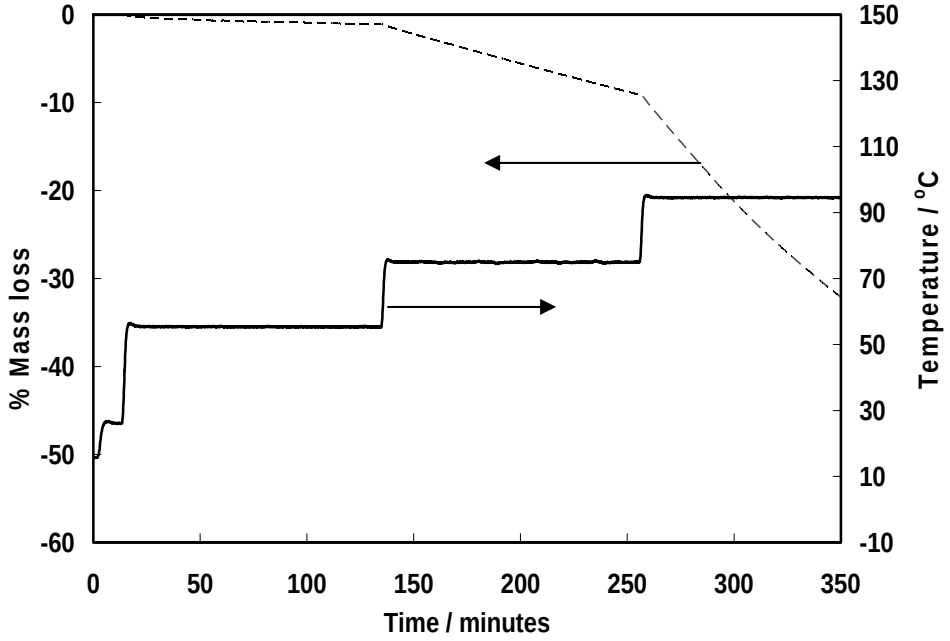

Figure 4.7: TG curve in short time isothermal mode for [Ni(cp)$_2$].

4.1.4 Lab synthesized precursors

1. Hafnium (Hf) and Zirconium (Zr) precursors

1. Zr(NEt$_2$)$_2$ (di-*ter*-butylmalonate)$_2$
2. Hf(NEt$_2$)$_2$ (di-*ter*-butylmalonate)$_2$
3. Hf(NEt$_2$)$_2$(deguan)$_2$

Isothermal TGA curve for these substances are shown in figure 4.8. Isothermal experiment for [Hf(NEt$_2$)$_2$(di-ter-butylmalonate)$_2$] at 116.2°C for 13 hours shows non linear curve indicating the decomposition is taking place with around 60.2% of the sample still remaining as residue. The TG curve from an isothermal TGA experiment for 20 hours at 95.8°C shows deviation from linearity with rapid decrease in mass for [Zr(NEt$_2$)$_2$(di-ter-butylmalonate)$_2$], which is a clear indication of decomposition taking place around 40% of the mass still remaining in the crucible. For [Hf(NEt$_2$)$_2$(deguan)$_2$] isothermal experiment at 58°C shows a nonlinear decrease in mass and attained a value of 64 % in about 4 hours and then remained constant indicating the decomposition of compound. All the precursors were found to be decomposing as indicated by TGA curves.

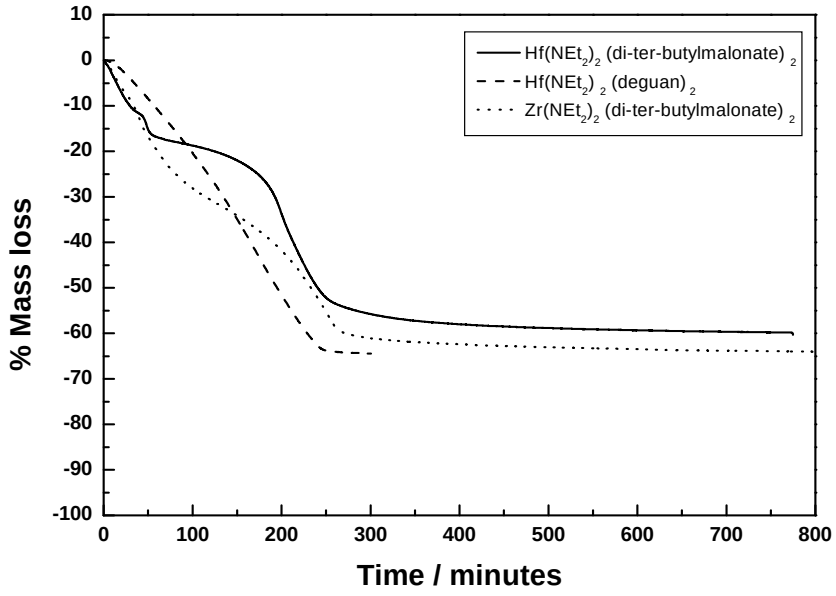

Figure 4.8: TG curve in isothermal mode for [Hf(NEt$_2$)$_2$(di-ter-butylmalonate)$_2$] at 116.2°C, [Zr(NEt$_2$)$_2$(di-ter-butylmalonate)$_2$] at 95.8°C, & [Hf(NEt$_2$)$_2$(deguan)$_2$] at 58°C.

2. Precursors for Gallium antimonide (GaSb) films:

1. [t- Bu$_2$GaSbEt$_2$]$_2$
2. [t- Bu$_2$GaSbPr$_2$]$_2$
3. [t- Me$_2$GaSbMe$_2$]$_2$
4. [t- Bu$_2$GaSbMe$_2$]$_2$

TGA curves for the above substances are shown in figure 4.9. For [t-Bu$_2$GaSbEt$_2$]$_2$ at about 40°C observable evaporation starts which later on proceed to a multi step evaporation processes around 150°C indicating the decomposition of compound. Around 80.7% mass loss was observed up to the temperature of 300 °C which then increased to 84% at 420°C (16% residual mass). A multi step evaporation process was observed for [t-Bu$_2$GaSbPr$_2$]$_2$ and [t-Me$_2$GaSbMe$_2$]$_2$ with 11% and 42% residual mass respectively at the temperature 500°C indicating the decomposition.

[t-Bu$_2$GaSbMe$_2$]$_2$ shows a two step evaporation process, the second step starts around the temperature of 150°C but the presence of 14% residue indicates that the decomposition might be taking place.

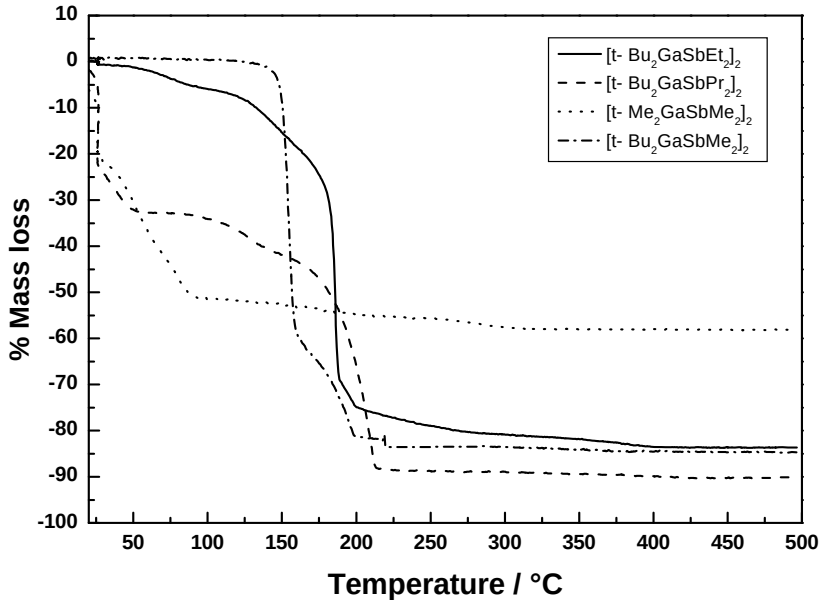

Figure 4.9: TG curve in non isothermal mode for (GaSb) complexes.

As shown in figure 4.9 for $[t\text{-}Bu_2GaSbEt_2]_2$ and $[t\text{-}Bu_2GaSbMe_2]_2$ TGA curves in non isothermal mode indicate that decomposition might not be accompanying evaporation at low temperatures. Therefore, isothermal experiment were done at the temperatures of 116.5°C for $[t\text{-}Bu_2GaSbEt_2]_2$ and 106.3°C for $[t\text{-}Bu_2GaSbMe_2]$ and the result are shown in figure 4.10.

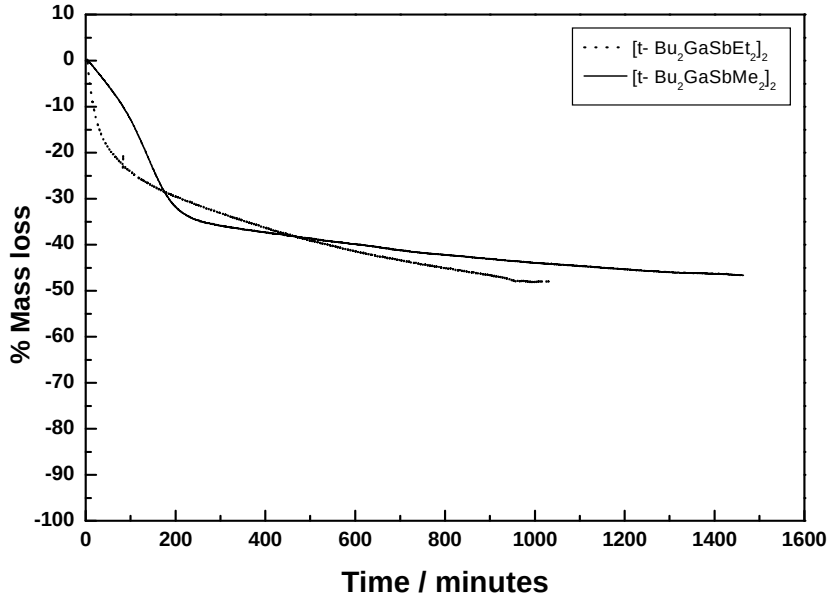

Figure 4.10: **TG curve in isothermal mode for $[t\text{-}Bu_2GaSbEt_2]_2$ at 116.5°C & $[t\text{-}Bu_2GaSbMe_2]_2$ at 106.3°C.**

Both substances show a nonlinear decrease in mass along with presence of large quantities of residue 52% and 56% for $[t\text{-}Bu_2GaSbEt_2]_2$ and $[t\text{-}Bu_2GaSbMe_2]_2$ respectively indicating the decomposition of the compound.

3. Ruthenium (Ru) precursors

1. [Ru (Benzene) (1, 3-Cyclohexadiene)]
2. [Ru (Benzene) (Isoprene)]
3. [Ru (Benzene) (2, 3-dimethyl butadiene)]
4. [Ru (Toluene) (1, 3-Cyclohexadiene)]
5. [Ru (Toluene) (2,3-dimethyl1,3 butadiene)]
6. [Ru $(C_7H_{11})_2$]
7. [Ru$(0C_6H_9)_2$]
8. [Ru(cp)(cp$CH_2N(CH_3)_2$)]

Figure 4.11 shows the TGA curves in non isothermal mode for the first three ruthenium complexes. For [Ru(Benzene) (1, 3-Cyclohexadiene)] a single step evaporation process is observed but the residual of around 9% was found after the temperature of 170°C which reduces to 3 % at higher temperature of 500°C indicating that decomposition might be taking place. The other two ruthenium complexes evaporate completely without leaving any residue.

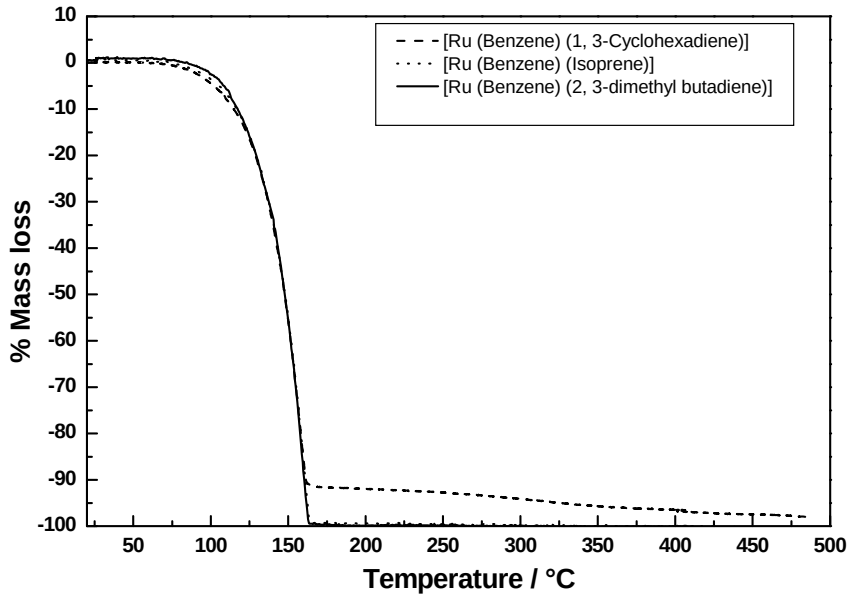

Figure 4.11: TG curve in non isothermal mode for Ru complexes.

The curves in isothermal mode are shown in figure 4.12.

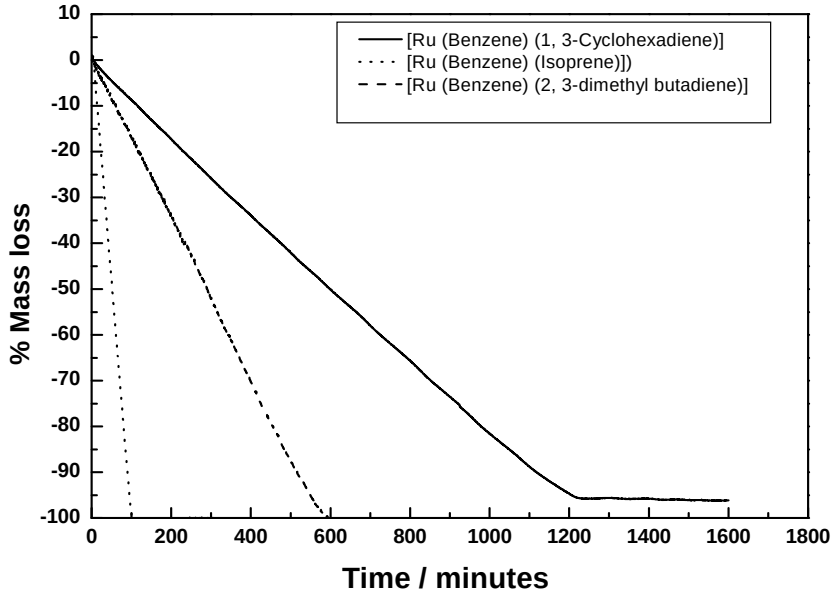

Figure 4.12: TG curve in isothermal mode for [Ru(Benzene) (1, 3-Cyclohexadiene)] at 97°C, [Ru (Benzene) (Isoprene)] at 96.5°C & [Ru (Benzene) (2, 3-dimethyl butadiene)] at 75.5°C.

For [Ru(Benzene) (1, 3-Cyclohexadiene)] a residual mass of 4% was found at 97°C. As the amount of residual mass was very less, therefore, it could be considered as thermally stable. [Ru (Benzene) (Isoprene)] and [Ru (Benzene) (2, 3-dimethyl butadiene)] were found to evaporate completely at 96.5°C and 75.5°C respectively.

The amount of [Ru (Toluene) (1, 3-Cyclohexadiene)] and [Ru (Toluene) (2,3-dimethyl1,3 butadiene)] available to us was very less in quantity, therefore, the thermogravimetric experiments were performed using stepwise isothermal temperature program at six temperatures between 56°C and 153°C keeping the sample at each temperature for two hours before going to the next temperature as shown in figure 4.13. [Ru (Toluene) (1, 3-Cyclohexadiene)] existed as liquid at room temperature and evaporate almost completely but [Ru (Toluene) (2,3-dimethyl1,3 butadiene)] leaves a residue of 8%, therefore, some isothermal experiment is needed to confirm its thermal stability.

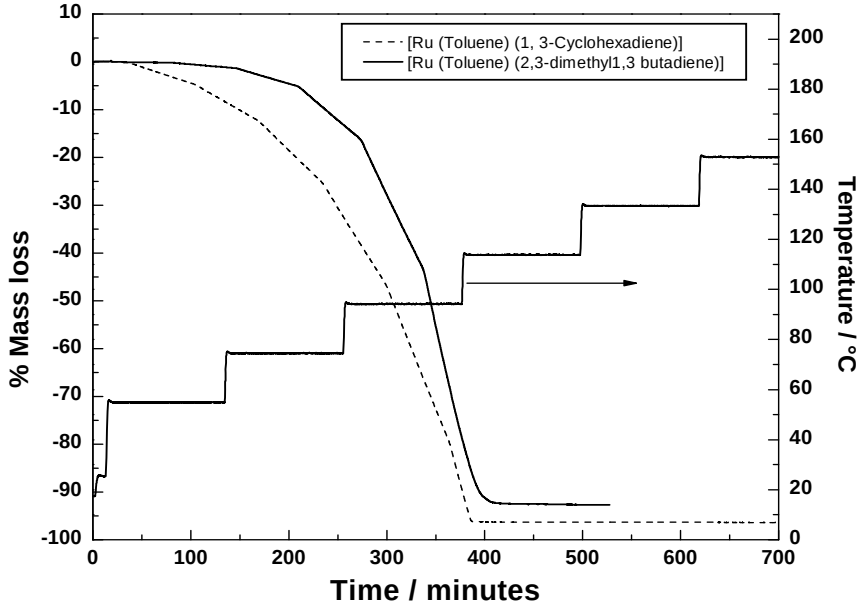

Figure 4.13: TG curve in short time isothermal mode for Ru complexes.

The experiments in long time isothermal mode for other ruthenium complexes viz. $[Ru(C_7H_{11})_2]$, $[Ru(0C_6H_9)_2]$ and $[Ru(cp)(cpCH_2N(CH_3)_2)]$ show a linear mass loss (see Figure 4.14). All the three precursors evaporate completely without leaving behind any residue or less than 2 % residue indicating that the clean evaporation is taking place (see Figure 4.14). The temperature for isothermal experiment in case of $[Ru(C_7H_{11})_2]$, $[Ru(Cp)(CpCH_2N(CH_3)_2)]$ was 95°C and for $[Ru(0C_6H_9)_2]$ it was 115°C.

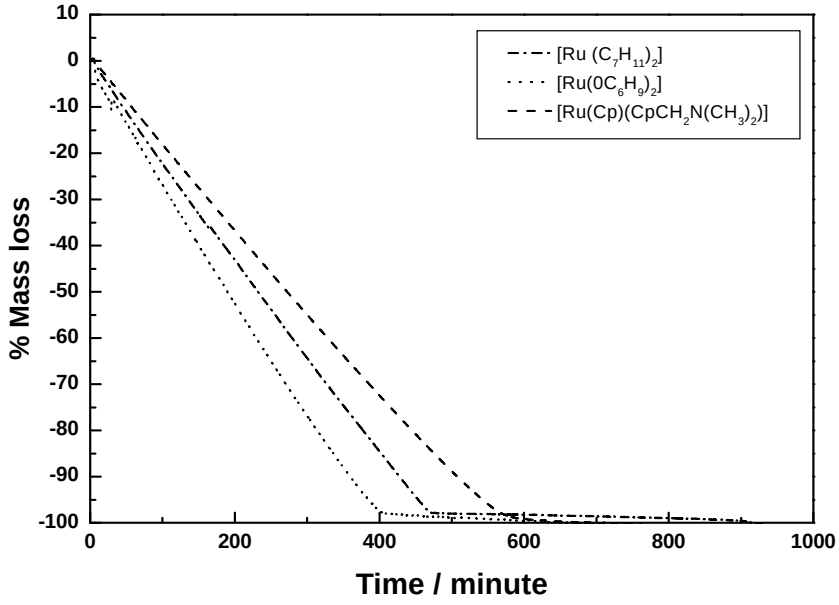

Figure 4.14: TG curve in isothermal mode for Ru complexes.

3. Tungsten (W) precursors

1. Cis [W (1, 3 Cyclohexadiene) $_2(CO)_2$]
2. Cis & trans [W (1, 3 Cyclohexadiene)$_2(CO)_2$]

Figure 4.15 shows the TGA curves in non isothermal mode for the above substances. For both tungsten complexes a single step evaporation process is observed but the residual around 35% was found upto the temperature of 500°C. Since curves in non isothermal shows a single step evapoartion process. It may be possible that decomposition is not accompanying evaporation at low temperatures. Therefore, isothermal experiments were done at the temperatures of 116.5°C and 106.3°C for both compounds and the result are shown in figure 4.15. The TGA curves in isothermal mode shows that both tungsten complexes leave appreciable amounts of residue. Therefore, they are not thermally stable as seen in figure 4.16.

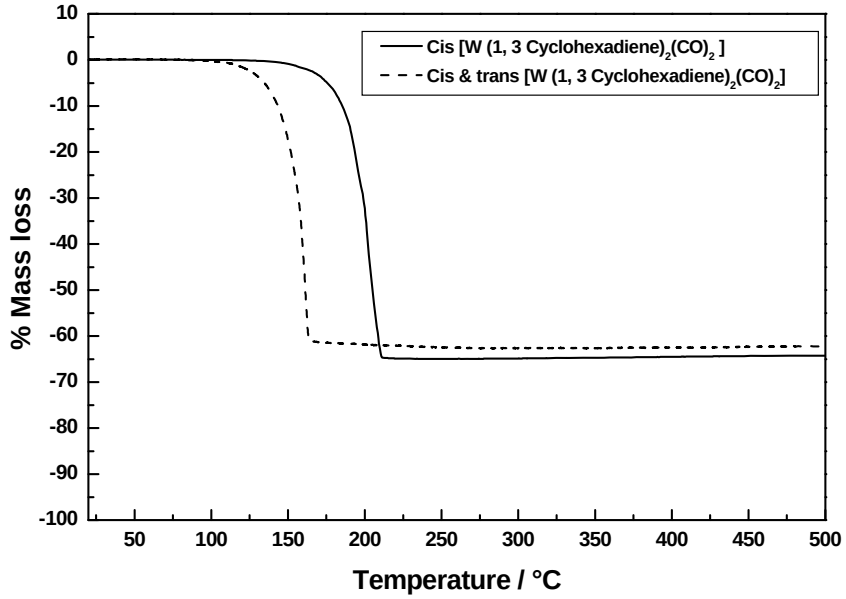

Figure 4.15: TG curve in non-isothermal mode for W complexes.

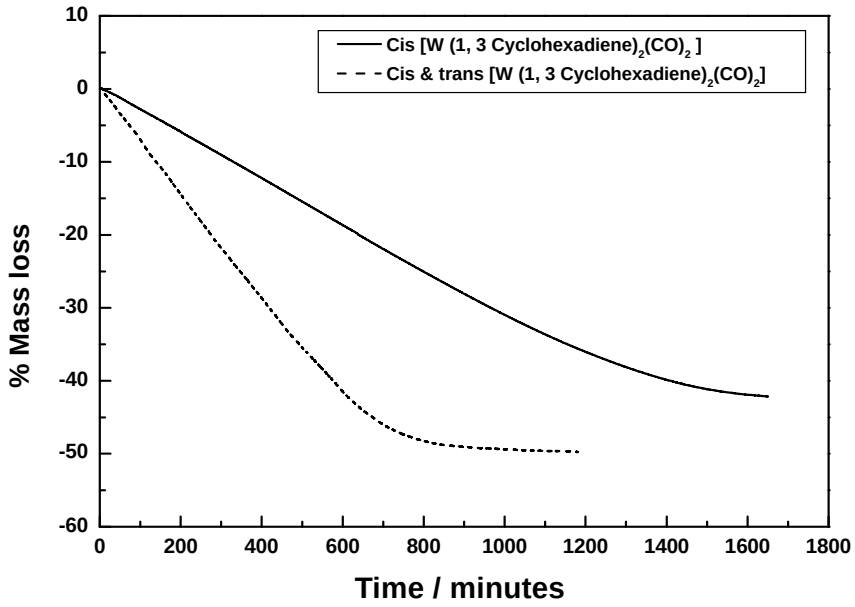

Figure 4.16: TG curve in isothermal mode for W complexes at 115.3°C.

5. Zinc (Zn) and Copper (Cu) precursor

1. Methylzinc isopropoxide
2. $[nBu_3P]_2Cu(acac)$

The isothermal TGA curve at 57°C for methylzinc isopropoxide show a linear curve up to 100 minutes and after that slope of the curve changes indicating certain decomposition. After 400 minutes, the mass loss becomes constant with around 65 % residual mass as shown in figure 4.17. For $[(nBu_3P)_2Cu(acac)]$ decomposition was noted due to the non linear mass loss curve and presence of around 10% residue at temperature of 96°C (see figure 4.17).

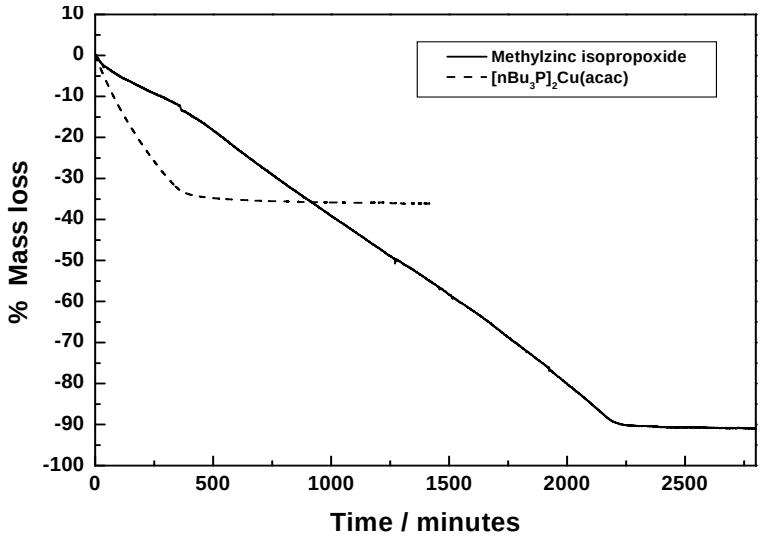

Figure 4.17: TG curve in isothermal mode for Methylzinc isopropoxide at 57°C & $[(nBu_3P)_2Cu(acac)]$ at 96°C.

4.2 Vapor pressure using the Knudsen effusion method
4.2.1 Polyaromatic hydrocarbon

Both anthracene and pyrene are recommended as a reference substance [112] for the measurement for the vapor pressures in the temperature range of 338 K-360 K and 350 K-420K respectively. These temperature ranges cover the pressure range between 0.1 Pa to 50 Pa. The vapor pressure of anthracene is shown in figure 4.18 and that of pyrene in figure 4.19 along with the available literature values. Vapor pressure of anthracene and pyrene has been studied by many groups covering a wide temperature range and all the available values agree quite well with each other. The results obatined in this study also agrees well with the available literature values for both of these compounds. In this study the enthalpy of sublimation derived from the temperature dependence of vapor pressure is 97.64 kJ/mol (339-399 K) for anthracene and 103.25 kJ/mol (341-418 K) for pyrene. The literature values for the enthalpy of sublimation along with Antoine constant for these two substances are given in Appendix B (Table B1).

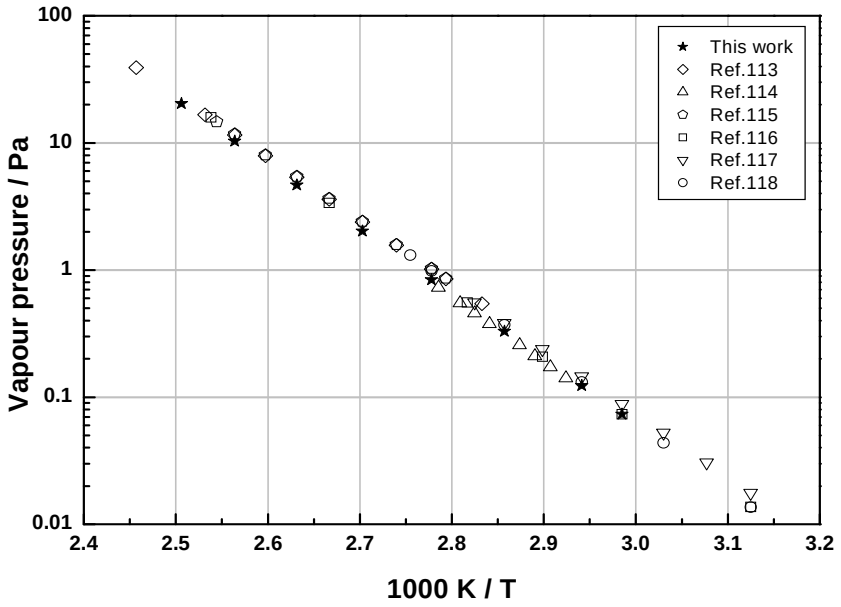

Figure 4.18: Vapor pressure of anthracene.

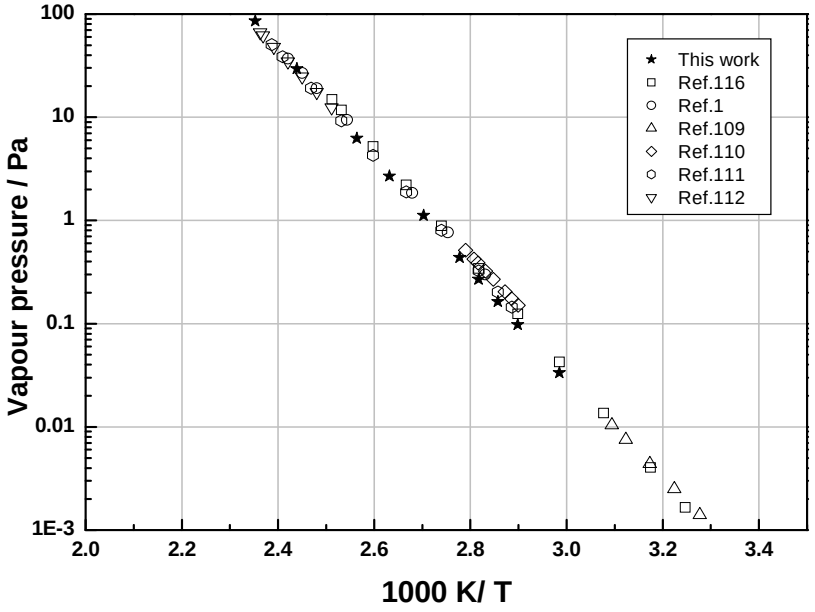

Figure 4.19: Vapor pressure of pyrene.

The values obtained for the vapor pressure for both substances agree with the available literature values quite well in the studied temperature range. Thus the experimental setup provides reliable vapor pressure values and these substances are, therefore, used as reference substances for the vapor pressure measurements.

4.2.2 Metal acetylacetonates [$M(acac)_n$]

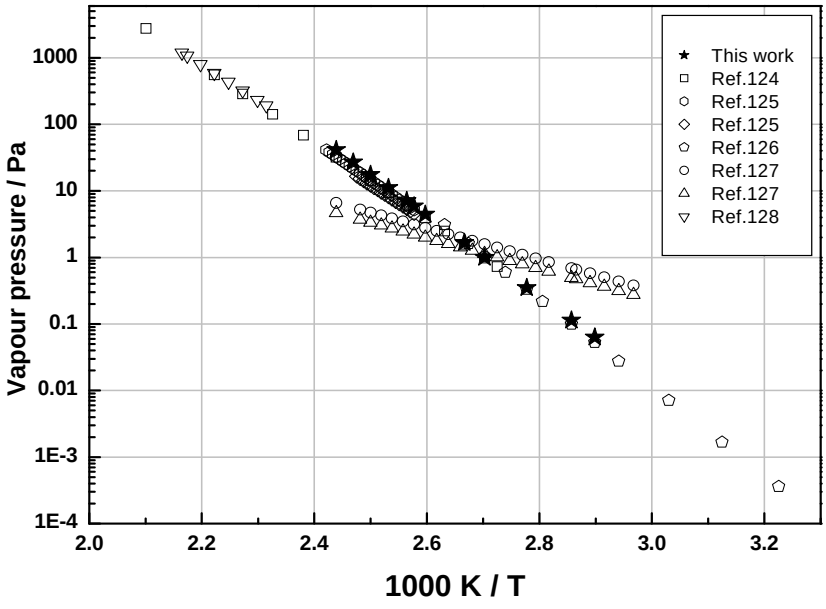

Figure 4.20: Vapor pressure of [$Al(acac)_3$].

The vapor pressure of aluminium acetylacetonate measured in the temperature range of 345-410K is shown in figure 4.20 as a function of *1/T*; literature values are also included. The enthalpy of sublimation derived from the vapor pressures is 117.31 kJ/mol (345-410 K). The values for the vapor pressure of $[Al(acac)_3]$ agree within experimental error with those of Semanikov et al [124], Sachindis and Hill [125] and Malkerova et al. [126], but differ appreciably from those of Teghil et al. [127]. Also the slope of *ln(p)* vs. *1/T* curve is quite different and hence the derived enthalpy of sublimation. The reported enthalpy of sublimation by Teghil et al. [127] is 47±1 kJ/mol (at 298K) and by Berg and Truemper [129] 20.5 kJ/mole is much lower than our vlaue and the other recently reported literature values of Semanikov et al. [124] (121.8 kJ/mol at 298K), Sachindis and Hill [125] (118.6±7.8 kJ/mol for temperature range of 388-413 K). Lazarev et al. [128] reported vapor pressures at higher temperatures (432-464 K) up to the melting point.

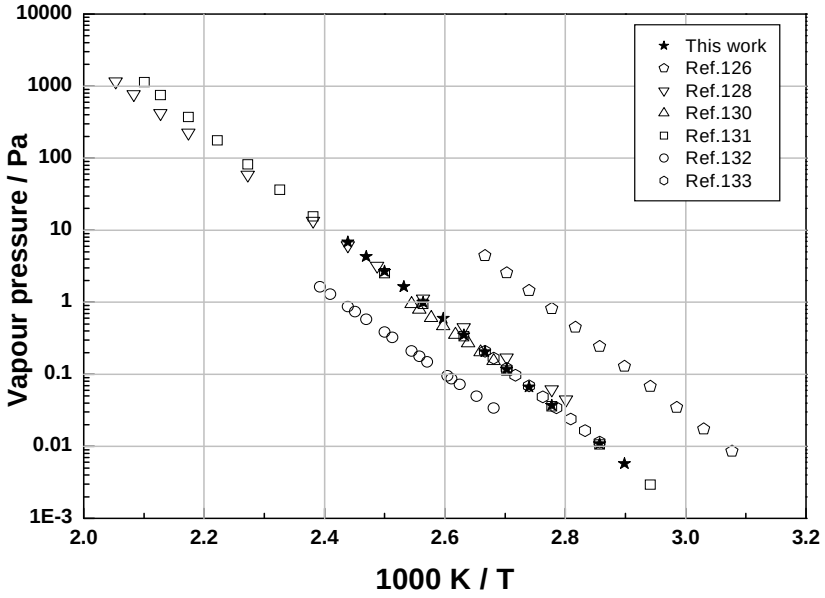

Figure 4.21: Vapor pressure of $[Cr(acac)_3]$.

The vapor pressure of chromium acetylacetonate was measured in the temperature range of 345- 410K and is shown in figure 4.21 as a function of *1/T*; literature values are also included. The enthalpy of sublimation derived from the vapor pressures is 128.20 kJ/mol (345-410K). For $[Cr(acac)_3]$ our values lie nearer to those reported by Malkerova [130] and Semyannikov et al [131]. Lazarev et al. [128] values also agree with ours except at lower temperatures. The vapor pressure values reported by Pankajvalli et al. [132] are much lower than ours and those of Malkerova et al. [126] are much higher. The heat of sublimation reported by Pankajvalli et al. [132] is 111.6±3 kJ/ mol. There

seems to be some systematic errors in these two sets of values. Pankajvalli et al. [132] used the transpiration method and the low value obtained could be due to the undersaturation of the carrier gas with the sample vapor. The experimental setup was also not tested with the substance with well established vapor pressure so the reliability of the data cannot be assured. The use of isoteniscope procedure by Malkerova et al. [115] for vapor pressure measurement is not recommended [131]. The values reported by Melia and Merrifield [133] also differ slightly from ours, who used benzoic acid as a reference substance in the temperature range of 338-370K, while the measurement were carried out within 383-403K. Therefore, the systematic error at higher temperatures could not be detected. In summary a more consistent picture of the vapor pressures is emanating from the present data sets.

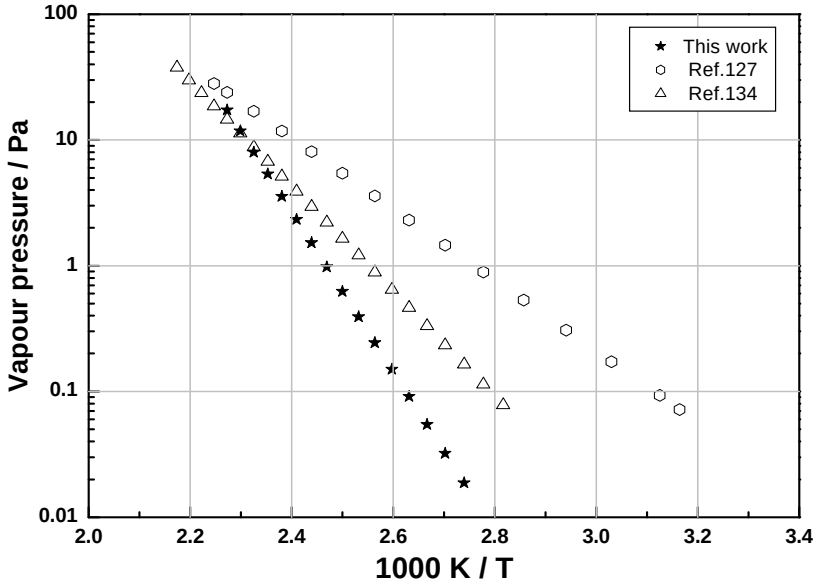

Figure 4.22: Vapor pressure of [Cu(acac)$_2$].

A number of vapor pressure studies for [Cu(acac)$_2$] are found in the literature [110, 127, 134, 135]. Two of these [127, 134] are over a large temperature range (353 – 453 K) but differ from each other considerably. This was also the reason to investigate this compound. The vapor pressure values for [Cu(acac)$_2$] measured by us are shown in figure 4.22 as a function of *1/T*; some literature values are also included. To account for the hygroscopic nature of [Cu(acac)$_2$], handling of the sample was done in the glove box. The TG experiments for [Cu(acac)$_2$] also did not show the presence of water. The enthalpy of sublimation derived from the vapor pressures is 121.6kJ/mol (363 – 443 K). The literature values are 57±1 kJ/mol (298K) [127] and 79.9 kJ/mol (353 – 453 K)[134].

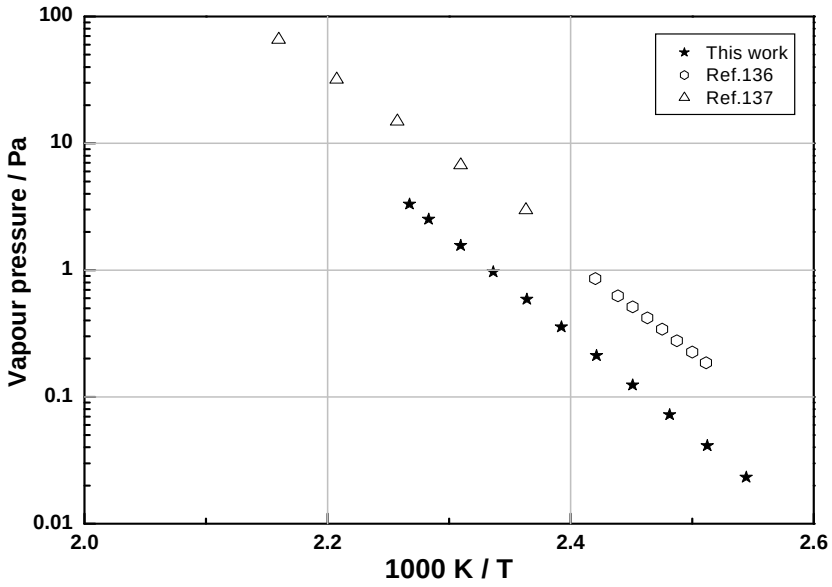

Figure 4.23: Vapor pressure of [Ru(acac)$_3$].

The measured values of vapor pressure for [Ru(acac)$_3$] is much lower than the values reported by Ribeiro de Silva et al. [136] and Bykov et al. [137]. Ribeiro de Silva et al. [136] and Bykov et al. [137] measured the sublimation pressure of [Ru(acac)$_3$] in the temperature range (398 – 413 K) and (423 – 493 K) respectively. Ribeiro de Silva et al. [136] also used the Knudsen cell method for the vapor pressure measurements. They synthesized [Ru(acac)$_3$] in the laboratory and purified it by crystallization from benzene. Its melting point was reported to be 260^{o}C and at this temperature it started to decompose. The purity of the sample was not mentioned and no care for the moisture and air-sensitiveness were taken into account during the handling and measurement. Bykov et al. [137] used the gas saturation method for vapor pressure measurement for the sample synthesized in the laboratory and purified by the zone sublimation method (the reported melting point was 240^{o}C). The purity of the sample was not mentioned and again no care for the moisture and air-sensitiveness were taken into account during the handling and measurement. Our measured vapor pressure values were lower than both of these values as shown in figure 4.23. The difference in vapor pressure values can be attributed to the following reasons:

1. Their samples were synthesized in the laboratory (purity doubtful), so there is a possibility of high volatile impurities (solvent) evaporation during measurements. The purity was not reported. The studied sample was the commercially available substance with 99% purity.
2. No care of moisture and air sensitiveness was taken into account.

3. Ribeiro de Silva et al. [136] used Benzoic acid and Ferrocene as reference substances, which are recommended at lower temperature (298-383K & 277-360K), while the measurements for [Ru(acac)$_3$] were done at higher temperature.

Acetylacetonates of iron, manganese, nickel, vanadium, zinc, thulium and dysprosium were found to be decomposing in isothermal TGA experiment. Therefore, no vapor pressure measurements could be obtained with the Knudsen cell method, which, as a gravimetric method, relies on the intact evaporation of the studied compound. For [Fe(acac)$_3$], [Mn(acac)$_3$] [V(acac)3] and [Ni(acac)$_2$] we find a number of publications reporting the sublimation/vapor pressures of these over a wide temperature range [110,125,126,129,133,138,139] although the decomposition of these have been reported in other publications in the past and recently [98,101-103,106,140].

4.2.3 Metal 2,2,6,6-tetramethyl-3,5-heptandionate [M(tmhd)$_n$)]

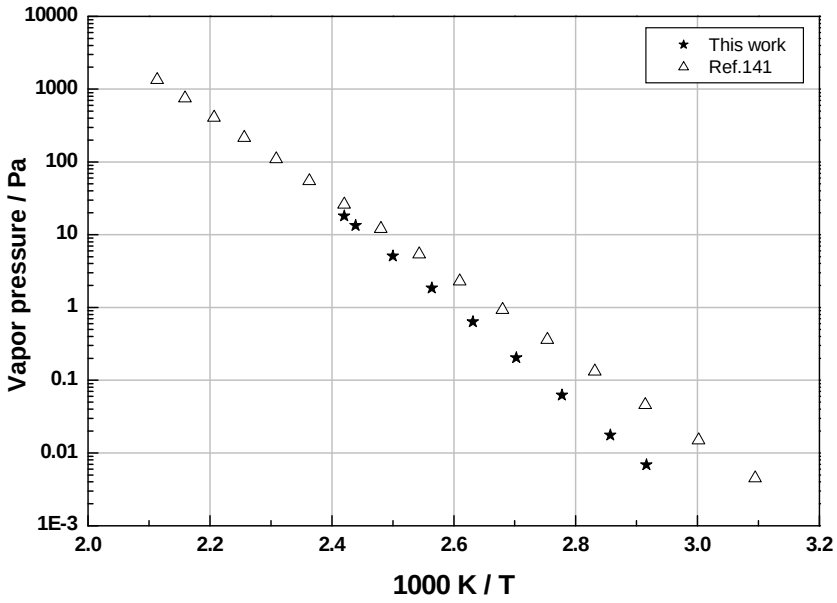

Figure 4.24: Vapor pressure of [Fe(tmhd)$_3$].

Vapor pressures for [Fe(tmhd)$_3$], [Mn(tmhd)$_3$], [Ni(tmhd)$_2$] , [Al(tmhd)$_3$], [Cr(tmhd)$_3$] and [Cu(tmhd)$_2$] were measured. The vapor pressure of [Fe(tmhd)$_3$] measured in the temperature range of 340- 405K is shown in figure 4.24 as a function of *1/T*; literature value is also included. The enthalpy of sublimation derived from the temperature dependence of vapor pressures is 131.94 kJ/mol (340-405 K). Sharply different from our data are the result reported by Brunner and Curtis [141] which were also obtained by

Knudsen effusion method as shown in figure 4.24. In low temperature region (up to 373K) vapor pressure values observed by them is higher by a factor of 3 and at higher temperature of 405K there exits a difference of factor 1.3. The difference in vapor pressure could be due the following facts:

1. The sample was synthesized in the laboratory and there is no mention of the sample purity. Therefore, the high values of vapor pressure could result from evaporation of some associated solvent or water as [Fe(tmhd)$_3$] is a hygroscopic substance and special care should be taken during its handling which was not taken into account.
2. Benzoic acid was used as reference substance, which is recommended at lower temperature (298-383K), while the measurement was done at higher temperature.

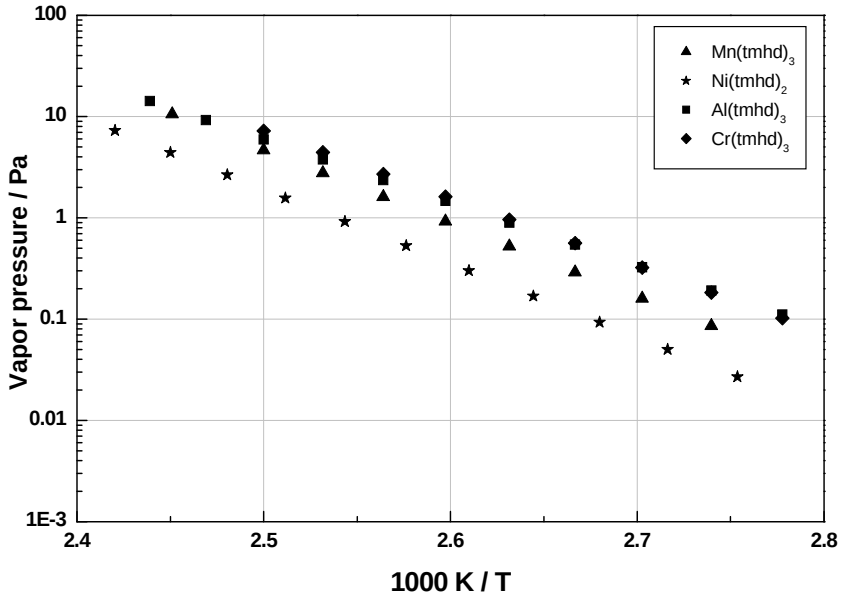

Figure 4.25: Vapor pressure of [Mn(tmhd)$_3$], [Ni(tmhd)$_2$], [Al(tmhd)$_3$], & [Cr(tmhd)$_3$].

Vapor pressure for [Mn(tmhd)$_3$], [Ni(tmhd)$_2$], [Al(tmhd)$_3$], & [Cr(tmhd)$_3$] are shown in figure 4.25 as function of *1/T*. The heat of sublimation derived from the vapor pressures are 138.59 kJ/mol (340-405 K), 139.74 kJ/mol (340-405 K), 119.12 kJ/mol (340-405 K), and 127.45 kJ/mol (340-405 K). No vapor pressure studies were found for these compounds in the literature.

The vapor pressure of [Cu(tmhd)$_2$] is shown in figure 4.26 as function of *1/T*, the derieved enthalpy of sublimation from vapor pressure data is 127.32 kJ / mol. The

values for the vapor pressure of [Cu(tmhd)$_2$] agree within experimental error with those of Tobaly and Lanchec [142] but the vapor pressure values reported by Yuhya et al.[143] are much higher than ours and those of Igunov et al. [144] (cited in [143]) are much lower. Yuhya et al. [143] used the transpiration method and no proof of saturation of carrier gas was given, this could lead to a underestimation of vapor pressure. Waffenschmidt et al. [145] reported the vapor pressure of decomposing [Cu(tmhd)$_2$], therefore, data provided by them does not seem to be reliable.

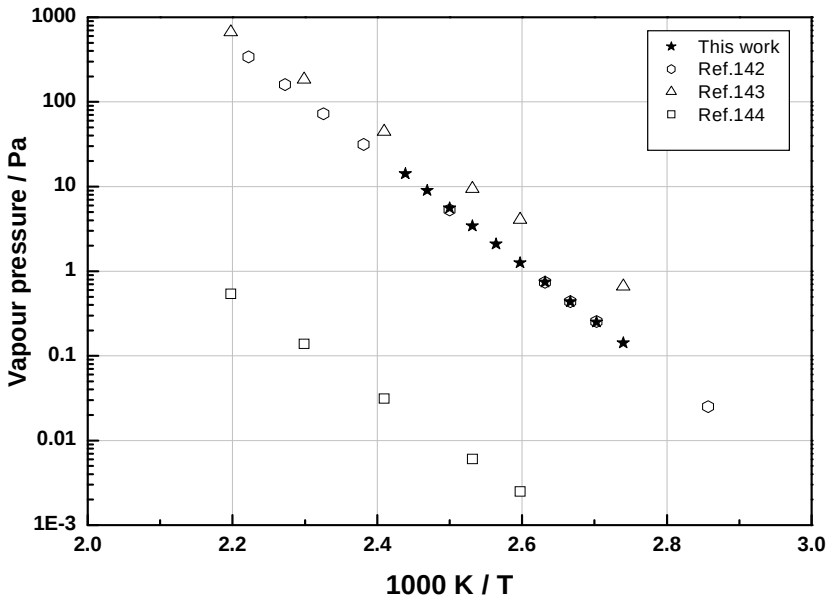

Figure 4.26: Vapor pressure of [Cu(tmhd)$_2$].

4.2.4 Metallocene

The vapor of ruthenocene is shown in figure 4.27 along with the available literature value of Cordes and Schreiner [146]. Ruthenocene is not sensitive to air. Its vapor pressure was measured in the range 331-351 K. Cordes and Schreiner [146] measured its vapor pressure in the range of 348-366 K. The values agree well with our extrapolated values to these temperatures and which are shown in figure 4.27. The enthalpy of sublimation derived from these vapor pressure values is 100.52 kJ/ mol. Nickelocene was found to be decomposing in isothermal TGA measurement, so no vapor pressure measurement were done. Vapor pressure of nickelocene was reported by Gomez et al. [147] in the temperature range 283-306K. The reported enthalpy of sublimation by Gomez et al. [147] is 71.47±0.63 kJ/mol (294.5K).

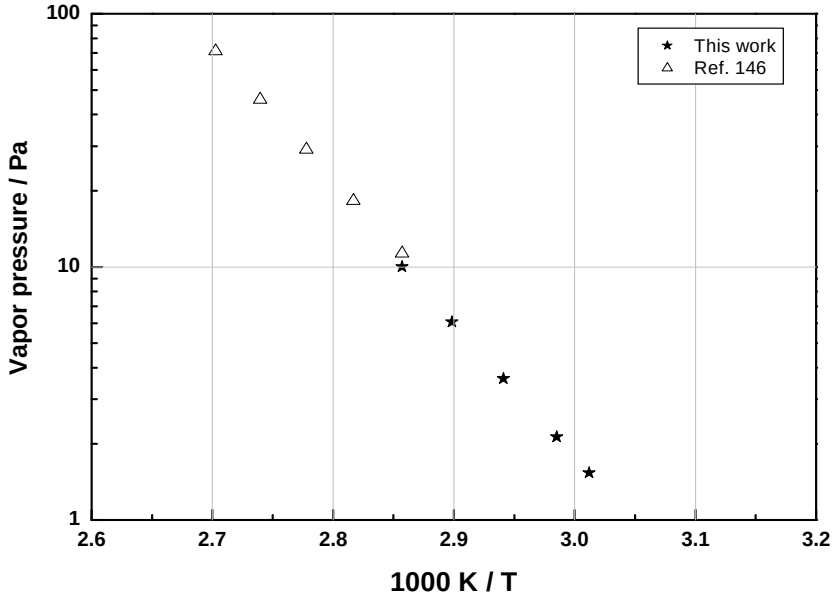

Figure 4.27: Vapor pressure of [Ru(cp)$_2$].

4.2.5 Lab synthesized precursors

Vapor pressure measurements were only done for those compounds which are found to be thermally stable in isothermal TGA experiments. It has been found that all the ruthenium complex were thermally stable and, therefore, subjected to vapor pressure measurements.The amount of [Ru (Toluene) (1,3-Cyclohexadiene)] and [Ru (Toluene) (2,3-dimethyl-1,3-butadiene)] provided was very small so no Knudsen cell measurements were possible. However, the thermogravimetric measurements were used to calculate the product of the vapor pressure and binary diffusion coefficient $p_A^{vap} D_{AB}$ at different temperatures by the method described in Siddiqi et al. [44] using the equation (2.106). The experimental mass loss ($\Delta m/\Delta t$) as a function of time t, the initial distance between the surface of the investigated substance and the top of the crucible (H) were needed. The diffusion coefficients of these substances were estimated from the expression [64]

$$D_{AB} = \frac{0.00266 T^{3/2}}{p M_{AB}^{3/2} \sigma_{AB}^2 \Omega_D} \tag{4.1}$$

Here p is the pressure in bar, T is the temperature in K,

$$M_{AB} = \frac{2}{(1/M_A + 1/M_B)}$$

where M_A and M_B are the molecular masses of substance A and the carrier gas B. The characteristic length σ_{AB} in Angstrom units (1°A= 10^{-10}m) and the diffusion collision integral Ω_D is calculated by selecting the intermolecular force law e.g. Lennard-Jones. In the absence of any data for Ru-complexes, the values of σ_{AB} and Ω_D calculated for ferrocene from the experimental vapor pressures determined by Knudsen cell method [44] were used to estimate the diffusion coefficients, σ_{AB} and Ω_D which were adopted for Ru complexes to obtain their diffusion coefficients and consequently the vapor pressures from the equation (2.106). The estimated vapor pressure values are shown in figure 4.28. The vapor pressure values at different temperature were estimated using the same method for [Ru(Benzene) (1, 3-Cyclohexadiene)] for which vapor pressure was measured using the Knudsen cell. From figure 4.26 it can be seen that the estimated values of the vapor pressure for [Ru(Benzene)(1, 3-Cyclohexadiene)] are in good with the values determined experimentally. In figure 4.28, the hollow symbol refers to values of vapor pressure estimated from diffusion coefficient and the filled symbols are used for experimentally determined values.

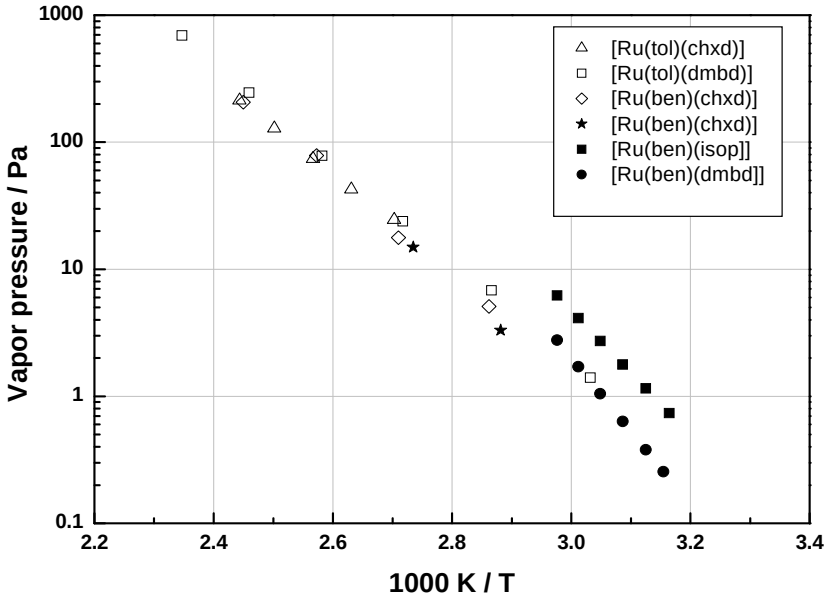

Figure 4.28: Vapor pressure of Ru complexes.

([Ru (ben)(isop)]-[Ru (Benzene) (Isoprene)], [Ru (ben) (dmbd)]-[Ru (Benzene)(2, 3-dimethylbutadiene)],[Ru(tol)(chxd)]-[Ru(Toluene)(1,3-Cyclohexadiene)], [Ru(tol)(dmbd)]-[Ru (Toluene) (2,3-dimethyl-1,3-butadiene), [Ru (ben)(chxd)]-[Ru (Benzene) (1,3-Cyclohexadiene)]]

The vapor pressure values for [Ru (Benzene) (Isoprene)] and [Ru (Benzene) (2, 3-dimethyl butadiene)] are also shown in figure 4.28 and the enthalpy of sublimation for these two compounds derived from vapor pressure data is 83.07 kJ/mol and 111.05 kJ/ mol respectively.

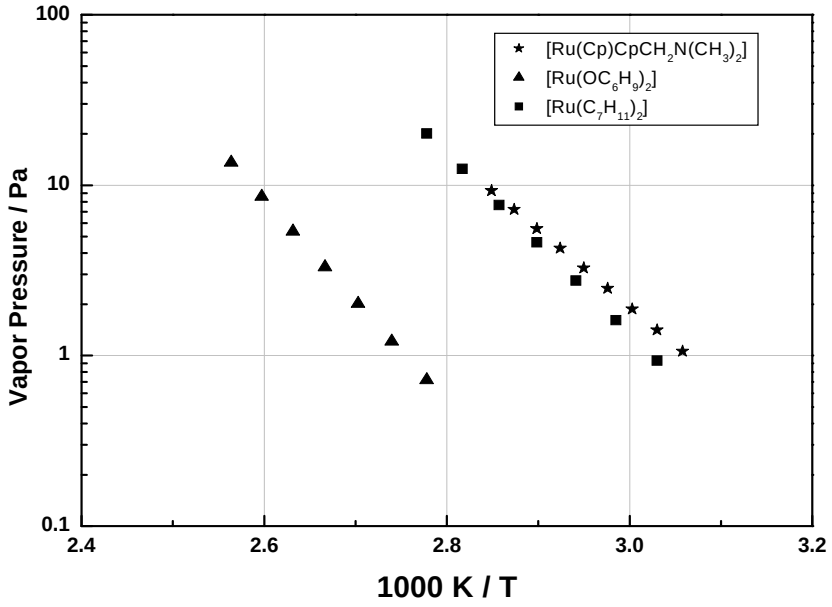

Figure 4.29: Vapor pressure of Ru complexes.

Since all the three precursors were found to be thermally stable, vapor pressure measurements was done at various temperatures using the Knudsen cell. The experimental vapor pressures for $[Ru(C_7H_{11})_2]$, $[Ru(0C_6H_9)_2]$ and $[Ru(cp)(cpCH_2N(CH_3)_2)]$ are plotted in figure 4.29 as a function of 1/T. The enthalpies of sublimation for these three compounds derived from vapor pressure data are 98.28 kJ/mol, 114.36 kJ/mol and 86.27 kJ/mol respectively.

4.3 Binary gaseous diffusion coefficient using TGA

The diffusion coefficient is in general unknown for organometallic compound. However, from the kinetic theory of gases an expression [64] can be derived for its calculation using equation (4.1). The characteristic length σ_{AB} in Angstrom units and the diffusion collision integral Ω_D can be calculated by selecting an intermolecular force law e.g. Lennard-Jones potential using viscosity data. The equation (4.1) shifts the problem to two new unknowns: the collision diameter σ_{AB} and the collision integral Ω_D. The latter is a function of temperature and could vary by 30-40% in the interesting temperature range, while the former can be estimated by XRD data (if available) and

should be only a weak function of temperature. For organic compounds there are empirical rules for their estimation, but little is known for organometallic compounds. Both can be determined by the methods of theoretical chemistry and molecular dynamics, but for validation experimental data is needed which lacks completely for organometallic compound. Therefore, the equation (4.1) cannot be used for the estimation of gaseous diffusion coefficient for organometallic compounds. There is complete lack of any sort of experimental or estimated data for the gaseous diffusion coefficient for organometallic compounds. In this study gaseous diffusion coefficient of some organomettalic compounds were measured along with two poly aromatic hydrocarbons (anthracene and pyrene).

4.3.1 Polyaromatic hydrocarbons

The diffusion coefficient for all the compounds was measured within the temperature range of vapor pessure measurements. This was done in order to avoid the extrapolation of vapor pressure value, which is needed for the calculation of gaseous diffusion coefficient. As already discussed, there are various empirical corelations for the estiamtion of diffusion coefficient for organic compounds and also quite a good number of experimental values for the organic compounds are available. Therefore, comparing these data with the data obtained from TG experiments will provide a good overview of the accuracy of TG method.

The diffusion coeffficients of naphthalene and phenanthrene in helium and nitrogen atmosphere were investigated by Siddiqi and Atakan [44] using the TG method. For napthalene experimental studies for D_{AB} in air was done previously by Mack [148], Caldwell [85], Cho et al. [86], Gustafson and Dickhut [87], Chen et al. [80] and Delgado et al. [72]. The mean value obtained from TG measurements of 0.085 cm^2s^{-1} at 307K is higher than the value of Chen et al. 0.0719 $cm^2\ s^{-1}$ and Cho et al. 0.0699 $cm^2\ s^{-1}$ but agrees quite well with 0.086 $cm^2\ s^{-1}$ at 303K measured by Caldwell, 0.088 $cm^2\ s^{-1}$ by Delgado et al. [72] and 0.088 $cm^2\ s^{-1}$ by Gustafson and Dickhut [87] as shown in figure 4.30.

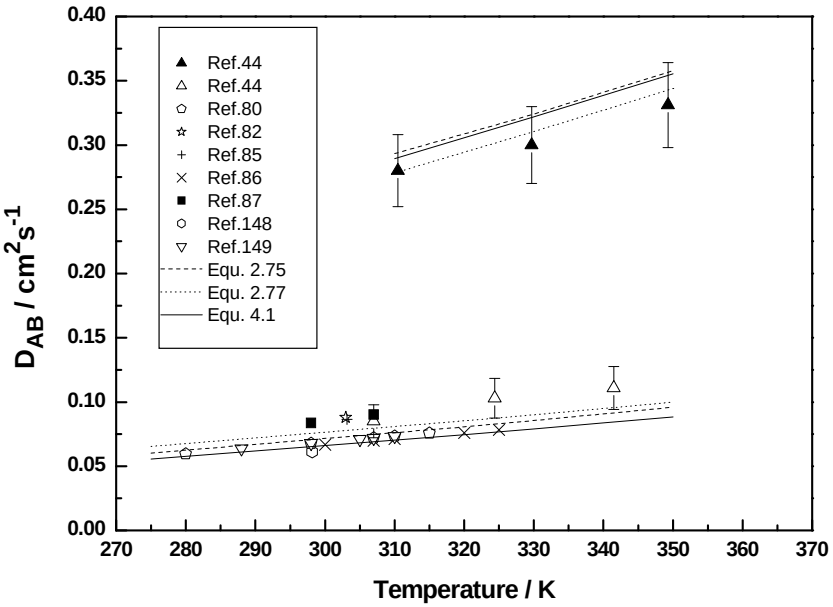

Figure 4.30: Gaseous D_{AB} for naphthalene in helium (▲) and nitrogen (△).

The value of Mack [147] had an error of using inaccurate vapor pressure data which had been already pointed out by other workers [81]. The possible sources of error in the method of Cho et al. [86] have been discussed in detail by Chen et al. The lower value of D_{AB} measured by Chen et al. could be attributed to the fact that the precision of the QCM technique depends upon how accurately the coating on the QCM i.e. film uniformity. The measured values of Siddiqi and Atakan [44], Caldwell [85], Delgado et al. [82], Gustafson and Dickhut [87] are slightly higher when compared with the values obtained from the correlation of Wilke & Lee [72] Fuller et al. [74] and Chapman & Enskog [64] values which has been recommened for use in the case of organic compounds. The values obtained from the TG measurement could be relied upon as discrepancies upto 20% between estimated and experimental values are possible [64].

In case of phenanthrene the mean value of TG measurements of Siddiqi and Atakan [44], of 0.075 cm²/s at 325 K agrees quite well with the values of Gustafson and Dickhut [87] of 0.077 cm²/s at 325 K obtained from T^2 dependence of his experimental values and also with the values obtained from the correlation of Wilke & Lee [72], Fuller et al. [74] and Chapman & Enskog [64] as shown in figure 4.31.

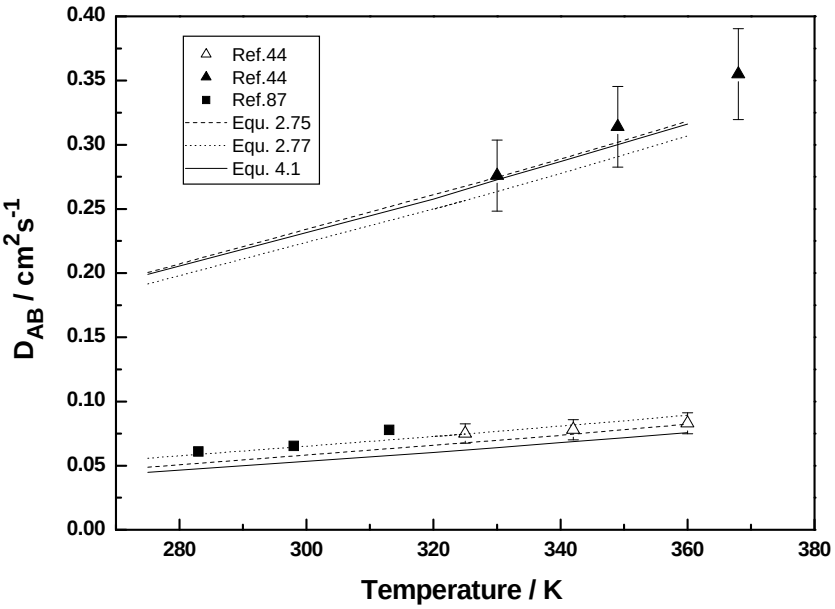

Figure 4.31: Gaseous D_{AB} for phenanthrene in helium (▲) and nitrogen (△).

As expected the gaseous diffusion coefficients in helium are throughout higher than in nitrogen. For both these compounds no experimental values in helium atmosphere were available in the literature, so a comparision of experimental TG values with values obtained from correlation of Chapman & Enskog [64], Wilke & Lee [72] and Fuller et al. [74] was made using the characterstic parameter from critical data. The estimated diffusion coefficient values in helium lie within the error limit of ±10% of the experimentally determined value. A temperature dependence of T^2 agrees quite well for these compounds both in nitrogen and helium atmosphere [44].

The diffusion coefficients of anthracene in nitrogen and in helium were determined using the TG method is shown in figure 4.32 as a function of temperature. The mean values for at least three runs are shown. As expected the binary diffusion coefficients in helium are throughout higher than in nitrogen. Gustafson and Dickhut [87] measured the diffusion coefficients of anthracene in air at 0, 10, 25 and 40 °C. Their values are also shown on the figure 4.32. Mack [148] reported a value of 0.0783cm^2s^{-1} for D_{AB} of anthracene in air.

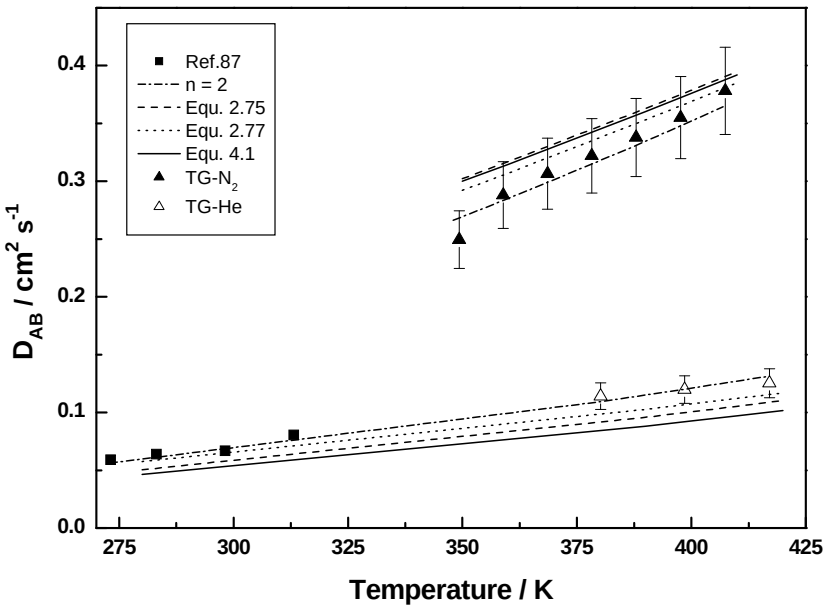

Figure 4.32: Gaseous D_{AB} for anthracene in helium (▲) and nitrogen (△).

The binary gaseous diffusion coefficients calculated with the correlation Wilke & Lee [72] Fuller et al. [74] and Chapman & Enskog [64] using the critical properties are also shown in figure 4.32. All the three methods give similar results which do not differ much from each other. The experimental values also agree with these values within experimental uncertainty. From simple gas kinetic theory a T^n dependence with n = 1.75-2 is expected [64]. A curve with n = 2 is also included in the diagram. The diffusion coefficients obtained in this study do not differ appreciably from those calculated with different methods.

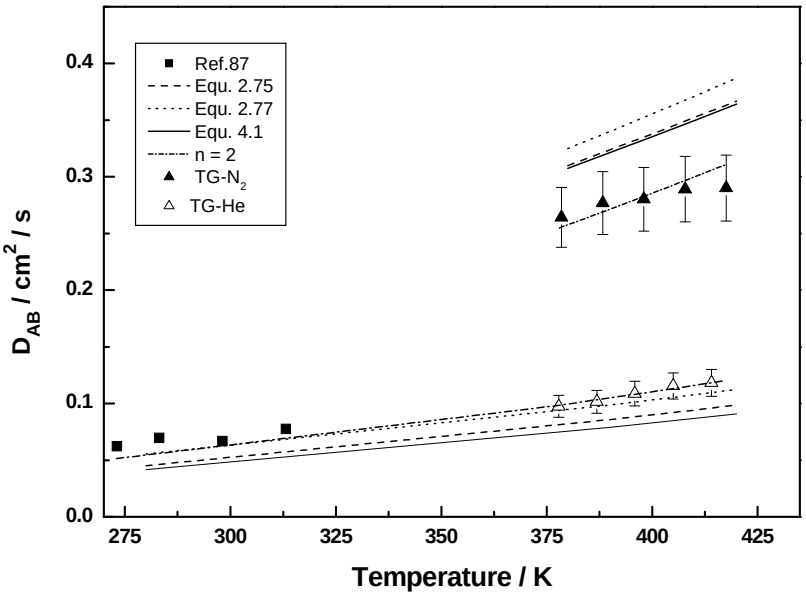

Figure 4.33: Gaseous D_{AB} for pyrene in in helium (▲) and nitrogen (△).

The diffusion coefficients of pyrene in nitrogen and in helium are shown in figure 4.33 as a function of temperature. The mean values for at least three runs are shown. The diffusion coefficients from the literature [87] and the correlations of Wilke & Lee [72] Fuller et al. [74] and Chapman & Enskog [64] are also shown. As the critical parameters for pyrene were not tabulated these were calculated using the correlations suggested in literature [64]. The discrepancies are here larger but acceptable. The binary diffusion coefficients in helium are throughout higher than in nitrogen.

The measured values for all the four PAH both in nitrogen and helium agree quite well with the values obtained from the correlation of Fuller et al. [86] which uses elemental diffusion volumes which are obtained from experimental diffusion coefficient using least square regression analysis of large number of data. Therefore, the correlation of Fuller et al. has better predictive qualities nearer to experimentally determined values. As of Chapman & Enskog [64] and Wilke and Lee [72] correlation, which are developed in the terms of σ and ε for pure components which can be obtained from critical properties or from Lennard-Jones potential using viscosity data. The data for σ_{AB} and ε_{AB} from viscosity data are considered to be accurate [60, 72] but due to lack of visocity data for number of substances these are usually not available and thus a great disadvantage of using these correlations. Usually σ_{AB} and ε_{AB} are estimated using the critical properties of the substances.

4.3.2 Metal acetylacetonates [M(acac)$_n$]

Figure 4.34 & 4.35 show the diffusion coefficients of [Al(acac)$_3$] and [Cr(acac)$_3$] in nitrogen and in helium. The mean values for at least three runs are shown in the plots as filled and hollow symbols for helium and nitrogen.

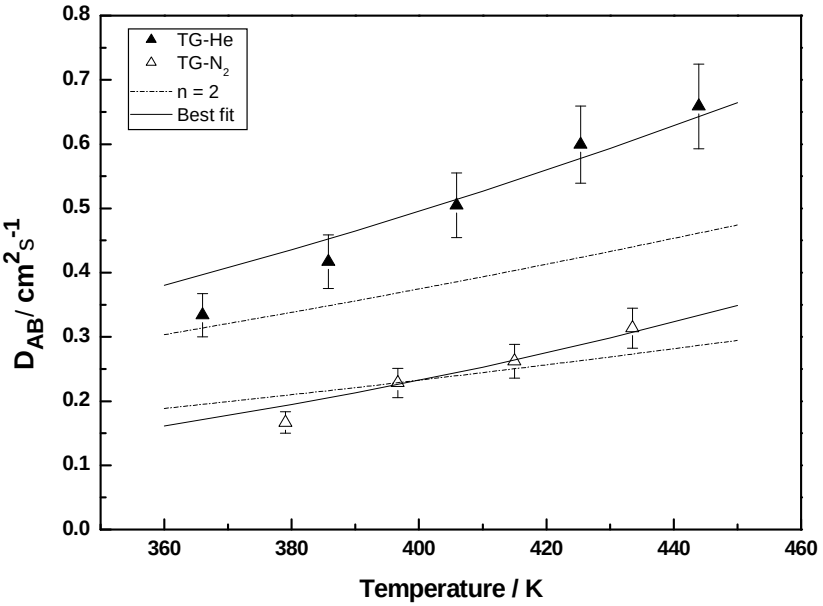

Figure 4.34: Gaseous D_{AB} for [Al(acac)$_3$] in helium (▲) and nitrogen (△).

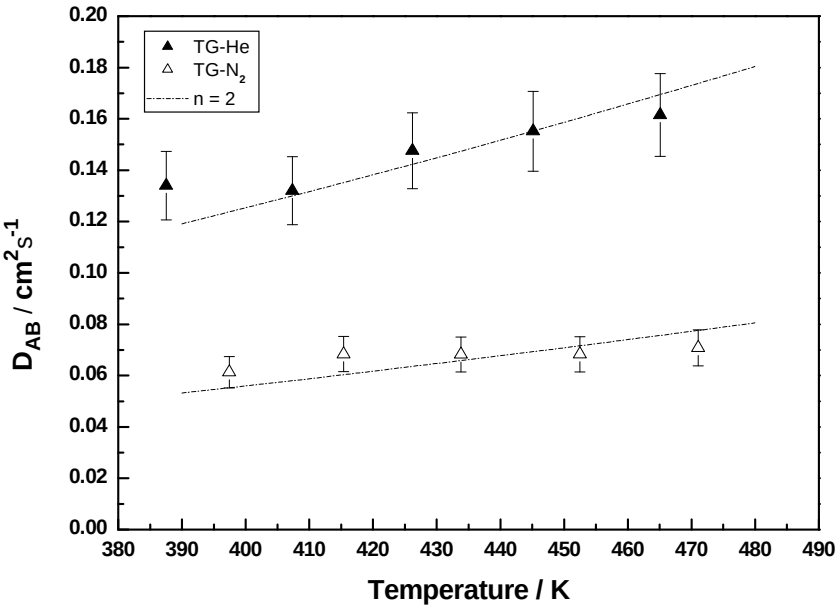

Figure 4.35: Gaseous D_{AB} for [Cr(acac)$_3$] in helium (▲) and nitrogen (△).

As expected the binary diffusion coefficients in helium are throughout higher than in nitrogen; also a lower diffusion coefficient for the chromium acetylacetonate compared to the one for aluminium acetylacetonate was expected due to its lower molecular mass.

A temperature dependence of n = 2 does not correspond well to the experimental data for $[Al(acac)_3]$ in helium and nitrogen atmosphere which is expected from gas kinetic theory [64] as shown in figure 4.34, while value of n =2 was found to be best fit with experimental D_{AB} for the chromium compound in both helium and nitrogen atmosphere. The best fits curves along with the temperature dependence of n =2 are included into to the diagrams.

The unexpected low values of D_{AB} for $[Cr(acac)_3]$ suggests that some dimerization of the chromium compound cannot be excluded but no such experimental evidence for dimerization of chromium compound could be found in the literature. Further theoritical investigation in terms intermolecular forces studies are needed to explain and understand this unexpected behaviour of $[Cr(acac)_3]$.

Figure 4.36 & 4.37 shows the diffusion coefficients of $[Cu(acac)_2]$ and $[Ru(acac)_3]$ in helium atmosphere. A temperature dependence of n =2 fits well to experimental data for both compounds in helium atmosphere.

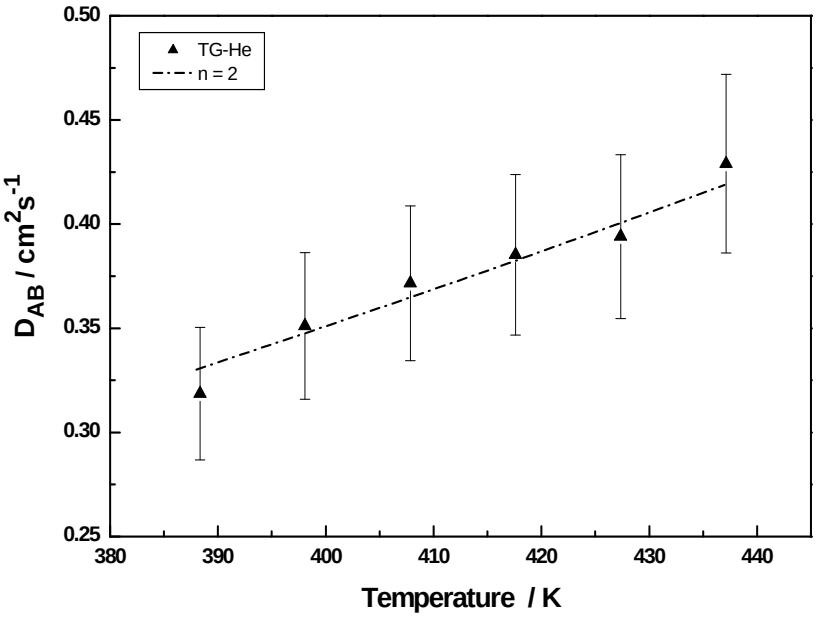

Figure 4.36: Gaseous D_{AB} for $[Cu(acac)_2]$ in helium.

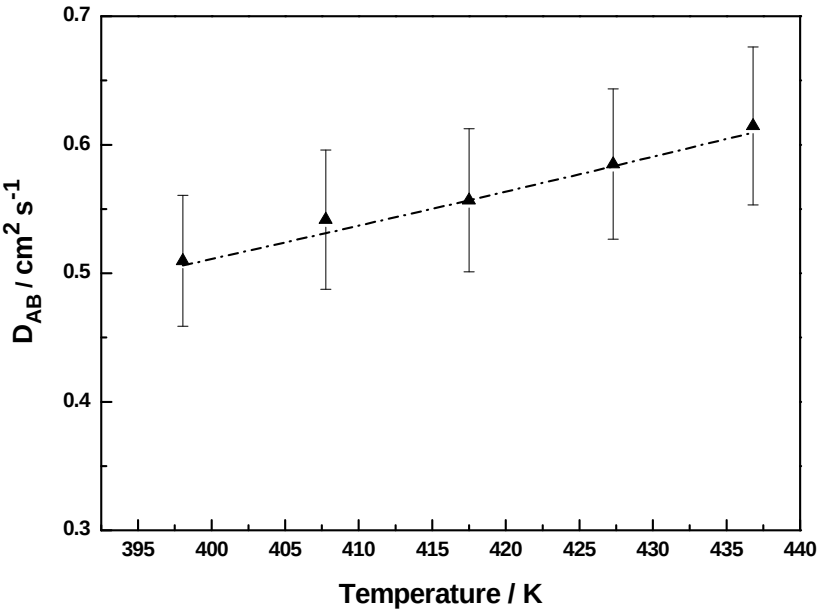

Figure 4.37: Gaseous D_{AB} for [Ru(acac)$_3$] in helium.

The diffusion coefficients for these metal acetylacetonates have been measured for the first time. The mass loss rate at lower temperatures in nitrogen was quite small both for [Cu(acac)$_2$] and [Ru(acac)$_3$] and hence the diffusion coefficients were not determined in nitrogen mixture. And also no correlations are yet available for the estimation of the binary gaseous diffusion coefficients of organometallic compounds hence these could not be calculated.

4.3.3 Metal 2, 2, 6, 6-tetramethyl-3, 5-heptandionate [M(tmhd)$_n$]

The gaseous diffusion coefficient of [Fe(tmhd)$_3$], [Mn(tmhd)$_3$], [Al(tmhd)$_3$] and [Cu (tmhd)$_2$] were measured in both helium and nitrogen atmosphere as shown in figures 4.38,4.39 and 4.40. No previous studies regarding the gaseous D_{AB} for [M(tmhd)$_n$] were found during the literature survey. These are reported for the first time. For [Cr(tmhd)$_3$] and [Ni(tmhd)$_2$], the mass loss in nitrogen was very small at low temperatures, therefore, for these two compounds, gaseous diffusion coefficient is being reported in helium only. As expected the binary diffusion coefficients in helium are throughout higher than in nitrogen for [M(tmhd)$_n$].

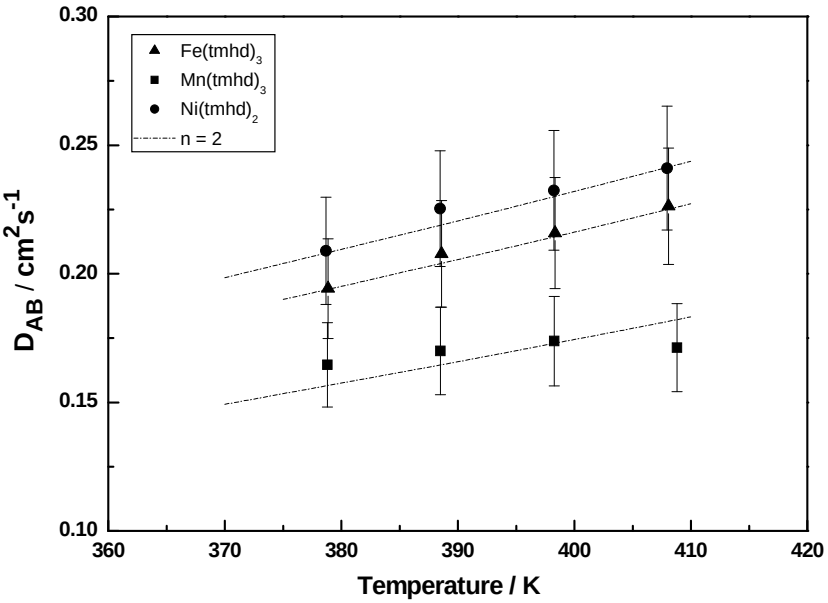

Figure 4.38: Gaseous D_{AB} for [Fe(tmhd)$_3$], [Mn(tmhd)$_3$], and [Ni(tmhd)$_2$] in helium.

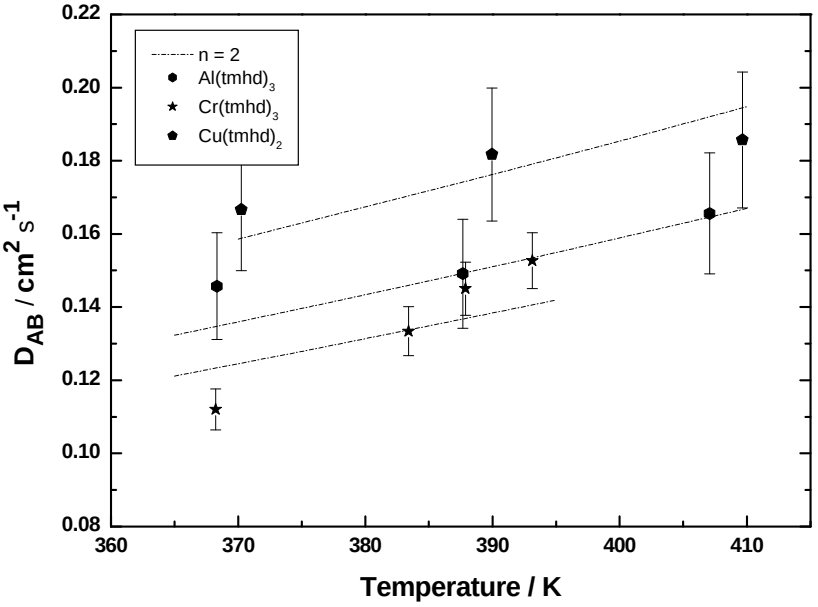

Figure 4.39: Gaseous D_{AB} for [Cr(tmhd)$_3$], [Cu(tmhd)$_2$], and [Al(tmhd)$_3$] in helium.

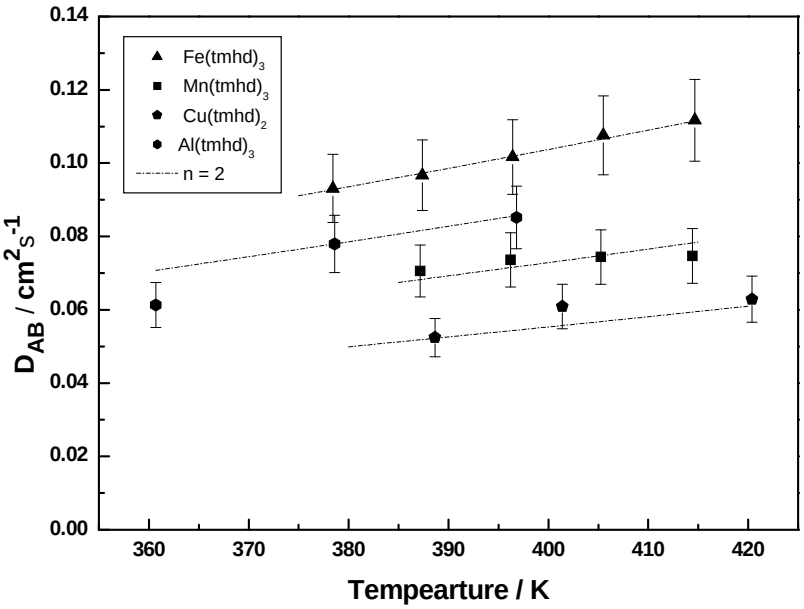

Figure 4.40: Gaseous D_{AB} for $[Fe(tmhd)_3]$, $[Mn(tmhd)_3]$, $[Al(tmhd)_3]$ and $[Cu(tmhd)_2]$ in nitrogen.

4.3.3 Metallocene $[M(cp)_n]$

The gaseous diffusion coefficient of $[Ru(cp)_2]$, was measured in nitrogen.

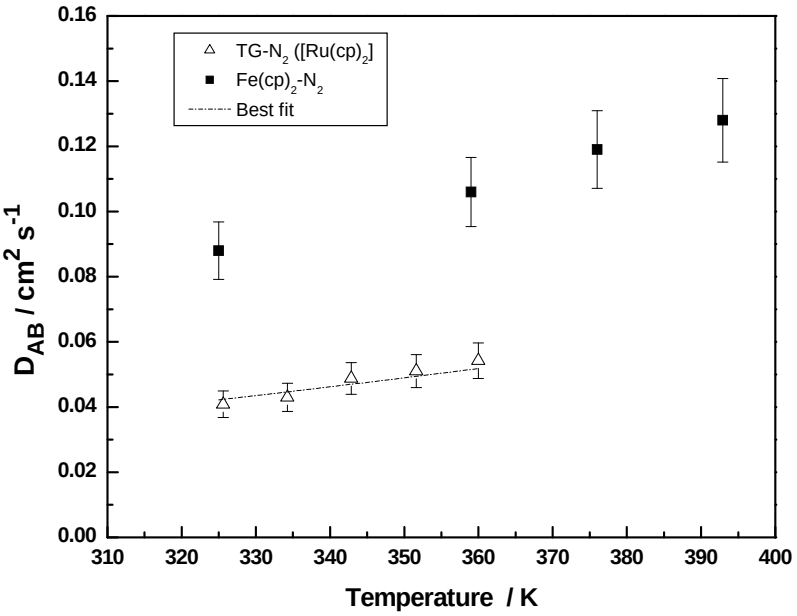

Figure 4.41: Gaseous D_{AB} for $[Ru(cp)_2]$, and $[Fe(cp)_2]$ in nitrogen.

Siddiqi and Atakan [44] reported the gaseous diffusion coefficient for $[Fe(cp)_2]$ in nitrogen and helium but no such study regarding $[Ru(cp)_2]$ has been found in the literature and is being reported for the first time. The mean value at different

temperatures of at least three runs for $[Ru(cp)_2]$ along with the literature value for $[Fe(cp)_2]$ is shown in figure 4.41. Lower diffusion coefficient for the $[Ru(cp)_2]$ when compared to the one for $[Fe(cp)_2]$ were expected due to the differences in their molecular mass. A temperature dependence of n = 2 fits well to the experimental data is also shown in figure 4.41.

4.4 Estimation of gaseous diffusion coefficient using hard sphere model

In some cases where mass loss was very small at low temperatures especially for $[Cu(acac)_2]$, $[Ru(acac)_3]$, $[Ni(tmhd)_2]$, and $[Cr(tmhd)_3]$ in nitrogen atmosphere, the gaseous diffusion coefficient could not be determined. Also neither any critical data are available for organomettallic compound which could be used for the calculation of σ_A and Ω to be used in equation nor any atomic diffusion volumes for the organometalic compounds are available to be used in the correlation of Fuller et al. [74] for estimation of D_{AB}. The binary gaseous diffusion coefficient in such cases were approximated by using the apporach which is based on Chapman rigid sphere model [59] and is represented as

$$D_{AB} = \frac{0.00146 T^{3/2} M_{AB}^{1/2}}{p\, \sigma_{AB}^2} \qquad (2.71)$$

Where M_1 and M_2 are the molecular masses of the substance and the carrier gas, n is the number density, k is Boltzmanns constant. Using the experimentally determined D_{AB} value in helium atmosphere at different temperatures and putting it into the equation (2.71) the value of σ^2_{AB} can be obtained. The σ_B value for helium was obtained from critical properties. Using the relation

$$\sigma_{AB} = \frac{\sigma_A + \sigma_B}{2}$$

one gets the value of σ_A. The average of the σ_A values that are obtained for different temperatures is then used to calculate the diffusion coefficient in nitrogen (σ for nitrogen is obtained from the critical properties) using equation (2.67). The estimated values $[Cu(acac)_2]$, $[Ru(acac)_3]$, $[Ni(tmhd)_2]$, and $[Cr(tmhd)_3]$ in nitrogen atmosphere are shown in figure 4.42

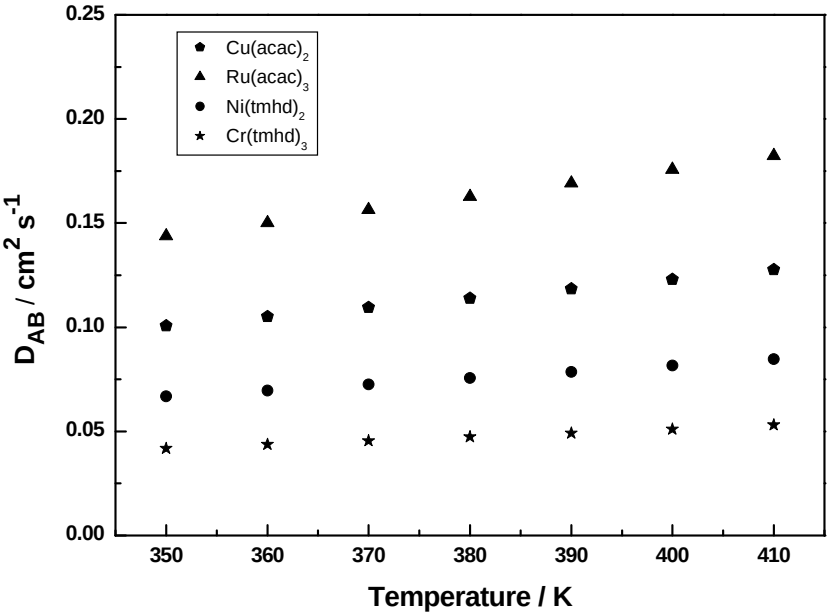

Figure 4.42: The estimated gaseous D_{AB} values for [Cu(acac)$_2$], [Ru(acac)$_3$] [Ni(tmhd)$_2$], and [Cr(tmhd)$_3$] in nitrogen.

Since the amount of the lab synthesized precursor was very small. It was sufficient enough for Knudsen cell measurement. Therefore, no gasesous diffusion coefficient measurements were done.

The reported values for the experimental gaseous diffusion coefficient for polyaromatic hydrocarbon anathracene and pyrene agree well with the measured values obtained from TGA measurements. The gaseous diifusion coefficient for some of the metal β-diketonates (acetylacetonates & TMHD) and metallocene were measured for the first time. For organometallic substances no empirical correlation for the estimation of gaseous diffusion coefficient is available. Therefore, a comparision of estimated values with experimental values was not done. Apart from the thermal stability and vapor pressure measurements, it was also desired to get some empirical correlation for the gaseous diffusion coefficient for the organometallic compounds but the number of experimental data was not sufficient to arrive on some conclusive empirical correlation.

CHAPTER 5

CONCLUSIONS

A systematic study of the evaporation behaviour and the transport properties of organometallic compounds was undertaken. The strategy followed was to first examine the thermal stability of the precursor in the isothermal mode, consequently those found to be thermally stable were subjected to vapor pressure and diffusion coefficient measurement.

Since some of the precursors are sensitive towards oxygen and moisture, they tend to degrade on exposure to the ambient atmosphere. Therefore, all the substances were stored and handled in the glove box to prevent any contact with the ambient atmosphere. The substances which showed nearly linear mass loss along with the negligible amount of residue in isothermal thermogravimetric were considered to be stable. The vapor pressures were measured by using the home built Knudsen cell. The experimental setup was tested with the reference substances, anthracene and pyrene, and provided reliable sublimation pressure over a large temperature range. The measured vapor pressure values were in good agreement with the available literature values for these reference substances. Among the metal acetylacetonates only $[Al(acac)_3]$, $[Cr(acac)_3]$, $[Ru(acac)_3]$ and $[Cu(acac)_2]$ evaporate without residuals and hence their vapor pressures were measured. All the $[M(tmhd)_n]$ except $[Eu(tmhd)_3]$ were found to be stable in isothermal thermogravimetry experiments and hence their vapor pressures at various temperatures were also reported for the first time. In case of the laboratory synthesized precursors, vapor pressure measurement was done only for the ruthenium complexes as they were found to be thermally stable. $[Ni(cp)_2]$ was found to decompose so vapor pressure measurements were only done for $[Ru(cp)_2]$. In all the cases, the temperature dependence of vapor pressure could be represented by an Antoine type expression within experimental errors and the coefficients were determined by the least square deviation method. The calculated enthalpies of sublimation for metal acetylacetonate are in the order of $[Al(acac)_3] < [Cu(acac)_2] < [Cr(acac)_3] < [Ru(acac)_3]$**.** For metal 2,2,6,6-tetramethyl-3,5-heptandionato the enthalpies of sublimation are in the order of $[Al(tmhd)_3] < [Cu(tmhd)_2] < [Cr(tmhd)_3] < [Fe(tmhd)_3] < [Mn(tmhd)_3] < [Ni(tmhd)_2]$. In case ruthenium precursors the enthalpy of sublimation lies between 86-116 $kJ \cdot mol^{-1}$.

The vapor pressures obtained using the Knudsen cell is combined with the TGA measurements to obtain the diffusion coefficients. The gaseous diffusion coefficient for well known organic compounds anthracene and pyrene in helium and nitrogen were also measured using TGA method. The experimental values for gaseous diffusion coefficient for these two substances agrees quite well with the estimated values from the well known correlation of Chapman & Enskog, Wilke & Lee and Fuller et al. for the organic compounds and also with the available literature values for these compounds.This showed that the goodness / quality of the proposed method. The gaseous diffusion coefficient for organometallic compounds in helium and nitrogen atmosphere was also determined and plotted as a function of temperature (T/K). For $[Cu(acac)_2]$, $[Ru(acac)_3]$, $[Ni(tmhd)_2]$ and $[Cr(tmhd)_3]$, the gaseous diffusion coefficient in nitrogen atmosphere could not be determined because the mass loss for these substances was very small at low temperatures. In such cases the gaseous diffusion coefficient was estimated using Chapman rigid sphere model. In absence of any experimental data or empirical correlation for the gaseous diffusion coefficient especially for organometallic compounds, the experimental values for the gaseous diffusion coefficient cannot be compared.

FUTURE WORK

The quartz crystal microbalance (QCM) has the advantage of measuring the weight changes in nano gram range. The low cost of the QCM compared to a conventional microbalance make this method attractive. In case of vapor pressure measurement, the effusing vapor of the substance is condensed on the QCM. The weight gain with time on the active surface of QCM is the mass loss rate from the effusion cell. For diffusion coefficient measurement the active surface of the QCM is coated with a thin film of the substance and the weight loss is determined in a particular atmosphere. The future work should in the direction of successful application QCM as a weighing device for the both the Knudsen effusion method and the gaseous diffusion coefficient measurements. Experiments for the measurement of gaseous diffusion coefficient using the QCM method is going on in our laboratory but further optimization of the method is needed in order to handle moisture sensitive substances. Further work is also needed in getting some empirical correlation for gaseous diffusion coefficient for organometallic compounds. After a reasonable amount of experimental data on gaseous diffusion

coefficient for organometallic compounds is collected. The approach of Chapman & Enskog, Wilke & Lee and Fuller et al. could be utilized in developing some empirical correlations for the gaseous diffusion coefficient of organometallic compunds.

REFERENCES

1. H. O. Pierson, "*Handbook of Chemical Vapor Deposition (CVD)*", Noyes Pub. / W. Andrew Pub., LLC, Norwich New York, USA. 1999.
2. D. L. Smith, *Thin-Film Deposition*", McGraw Hill, 1995.
3. M. Ohring, *Material Science of Thin Films*, 2nd Ed. AP, 2001.
4. H. Lamprey, *Ann. N. Y. Acad. Sci.*, **88**, (1960) 519.
5. K. Binnemans, *Handbook on the physics and chemistry of rare earths*, Elsevier, 2005.
6. R. E. Sievers, J. E. Sadlowski, *Science*, **201**, (1978) 217.
7. M. D. Rausch, J. M. Birmingham , *Ann. N. Y. Acad. Sci.*, **125**, (1965) 57.
8. E.F. Rivera, B. Atakan, and K. Kohse-Höinghaus, *Journal de Physique IV*, **11**, (2001) Pr3-629.
9. E.F. Rivera, B. Atakan, and K. Kohse-Höinghaus, *Proceedings of the CVD XVI/EUROCVD 14 Meeting, The Electrochemical Society*, Paris, (2003)1455.
10. A. Rautiainen, M. Lindblad, V. Backmann, R.L. Puurunen, *PCCP*, **4**, (2002) 2466.
11. R.G. Charles, P.G. Haverlack, *J.Inorg. Nucl. Chem.*, **31**, (1969) 995.
12. B. Atakan, and M. A. Siddiqi, *Proceedings of the Fifteenth European Conference on Chemical Vapor Deposition*, The Electrochemical Society Inc., U. S. A., **9** , (2005) 229.
13. N. E. Fedotava, N. V. Gelfond, I. K. Igumenov, A. N. Mikheev, N. B. Morozova, R. H. Tuffias, *Int. J. Therm. Sci.* **40**, (2001) 469.
14. N. E. Fedotava, N. V. Gelfond, I. K. Igumenov, A. N. Mikheev, N. B. Morozova, R. H. Tuffias, *Journal de Physique IV*, **9**, (1991) Pr8-251.
15. K. S. Chou, M. J. Hwang, M. Y. Shu, *Thermochimica Acta*, **233**, (1994) 141.

16. G. Wahl, W. Decker, M. Pulver, R. Stolle, O.Y. Gorbenko, A. R. Kaul, Y. Y. Erokhin, I. E. Graboy, M. Sommer, U. Vogt, *Physica C*, **209**, (1993), 195.

17. M. A. Siddiqi, B.Atakan, *J. Chem. Eng. Data*, **51**, (2006) 1092.

18. M. A. Siddiqi, R. A. Siddiqui, B.Atakan, *Surface and Coating Technology*, **201**, (2007) 9055.

19. A. Schneider, N. Popovska, I. Jipa, B. Atakan, M. A. Siddiqi, R. Siddiqui, U. Zenneck *Chemical Vapor Deposition*, **13**, (2007) 389.

20. D. Ambrose, in: B. Le Neindre, B. Vodar (Eds.), *Experimental Thermodynamics Vol. II*, Butterworths, London, (1975) p.607.

21. S. Vervekin, *Measurement of the thermodynamic properties of multiple phases, VII*, Elsevier, 2005

22. M. Knudsen, *Ann. Phys*. **34**, (1911) 593.

23. P. Atkins, J. de Paula, *Atkins´ Physical Chemistry*, Oxford University Press, 2002

24. P. Clausing, *Ann. Phys.* **12**, (1932) 961.

25. T. A. O'Donnell, *Aust. J. Chem.*, **8**, (1955) 485.

26. K. Motzfeldt, *J. Phy. Chem.*, **59**, (1955) 139.

27. C. I. Whitman, *J. Chem. Phy.*, **20**, (1952) 161.

28. K. D. Carlson, P. W. Giles, R. J. Thorn, *J. Chem. Phy.* **38**, (1963) 2064.

29. A. W. Searcy, R. A. McNees Jr., *J. Am. Chem. Soc.* **75**, (1953) 1578.

30. R. P. Iczkowski, J. L. Margrave, S. M. Robinson, **67**, (1963) 229.

31. D. W. Morecroft, *J. Chem. Eng. Data.*, **9**, (1964) 488.

32. E. M. Suuberg, V. Oja, *Anal. Chem.*, **69**, (1997) 4619.

33. H. G. Wiedemann, *Thermochimica Acta*, **3**, (1972) 355.

34. W. L. Winterbottom, J. P. Hirth, *J. Chem. Phys*. **37**, (1962) 784.

35. C. L. Rosen, *Rev. Sci. Inst.*, **31**, (1960) 837.

36. C. G. de Kruif, C. H. D. van Ginkel, *J. Physics E: Sci. Inst.*, **6**, (1973) 764.

37. O. T. Glukhova, N. M. Arkhangelova, A. B. Teplitsky, L. F. Sukhodub, I. K. Yanson, Miron Kaminski, *Thermochimica Acta*, **95,** (1985) 133.

38. M. A. Goodman, *J. Chem. Eng. Data*, **42**, (1997) 1227.

39. S. R. Dharwadkar, A. S. Kerkar, M. S. Samant, *Thermochimica Acta*, **217**, (1993) 175.

40. R. Vishwanathan, *Personal communication.*

41. P. G. Wahlbeck, *High Temperature Science*, **21**, (1986) 189.

42. D. M. Price, M. Hawkins, *Thermochimica Acta*, **315**, (1998) 19.

43. M. D. Nyman, S. B. Desu, C. H. Peng, *Chem. Mater.* **5**, (1993) 1636.

44. M. A. Siddiqi, B. Atakan, *Thermochimica Acta*, **452**, (2007) 128.

45. N. Pieterse, W. W. Focke, E. Vuorinen, I. Rácz, *Corr. Sci.* **48**, (2006) 1986.

46. B. J. Hinds, R. J. McNeely, D. B. Studebaker, T. J. Marks, T. P. Hogan, J. L. Schindler, C. R. Kannewurf, X. F. Zhang, D. J. Miller, *J. Mat. Res.*, **12**, (1997) 1214.

47. D. J. Hamilton, *J. Chromatography*, **195**, (1980) 75.

48. R. Fuchs, L. A. Peacock*, J. Am. Chem. Soc.*, **99**, (1977) 5524.

49. J. S. Chickos, S. Hosseini, D. G. Hesse, *Thermochimica Acta*, **249**, (1995) 41.

50. J. S. Chickos, D. G. Hesse, S. Hosseini, J. F. Liebman, G. D. Mendenhall, S. P. Verevkin, K. Rakus, H. D. Beckhaus, C. Rüchardt, *J. Chem. Thermodyn.*, **27**, (1995) 693.

51. J. S. Chickos, W. Hanshaw, *J. Chem. Eng. Data*, **49**, (2004) 77.

52. K. Ruzicka,, M. Fulem, V. Ruzicka, *J. Chem. Eng. Data*, **50**, (2005) 1956.

53. G. Thompson, *Chem. Rev.*, **38**, (1940) 1.

54. L. Riedel, *Chem.-Ing.-Tech.*, **26** (1954) 83.

55. Y. Nannoolal, Ph.d Thesis, University of Kwazulu-Natal, Durban Campus, 2006.

56. W. Wagner, *Cyrogenics*, **13**, (1973) 470.

57. J. Wisniak, *J. Ph. Equil. Diff.*, **22**, (2007) 623.

58. T. R. Marrero, E. A. Mason, J. Phys. Chem. Ref. Data, **1**, (1972) 3.

59. Chapman & Cowling "*The mathematical theory of nonuniform gases*" Cambridge University press, Great Britain, 1970.

60. E. N. Fuller, J.C. Giddings, *J. Gas Chromatography*, **3**, (1965) 222.

61. S.L. Seager, L.R. Greetson, J.C. Giddings*, J. Chem. Eng. Data,* **8**, (1963) 168.

62. R. F Barr, H. Watts, *J. Chem. Eng. Data*, **17**, (1972) 45.

63. E. R. Gilliland, *Ind. & Eng. Chem.*, **26**, (1934) 681.

64. B. E. Pauling, J. M. Prausnitz, J. P. O`Connell "*The properties of gasses and liquids*" p. 277, McGraw Hill, NY, 2000.

65. J. H. Arnold, *Ind. & Eng. Chem.*, **22**, (1930) 1091.

66. Sutherland, *Phil. Mag*., **36**, (1893) 504.

67. L. Andrussow, *Z. Elektrochem*. **54**, (1950) 566.

68. J. O. Hirschfelder, R. B. Bird, E. L. Spotz, *J. Chem. Phys.*, **16**, (1948) 968.

69. J. O. Hirschfelder, R. B. Bird, E. L. Spotz, *Chem. Rev.*, **44**, (1949) 205.

70. P. D. Neufeld, A. R. Jansen, A. R. Aziz, *J. Chem. Phys.,* **49**, (1975)1404.

71. N. H. Chen, D. F. Othmer, *J. Chem. Eng. Data*, **7**, (1962) 37.

72. C. R. Wilkee, C. Y. Lee, *Ind.& Eng. Chem.* **47**, (1955) 1253.

73. R.C. Reid, T. K. Sherwood "*The properties of gasses and liquids*" p. 277, McGraw Hill, NY, 1958.

74. E. N. Fuller, P. D. Schettler, J. C. Giddings, *Ind. Eng. Chem.* **58**, (1966)19.

75. E. P. Ney, F. C. Armistead, *Phys. Rev.*, **71**, (1947) 14.

76. J. C. Giddings, S. L. Seager, *Ind. & Eng. Chem. Fund.* **1**, (1962) 277.

77. A. P. Altshuller, I. R. Cohen, *Anal. Chem.* **32**, (1960) 802.

78. C. Y. Lee, C. R. Wilkee, *Ind. & Eng. Chem.* **46**, (1954) 2831.

79. R. E. Walker, A. A. Westenberg, *J. Chem. Phy.*, **29**, (1958) 1139.

80. P. H. Chen, J. M. Miao, C. S. Jian, *Rev. Sci. Instrum.* **67**, (1996) 2831.

81. G. Sauerbery, *Z. Phys*., **155**, (1959) 206.

82. J. M. P. Q. Delgado, M. A. Alves, J. R. F. Guedes de Carvalho, *J. Ph. Equil. & Diff.* **26**, (2005) 447.

83. J. M. P. Q. Delgado, M. A. Alves, *AIChE*, **45**, (1999) 2495.

84. R. B. Bird, W. E. Stewart, E. N. Lightfoot, "*Transport Phenomenon"*, John Wiley & Sons, New York, 2002.

85. L. Caldwell, *J. Chem. Eng. Data*, **29**, (1984) 60.

86. K. Cho, T. F. Irvine, J. Karni, *Intl. J. Heat Mass Transfer*, **35**, (1992) 957.

87. K. E. Gustafson, R. M. Dickhut, *J. Chem. Eng. Data*, **39**, (1994) 286.

88. S. Tashiro, N. Sagawa, *J. Nucl. Sci. Tech*., **38**, (2001) 551.

89. P. J. Gardner, S. R. Preston, *J.Chem.Soc. Faraday Trans.*, **88**, (1992) 1993.

90. R. Battino, E. Wilhelm, *Monathefte für Chemie*, **106**, (1975) 347.

91. G. A. M. Cummings, A. R. Ubbelohde , *J. Chem. Soc.*, 3751,1953.

92. A. Milanov, R. Bhakta, A. Baunemann, H. Becker, R. Thomas, P. Ehrhart, M. Winter, A. Devi, *Inorg. Chem.*, **45,** (2006)**,** 11008.

93. A. Milanov, R. Bhakta, R. Thomas, P. Ehrhart, M. Winter, R. Wasser, A. Devi, *J. Mater. Chem.*, **16**, (2006)**,** 437.

94. F. Reilmann, L.C. Salameh, N. Bahlawane, K. Kohse-Höinghaus, S. Fahrenholz, S. Schulz, *Sixteenth European Conference on Chemical Vapor Deposition September 2007*, Den Haag, Netherlands.

95. B. Atakan, N. Popovska, K. Michkova, I. Jipa, M. Aslam Siddiqi, R. A. Siddiqui, U. Zenneck, *Sixteenth European Conference on Chemical Vapor Deposition*

September 2007, Den Haag, Netherlands.

96. I. Jipa, K. Michkova, N. Popovska, U. Zenneck, *Sixteenth European Conference on Chemical Vapor Deposition September 2007*, Den Haag, Netherlands.
97. N. Roth, A. Jakob, T. Waechtler, S. Schulz, T. Gessner, H. Lang, *Surface and Coating Technology*, **201**, (2007) 9089.
98. G. Beech, R. M. Lintonbon, Therm*ochimica Acta*, **3**, (1971) 97.
99. Y. Pauleau, A.Y. Fasasi, *Chem. Mater.* **3**, (1991) 45.
100. M. Lashdaf, T. Hatanpää, M. Tiitta, *J. Therm. Anal.*, Cal. **64**, (2001) 1171.
101. V. A.Varnek, I. K. Igumenov, L.N. Mazalov, *J.Struct. Chem.*, **42** (2001) 860.
102. P. O Brien, Y. Li, M. Afzaal, *J. Mater. Chem.*, **16**, (2006) 2175.
103. J.P Murray, J.O. Hill, *Thermochimica Acta*, **109**, (1987) 383.
104. T. Arii, A. Kishi, *J. Therm. Anal. Cal.*, **83**, (2006) 253.
105. G.V. Bazuev, L. D. Kurbatova, *Russ. Chem. Rev.*, **62**, (1993) 981.
106. J. N. Hoene, R. G. Charles, W. M. Hickman , *J.Phys. Chem.*, **62**, (1958) 1098.
107. E. Hosono, S. Fujihara, M. Onuki, T. Kimura, *J. Am. Ceram. Soc.* **87**, (2004) 1785.
108. D. P. Gardon, Coordin. *Chem. Rev.*, **4**, (1969) 1.
109. V. A. Logvinenko, N. E. Fedotova, L K. Igumenov , G. V. Gavrilova, *J. Therm. Anal.*, 34, (1988) 259.
110. B. D. Fahlman, A. R. Barron, *Adv. Mater. Opt . Electron.,* **10**, (2000) 223.
111. J-K. Kang, S-W. Rhee, *J. Mater. Res.* **15**, (2000) 1828.
112. R. Sabah, An Xu-wu, J. S. Chickos, M. L. Planas Leitao, M.V. Roux, L. A. Torres, *Thermochimica Acta*, **331**, (1999) 93.
113. R. Bender, V. Bieling, G. Maurer, *J. Chem. Thermodyn*., **15**, (1983) 585.
114. J. D. Kelley, F. O. Rice, *J. Phys. Chem*. **68**, (1964) 3794.
115. A. B. Macknick, J. M. Prausnitz, *J. Chem. Eng. Data*, **24**, (1979) 175.

116. V. Oja, E. M. Suuberg, *J. Chem. Eng. Data,* **43**, (1998) 486.

117. X. Chen, V. Oja, W. G. Chan, M. R. Hajaligol, *J. Chem. Eng. Data*, **51**, (2006) 386.

118. P. C. Hansen, C. A. Eckert, *J. Chem. Eng. Data*, **31**, (1986) 1.

119. K. Sasse, J. Jose, J.-C. Merlin, *Fluid Phase Equilibria,* **42**, (1988) 287.

120. W. J. Sonnefeld, W. H. Zoller, W. E. May, *Anal. Chem*., **55**, (1983) 275.

121. R. S. Bradley, T. G. Cleasby, J. Chem. Soc. **2**, (1953) 1690.

122. L. Malaspina, G. Bardi, R. Gigli, J. Chem. Thermodyn. **6**, (1974) 1053.

123. N. K. Smith, R. C. Stewart Jr., A. G. Osborn, D. W. Scott, J. Chem. Thermodyn., **12** (1980) 919.

124. P. P. Semyannikov, I. K. Igumenov, S. V. Trubin, T. P. Chusova, Z. I. Semenova , *Thermochimica Acta*, **451**, (2006) 91.

125. J. Sachindis, J. O. Hill, *Thermochimica Acta*, **35**, (1980) 59.

126. I. P. Malkerova, A. S. Alikhanyan, V. B Lazarev, V. A. Bogdanov, V. I. Gorgoraki, Ya. Kh. Grinberg, *Russ. J. Phys. Chem.,* **292**, (1987) 376 (Engl.Transl.).

127. R. Teghil, D. Ferro, M. Pelino, , *Thermochimica Acta*, **44**, (1981) 213.

128. V. B Lazarev, J. H. Greenberg, Z. P. Ozerova, G. A.Sharpataya, *J. Therm. Ana.,* **33**, (1988) 797.

129. E. W. Berg, J. T. Truemper, *Anal. Chim. Acta,* **32**, (1965) 245.

130. I. P. Malkerova, A. S. Alikhanyan, V. G. Sevastyanov, Ya. Kh. Grinberg, V. I. Gorgoraki, *J. Inorg. Chem.USSR,,* **35** (1990) 413 (Engl.Transl.).

131. P. P. Semyannikov, I. K. Igumenov, S. V. Trubin, T. P. Chusova, Z. I. Semenova , *Thermochimica Acta*, **432** , (2005) 91.

132. R. Pankajavalli, C. Mallika, O. M.Shreedharan, P. AntonyPremkumar, K. S. Nagaraja, V. S. Rangunath, *Chem. Engg. Sci.,* **57**, (2002) 3603.

133. T. P. Melia, R. Merrifield, *J. Inorg. Nucl. Chem.,* **32**, (1970) 1489.

134. A. G. Nasibulin, P. P. Ahonen, O. Richard, E. I. Kauppinen, I. S. Altman, *J. Nanoparticle Research,* **3**, (2001) 385.

135. D. Tonneau, R. Pierrisnard, H. Dallaporta, W. Marine, *Journal de Physique IV,* **5**, (1995) C5-629.

136. M. A. V. Ribeiro da Silva, E. Giera, M. J. S. Monte, *J. of Alloys and Compounds,* **197**, (1993) 105.

137. A. F. Bykov, N. B. Morozova, I. K. Igumenov, S. V. Sysoev, *Journal of Thermal Analysis,* **46**, (1996) 1551.

138. J. L .Wood, M. M. Jones, *Inorg. Chem.* **3**, (1964) 1533.

139. P. P. Semyannikov, I. K. Igumenov, S. V. Trubin, I. P. Asanov, *J.Phys.France IV*, **11** (2001) 995.

140. R. G. Charles, M. A. Pawlikowski, *J.Phys. Chem.*, **62**, (1958) 440.

141. H. R. Brunner, B. J. Curtis, *Journal of Thermal Analysis*, **5**, (1973) 111.

142. P. Tobaly, G. Lanchec, *J. Chem. Thermodynamics*, **25**, (1993) 503.

143. S.Yuhya, K. Kikuchi, M. Yoshida, K. Sugawara, Y. Shiohara, *Mol. Cryst. Liq. Cyrst.*, **184**, (1990) 231.

144. I. K. Igunov, Yu. V. Chumachenko, S. V. Zemskov, *Khim. Termodin. Termokhim.*, **65**, (1979) 6 (Russian).

145. E. Waffenschmidt, J. Musolf, M. Heuken, K. Heime., *Journal of Superconductivity*, **5**, (1992) 119.

146. J. F. Cordes, S. Schreiner, *Zeitschrift für anorganische und allgemeine Chemie,* **299** (1959) 87.

147. L. A. T. Gomez, G. B. Rodriguez, F. M. Ruiz., *Thermochimica Acta*, **124**, (1988) 179.

148. Jr. E. Mack, *J. Am. Chem. Soc.*, **47**, (1925**)** 2468.

149. R. J. Goldstein, H. H. Cho, *Exp. Thermal & Fluid Sci.*, **10,** (1995) 416.

APPENDIX A

Table A1: Clausing correction factor

Hole Dia. (mm)	Thickness (mm)	l/r	Clausing Factor
0.416	0.07	0.33653846	0.854382
0.509	0.07	0.27504912	0.877606
0.513	0.07	0.27290448	0.878443
0.517	0.07	0.27079304	0.879269
0.656	0.07	0.21341463	0.902402
0.678	0.07	0.20648968	0.905283
0.691	0.07	0.20260492	0.906907
0.696	0.07	0.20114943	0.907518
0.703	0.07	0.19914651	0.908359
0.715	0.07	0.1958042	0.909766
0.719	0.07	0.19471488	0.910225
0.795	0.08	0.20125786	0.907472

Table A2: Pyrene - Details for Knudsen cell measurements

Hole Dia.(mm)	Time (hr)	Mass.Evap. (mg)	Temperature (K)	1/T (1/K)	Vapor Pressure (Pa)
0.715	15.15	5.08	341.45	0.0029287	0.075
0.715	15.175	11.38	351.05	0.0028486	0.171
0.715	2.15	8.07	369.85	0.0027038	0.882
0.691	3.2	18.6	373.95	0.0026742	1.475
0.715	1.6	13.34	379.55	0.0026347	1.974
0.691	1.65	30.48	383.95	0.0026045	4.727
0.715	1.125	25.17	389.05	0.0025704	5.393
0.691	1.89	61.53	392.25	0.0025494	8.464
0.715	0.958	41.91	398.55	0.0025091	10.670
0.691	1.25	78.95	402.05	0.0024873	16.624
0.416	1.116	39.27	408.05	0.0024507	27.310

Table A3: Anthracene - Details for Knudsen cell measurements

Hole Dia.(mm)	Time (hr)	Mass.Evap. (mg)	Temperature (K)	1/T (1/K)	Vapor Preesure (Pa)
0.691	15.45	6.25	339.25	0.0029477	0.104
0.691	4.12	4.57	348.35	0.0028707	0.289
0.719	4.12	5.34	350.92	0.0028497	0.312
0.691	3.55	7.76	356.45	0.0028054	0.577
0.719	1.13	5.17	360.44	0.0027744	1.113
0.715	1.175	4.65	360.45	0.0027743	0.978

0.678	2.87	16.34	365.66	0.0027348	1.580
0.715	1.3	9.43	369.85	0.0027038	1.816
0.678	2.44	26.98	373.95	0.0026742	3.110
0.656	1.975	23.4	376.95	0.0026529	3.586
0.715	1.208	19.84	379.55	0.0026347	4.164
0.678	1.99	47.93	383.95	0.0026045	6.860
0.656	1.35	35.81	386.45	0.0025877	8.130
0.513	1.025	17.38	389.05	0.0025704	8.759
0.513	1.158	21.58	389.05	0.0025704	9.624
0.678	1.67	86.28	392.95	0.0025449	14.86
0.513	1.116	26.03	393.75	0.0025397	12.115
0.513	1	23.93	393.75	0.0025397	12.437
0.715	0.94	63.93	398.05	0.0025122	17.633
0.513	1.23	42.78	398.55	0.0025091	18.137
0.513	0.95	33.62	398.55	0.0025091	18.5

Table A4: $[Al(acac)_3]$- Details for Knudsen cell measurements

Hole Dia.(mm)	Time (hr)	Mass Evap. (mg)	Temperature (K)	1/T (1/K)	Vapor Pressure (Pa)
0.795	1.05	3.18	361.47	0.00276648	0.44
0.795	3.7	1.61	345.8	0.00289184	0.063
0.93	3.27	14.76	362.3	0.00276014	0.479
0.93	2.26	3.46	353.94	0.00282534	0.16
0.93	2.95	1.98	345.58	0.00289369	0.069
0.678	2.47	34.64	379.03	0.00263831	2.93
0.678	2.81	6.77	362.3	0.00276014	0.493
0.678	2.33	59.15	387.39	0.00258138	5.37
0.678	4.2	23.69	370.66	0.00269789	1.17
0.678	1.61	79.88	395.75	0.00252685	10.59
0.691	1.81	83.79	392.95	0.00254485	9.48
0.691	1.53	34.21	383.95	0.00260451	4.53
0.691	15.05	44.58	365.66	0.00273478	0.586
0.691	20.38	20.31	356.45	0.00280544	0.195
0.691	1.42	138.55	402.95	0.0024817	20.23
0.691	2.15	17	373.95	0.00267415	1.58

Table A5: $[Cr(acac)_3]$ - Details for Knudsen cell measurements

Hole Dia.(mm)	Time (hr)	Mass Evap. (mg)	Temperature (K)	1/T (1/K)	Vapor Pressure (Pa)
0.795	1.29	4.93	383.12	0.00261015	0.562
0.795	1.55	15.96	394.91	0.00253222	1.53
0.795	1.5	34.62	401.6	0.00249004	3.48
0.795	3.41	1.15	362.3	0.00276014	0.048
0.795	3.44	3.4	370.66	0.00269789	0.143

0.678	2.33	35.51	404.11	0.00247457	3.17
0.678	2.16	2.8	379.03	0.00263831	0.261
0.678	1.26	4.49	387.39	0.00258138	0.724
0.691	19.35	16.3	373.95	0.00267415	0.162
0.691	1.8	12.19	392.95	0.00254485	1.28
0.691	1.41	23	402.05	0.00248725	3.25
0.691	22.33	3.21	356.45	0.00280544	0.027
0.691	1	31.58	410.75	0.00243457	6.33
0.691	14.93	43.31	383.95	0.00260451	0.57

Table A6: [$Cu(acac)_2$] - Details for Knudsen cell measurements

Hole Dia.(mm)	Time (hr)	Mass Evap. (mg)	Temperature (K)	1/T (1/K)	VaporPressure (Pa)
0.715	17	18.3	367.65	0.00271998	0.022
0.715	1.7	9.31	405.05	0.00246883	1.184
0.715	1.53	18.04	414.35	0.00241342	2.573
0.715	1.708	37.06	423.85	0.00235933	4.798
0.715	1.85	76.66	433.65	0.00230601	9.27
0.715	1.28	113.51	442.85	0.0022581	19.9
0.715	16.5	13.52	386.45	0.00258766	0.172
0.715	5.18	9.67	395.55	0.00252813	0.398
0.715	18.01	5.93	376.95	0.00265287	0.068
0.715	4.3	14.1	400.64	0.00249601	0.705
0.715	17.679	9.3	381.83	0.00261897	0.11
0.715	23.88	1.87	363.02	0.00275467	0.016
0.715	18.36	3.5	372.42	0.00268514	0.039

Table A7: [$Ru(acac)_3$] - Details for Knudsen cell measurements

Hole Dia.(mm)	Time (hr)	Mass Evap. (mg)	Temperature (K)	1/T (1/K)	Vapor Pressure (Pa)
0.719	50.12	8.80	393.75	0.0025397	0.029
0.719	17.82	4.02	398.51	0.0025093	0.038
0.719	23.18	7.75	403.26	0.0024798	0.057
0.715	7.54	4.56	408.02	0.0024509	0.106
0.715	21.36	17.44	412.78	0.0024226	0.142
0.715	2.17	5.40	417.54	0.0023950	0.443
0.715	2.62	8.66	422.30	0.0023680	0.592
0.715	2.07	10.24	427.15	0.0023411	0.891
0.715	1.71	13.17	431.81	0.0023158	1.395
0.715	1.06	10.71	436.57	0.0022906	1.841
0.715	0.99	19.14	441.33	0.0022659	3.530

Table A8: [Fe(tmhd)$_3$] - Details for Knudsen cell measurements

Hole Dia.(mm)	Time (hr)	MassEvap. (mg)	Temperature / K	1/T	Vapor Pressure (Pa)
0.715	1.63	25.72	391.23	0.00255604	2.199
0.715	1.35	31.91	395.93	0.0025257	3.301
0.715	1.625	16.23	386.53	0.00258712	1.38
0.715	2.53	13.92	381.83	0.00261897	0.758
0.715	6.74	9.04	376.95	0.00265287	0.341
0.715	6.86	6.65	367.72	0.00271946	0.131
0.715	1.26	87.39	405.34	0.00246706	9.81
0.715	3.65	6.48	372.42	0.00268514	0.241
0.696	1.6	10.13	384.23	0.00260261	0.927
0.696	1.13	12.81	389.05	0.00257036	1.665
0.696	15.66	9.71	360.45	0.00277431	0.087
0.513	0.84	57.38	408.05	0.00245068	19.567
0.513	0.88	13.56	398.55	0.0025091	4.354
0.513	1.15	6.88	389.05	0.00257036	1.676
0.696	3.125	3.53	369.85	0.0027038	0.162
0.696	1.6	5.74	379.55	0.0026347	0.519
0.696	18.15	2.14	351.05	0.0028486	0.016
0.719	21.1	5.41	355.68	0.00281152	0.033
0.719	52.45	3.88	341.45	0.00292869	0.008

Table A9: [Mn(tmhd)$_3$] - Details for Knudsen cell measurements

Hole Dia.(mm)	Time (hr)	Mass Evap.(mg)	Temperature (K)	1/T (1/K)	Vapor Pressure (Pa)
0.715	1.34	28.23	395.93	0.0025256	2.959
0.715	1.63	14.54	386.53	0.0025871	1
0.715	3.21	8.73	377.13	0.0026516	0.372
0.715	1.75	24.2	391.23	0.0025560	1.924
0.715	5.53	5.18	367.72	0.002719	0.126
0.715	2.36	10.86	381.83	0.0026189	0.633
0.715	1.425	49.02	400.64	0.0024960	4.866
0.715	1.2	68.34	405.34	0.0024670	8.103
0.715	3.69	5.38	372.42	0.0026851	0.198
0.513	1.075	36.07	408.03	0.0024508	9.637
0.715	6.38	7.18	369.95	0.0027030	0.152
0.715	2.15	17.94	388.98	0.0025708	1,158
0.513	1.075	34.77	408.03	0.0024508	9.29
0.715	1.125	28.93	398.51	0.0025093	3.628
0.715	1.18	41.88	403.27	0.0024797	5.023
0.715	4.74	15.84	379.48	0.0026351	0.459
0.719	20.38	7.43	360.44	0.0027743	0.048
0.719	49.23	6.31	350.92	0.0028496	0.0167
0.719	23.2	13.77	365.2	0.0027382	0.079
0.719	46.18	9.36	355.68	0.0028115	0.0266

Table A10: [Ni(tmhd)$_2$] - Details for Knudsen cell measurements

Hole Dia.(mm)	Time (hr)	Mass Evap. (mg)	Temperature (K)	1/T (1/K)	Vapor Pressure (Pa)
0.715	5.91	5.56	377.13	0.0026516	0.153
0.715	4	10	386.53	0.0025871	0.413
0.715	1.62	8.69	391.23	0.0025560	0.891
0.715	1.11	5.33	393.75	0.0025397	0.798
0.513	1.05	5.75	398.15	0.0025116	1.852
0.715	1.65	18.57	400.64	0.0024960	1.889
0.513	1.08	8.49	403.27	0.0024797	2.668
0.513	1.05	12.74	408.03	0.0024508	4.156
0.719	15.88	12.34	374.72	0.0026687	0.125
0.719	5.44	23.68	393.75	0.0025397	0.718
0.719	6.54	19.74	388.92	0.0025712	0.484
0.719	4.025	18.79	393.75	0.0025397	0.772
0.719	17.38	15.14	374.72	0.0026687	0.140
0.719	42.43	5.77	360.43	0.0027745	0.021
0.719	38.83	10.19	365.19	0.0027383	0.041
0.719	3.9	8.5	384.23	0.0026026	0.358
0.719	16.3	8.66	369.95	0.0027031	0.084
0.719	5.84	6.83	379.47	0.0026353	0.189

Table A11: [Al(tmhd)$_3$] - Details for Knudsen cell measurements

Hole Dia.(mm)	Time (hr)	Mass Evap. (mg)	Temperature (K)	1/T (1/K)	Vapor Pressure (Pa)
0.719	1.35	45.75	398.05	0.00251225	4.836
0.719	1.18	18.17	388.96	0.00257096	2.166
0.715	2.06	14.06	379.47	0.00263525	0.959
0.715	2.45	6.28	369.95	0.00270307	0.356
0.715	1.125	12.1	384.23	0.00260261	1.525
0.715	25.04	5.8	350.92	0.00284965	0.031
0.715	39.81	7.45	346.16	0.00288884	0.025
0.715	6.61	6.85	365.19	0.0027383	0.143
0.715	65.19	6.06	341.4	0.00292912	0.012
0.509	1.61	37.79	403.26	0.00247979	6.949
0.509	0.98	39.08	408.22	0.00244966	11.88
0.715	15.84	6.76	355.68	0.00281152	0.058
0.509	1.058	5.14	412.78	0.0024226	14.607

Table A12: [Cr(tmhd)$_3$] - Details for Knudsen cell measurements

Hole Dia.(mm)	Time (hr)	MassEvap. (mg)	Temperature (K)	1/T (1/K)	Vapor Pressure (Pa)
0.715	14.03	5.36	355.66	0.0028117	0.051
0.715	1.66	21.49	388.98	0.0025708	1.801
0.715	1.44	8.64	379.47	0.0026353	0.827

0.715	1.86	22.2	384.23	0.0026026	1.651
0.715	1.95	9.57	374.71	0.0026687	0.67
0.715	19.5	4.36	350.92	0.0028497	0.029
0.715	1.041	29.22	393.74	0.0025397	3.94
0.715	19.87	13.75	360.43	0.0027745	0.093
0.715	16.81	19.24	365.19	0.0027383	0.154
0.715	6.46	18.3	369.95	0.0027031	0.385
0.715	46.2	7.6	346.16	0.0028888	0.0216
0.715	1	17.57	398.5	0.0025094	5.083

Table A13: [Cu(tmhd)$_2$] - Details for Knudsen cell measurements

Hole Dia.(mm)	Time (hr)	Mass Evap. (mg)	Temperature (K)	1/T (1/K)	Vapor Pressure (Pa)
0.703	1.25	32.04	398.5	0.0025094	4.413
0.703	1.05	74.71	408.2	0.0024498	12.38
0.703	1.77	79.8	403.64	0.0024775	7.842
0.703	17.02	15.36	365.19	0.0027383	0.149
0.703	5.94	11.74	369.95	0.0027031	0.329
0.703	4.49	34.55	384.23	0.0026026	1.266
0.703	0.91	19.69	393.74	0.0025397	3.70
0.703	7.77	23.18	374.71	0.0026687	0.501
0.703	1.39	17.47	388.98	0.0025708	2.149
0.703	3.25	12.09	379.47	0.0026353	0.629

Table A14: [Ru(cp)$_2$] - Details for Knudsen cell measurements

Hole Dia.(mm)	Time (hr)	Mass Evap. (mg)	Temperature (K)	1/T (1/K)	Vapor Pressure (Pa)
0.703	2.02	14.45	331.88	0.0030131	1.539
0.517	1.92	18.12	341.4	0.0029291	3.933
0.517	1.18	7.43	336.34	0.0029732	2.604
0.517	1.04	16.82	346.16	0.0028888	6.79
0.517	1.18	24.57	350.92	0.0028497	24.57

Table A15: [Ru(C_7H_{11})$_2$] - Details for Knudsen cell measurements

Hole Dia. (mm)	Time (hr)	Mass Evap. (mg)	Temperature (K)	1/T (1/K)	Vapor Pressure (Pa)
0.517	1.35	4.56	331.88	0.0030131	1.237
0.517	1.34	6.45	336.64	0.0029705	1.774
0.517	1.01	9.28	341.4	0.0029291	3.392
0.517	1.11	16.04	346.16	0.0028888	5.375

0.517	1.26	25.22	350.92	0.0028496	7.502
0.517	1.25	67.53	360.43	0.0027744	20.63

Table A16: [Ru(Cp)($CpCH_2N(CH_3)_2$)] - Details for Knudsen cell measurements

Hole Dia.(mm)	Time (hr)	Mass Evap. (mg)	Temperature (K)	1/T (1/K)	Vapor Pressure (Pa)
0.517	2.15	10.52	331.88	0.003013137	1.798
0.517	1.77	13.32	336.64	0.002970532	2.788
0.517	1.18	19.67	346.16	0.002888838	6.264
0.517	1.01	23.46	350.92	0.002849652	8.755
0.517	1.04	10.82	341.4	0.002929115	3.88
0.517	3.26	8.48	327.13	0.003056889	0.951

Table A17: [$Ru(OC_6H_9)_2$] -Details for Knudsen cell measurements

Hole Dia.(mm)	Time (hr)	Mass Evap. (mg)	Temperature (K)	1/T (1/K)	Vapor Pressure (Pa)
0.517	2.01	8.84	369.95	0.0027031	1.687
0.517	1.05	30.86	388.98	0.0025708	11.6
0.703	3.3	12.66	360.43	0.0027745	0.763
0.703	1.51	25.98	374.71	0.0026687	3.474
0.703	0.95	25.61	379.47	0.0026353	5.502

Table A18: [Ru (Benzene) (2, 3-dimethyl butadiene)] -Details for Knudsen cell measurements

Hole Dia.(mm)	Time (hr)	Mass Evap. (mg)	Temperature (K)	1/T (1/K)	Vapor Pressure (Pa)
0.513	0.933	4.35	331.89	0.0030130	1.854
0.513	0.633	4.41	336.65	0.0029704	2.79
0.513	0.775	1.14	322.37	0.0031020	0.576
0.513	2.1	1.13	317.62	0.0031484	0.209

Table A19: [Ru (Benzene) (Isoprene)] - Details for Knudsen cell measurements

Hole Dia.(mm)	Time (hr)	Mass Evap. (mg)	Temperature (K)	1/T (1/K)	Vapor Pressure (Pa)
0.513	0.725	13.82	336.64	0.0029705	7.185
0.513	0.833	4.96	327.13	0.0030569	2.405
0.513	0.791	1.68	317.61	0.0031485	0.845
0.513	0.691	2.54	322.37	0.0031020	1.437

Table A21: [Ru(Benzene) (1, 3-Cyclohexadiene)] - Details for Knudsen cell measurements

Temperature (K)	1/T (1/K)	Vapor Pressure (Pa)
336.64	0.0029705	7.185
327.13	0.0030569	2.405

Table A22: Estimated vapor pressure values using thermogravimetric method.

Substance	Temperature / K	D_{AB} / m^2 / s	Vapor Pressure (Pa)
[Ru (Toluene) (1,3 cyclohexadiene)]	370	3.21×10^{-5}	24.5
	380.1	3.35×10^{-5}	42.6
	389.6	3.49×10^{-5}	74.2
	399.7	3.65×10^{-5}	128.5
	409.3	3.80×10^{-5}	213.2
[Ru (Toluene) (2,3 dimethyl1,3 butanediene)]	329.8	2.64×10^{-5}	1.4
	348.9	2.90×10^{-5}	6.8
	368	3.18×10^{-5}	23.9
	387.3	3.46×10^{-5}	78.3
	406.6	3.75×10^{-5}	245.8
	426.1	4.07×10^{-5}	692.2
[Ru(Benzene) (1, 3-Cyclohexadiene)]	349.4	2.91 x 10-5	5.1
	369	3.19 x 10-5	17.7
	388.7	3.48 x 10-5	78.6
	408.2	3.78 x 10-5	207.1
	370	3.21 x 10-5	24.5

Table A23: Experimental Diffusion coefficient for poly aromatic hydrocarbon

Studied system	Average temperature (K)	Average diffusion coefficient (cm^2 / s)
Anthracene-N_2	380.15 398.51 417.06	0.1141 0.1198 0.1253
Anthracene-He	349.33 358.93 368.57 378.25 387.93 397.65 407.38	0.2495 0.2880 0.3065 0.3220 0.3377 0.3550 0.3782
Pyrene-N_2	377.88 386.89 395.90 404.97 414.09	0.0975 0.1015 0.1087 0.1155 0.1181
Pyrene-He	378.52 388.26 398.01 407.78 417.56	0.2641 0.2768 0.2801 0.2891 0.2901

Table A24: Experimental Diffusion coefficient for [M(acac)$_n$]

Studied system	Average temperature (K)	Average diffusion coefficient (cm^2 / s)
[Al(acac)$_3$]-N_2	379.05 396.68 415.01 433.51 452.28	0.1665 0.2282 0.2623 0.3135 0.3549
[Al(acac)$_3$]-He	366.00 385.75 405.88 425.35 443.95	0.3307 0.4168 0.5048 0.5992 0.6587
[Cr(acac)$_3$]-N_2	397.45 415.40 433.81 452.49 471.03	0.0613 0.0684 0.0682 0.0683 0.0708
[Cr(acac)$_3$]-He	387.55 407.35 426.18 445.15 465.10	0.1340 0.1320 0.1476 0.1552 0.1615
[Cu(acac)$_2$]-He	338.34 398.02 407.85 417.17 427.35 437.14	0.3185 0.3511 0.3715 0.3852 0.3939 0.4289
[Ru(acac)$_3$]-He	398.04 407.77 417.17 427.29 436.80	0.5097 0.5417 0.5567 0.5849 0.6147

Table A25: Experimental diffusion coefficient for [M(tmhd)$_n$]

Studied system	Average temperature (K)	Average diffusion coefficient (cm² / s)
[Fe(tmhd)$_3$]-N_2	378.42 387.39 396.43 405.50 414.66	0.0931 0.0967 0.1017 0.1076 0.1117
[Fe(tmhd)$_3$]-He	378.87 388.61 398.35 408.10	0.1948 0.2107 0.2207 0.2313
[Mn(tmhd)$_3$]-N_2	387.18 396.20 405.26 414.43	0.0706 0.0736 0.0744 0.0747
[Mn(tmhd)$_3$]-He	378.81 388.51 398.26 408.21	0.1646 0.1700 0.1738 0.1713
[Cr(tmhd)$_3$]-He	348.94 368.24 383.42 387.88 393.14	0.0681 0.1120 0.1334 0.1450 0.1527
[Ni(tmhd)$_2$]-He	378.69 388.47 398.23 407.96	0.2089 0.2253 0.2324 0.2410
[Al(tmhd)$_3$]-N_2	360.69 378.60 396.80	0.0613 0.0779 0.0840

$[Al(tmhd)_3]$-He	368.32 387.67 407.08	0.1457 0.1491 0.1656
$[Cu(tmhd)_2]$-He	370.24 389.95 409.64	0.1666 0.1817 0.1855
$[Cu(tmhd)_2]$-N_2	382.65 401.41 420.40	0.0524 0.0609 0.0629

Table A26: Experimental diffusion coefficient for $[M(cp)_n]$

Studied system	**Average temperature / K**	**Average diffusion coefficient / cm² / s**
$[Ru(cp)_2]$-N_2	325.62 334.23 342.85 351.61 360.00	0.0408 0.0429 0.0487 0.0510 0.0542

Table A27: Estimated gaseous diffusion coefficient

Studied system	Average temperature (K)	Average diffusion coefficient (cm^2 / s)
$[Cu(acac)_2]$-N_2	350 360 370 380 390 400 410	0.1006 0.1050 0.1094 0.1139 0.1184 0.1230 0.1276
$[Ru(acac)_3]$-N_2	350 360 370 380 390 400 410	0.1438 0.1500 0.1563 0.1627 0.1691 0.1757 0.1823
$[Ni(tmhd)_2]$-N_2	350 360 370 380 390 400 410	0.0667 0.0696 0.0725 0.0755 0.0785 0.0815 0.0846
$[Cr(tmhd)_3]$-N_2	350 360 370 380 390 400 410	0.04179 0.04359 0.04540 0.04728 0.04915 0.05106 0.05298

APPENDIX B

Table B1: The Antoine constants and the enthalpies of sublimation for the substances studied in this work

Substance	A_i	B_i	$\Delta_{sub}H_m$ (Temperature) / kJ · mol^{-1}
Anthracene	11.09± 0.21	5100.00±80.66	97.64± 1.27* (339-399 K)
			100 ± 2.8[a] (318-363 K)
			94.6[b] (354-399 K)
			98.5[c] (342-353 K)
			94.8[d] (358-392 K)
Pyrene	11.62±0.34	5393.20±131.75	103.25±2.05* (341-418 K)
			103.1 ± 6.5[a] (308-398 K)
			97.7[e] (353-413 K)
			91.2[f] (283-323 K)
			93.9[g] (345-358 K)
[Al(acac)$_3$]	13.55±0.27	6126.81±101.86	117.31±1.67* (345-410 K)
			111 ± 4[h] (345-410K)
			105 ±2[h] (388-413 K)
			47 ± 1[i] (298 K)
			102 ± 3.2[j] (432-464 K)
[Cr(acac)$_3$]	14.16±0.29	6695.43±112.42	128.20±1.60* (345-410 K)
			127.28 ± 0.22[k] (320-478 K)
			113.0 ± 4.8[j] (357-486 K)
			111.6 ± 3.0[l] (374-418 K)
			110.77 ± 0.2[m] (320-478 K)
[Cu(acac)$_2$]	12.67± 0.21	6350.2±82.99	121.58±1.40* (363-443 K)
			57±1[i] (298 K)
			79.9[n] (353-453 K)
[Ru(acac)$_3$]	15.14±0.74	7772.40±309.39	148.79±5.35* (394-441 K)
			139.7 ± 2.5[o] (398-413 K)
			127.0 ±0.9[p] (423-493 K)
[Fe(tmhd)$_3$]	14.93±0.45	6891.10±170.67	131.94±4.00* (341-408K)
			106.69[q] (313-523K)
[Mn(tmhd)$_3$]	15.76±0.24	7238.45±92.03	138.59±5.48* (350-408K)
[Ni(tmhd)$_2$]	15.53±0.53	7299.91±204.16	139.77±5.27* (360-408K)
[Al(tmhd)$_3$]	13.32±0.31	6221.52±116.29	119.12±2.72* (341-412K)
[Cr(tmhd)$_3$]	14.50±0.57	6656.58±201.52	127.45±2.81* (350-398K)

[Cu(tmhd)$_2$]	14.37±0.54	6649.99±208.91	127.38±2.33*	(365-408K)
			124.65[r]	(350-450 K)
			106.09[s]	(365-550 K)
			111.85[t]	(365-550 K)
[Ru(cp)$_2$]	13.00±0.84	5249.99±285.57	100.52±1.86*	(331-351K)
			98.74[u]	(356-370K)
[Ru(C$_7$H$_{11}$)$_2$]	12.54±0.53	5133.29±182.97	98.28± 0.66*	(331-360K)
[Ru(cp)(cpCH$_2$N(CH$_3$)$_2$)]				
	10.80±0.63	4505.81±204.52	86.27±0.83*	(327-350K)
[Ru(OC$_6$H$_9$)$_2$]	13.45±0.97	5974.61±364.88	114.39±1.81*	(360-380K)
[Ru(benzene) (Isoprene)]				
	13.97±0.68	5418.46±222.07	91.58±1.25*	(317-337K)
[Ru(benzene) (2-3,dimethyl butadiene)]				
	15.60±1.97	6095.74±646.49	116.71± 3.87*	(317-332K)

*) This work; **a**) Ref. [113]; **b**) Ref. [114]; **c**) Ref. [115]; **d**) Ref. [116]; **e**) Ref. [120]; **f**) Ref. [121]; **g**) Ref. [122]; **h**) Ref. [125]; **i**) Ref. [127]; **j**) Ref. [128]; **k**) Ref. [131]; **l**) Ref. [132]; **m**) Ref. [133]; **n**) Ref. [134]; **o**) Ref. [136]; **p**) Ref. [137] ; **q**) Ref. [141]; **r**) Ref. [142]; **s**) Ref. [143]; **t**) Ref. [144]; **u**) Ref. [146].

Table B2: The constants for the equation of temperature dependence of diffusion coefficient

Studied system	A	n
Anthracene-N_2	7.56×10^{-7}	2
Anthracene-He	2.20×10^{-6}	2
Pyrene-N_2	6.899×10^{-7}	2
Pyrene-He	1.787×10^{-6}	2
[Al(acac)$_3$]-N_2	2.375×10^{-10}	3.45
[Al(acac)$_3$]-He	1.547×10^{-7}	2.5
[Cr(acac)$_3$]-N_2	3.497×10^{-7}	2
[Cr(acac)$_3$]-He	6.870×10^{-7}	2
[Cu(acac)$_2$]-He	2.193×10^{-6}	2
[Ru(acac)$_3$]-He	3.218×10^{-6}	2
[Fe(tmhd)$_3$]-N_2	6.106×10^{-7}	2
[Fe(tmhd)$_3$]-He	1.351×10^{-6}	2
[Mn(tmhd)$_3$]-N_2	4.552×10^{-7}	2
[Mn(tmhd)$_3$]-He	1.090×10^{-6}	2
[Al(tmhd)$_3$]-N_2	5.174×10^{-2}	2
[Al(tmhd)$_3$]-He	9.929×10^{-7}	2
[Cr(tmhd)$_3$]-He	9.094×10^{-7}	2
[Cu(tmhd)$_2$]-N_2	3.455×10^{-7}	2
[Cu(tmhd)$_2$]-He	1.158×10^{-6}	2
[Ni(tmhd)$_2$]-He	1.449×10^{-6}	2
[Ru(cp)$_2$]-N_2	3.996×10^{-7}	2

Lebenslauf

Personal Daten:

Name	Rehan Ahmad Siddiqui
Geburtsdatum	19-11-1977
Geburtsort	Lucknow, Indien
Nationalität	Indisch
Familienstand	Ledig
Kontakt Adresse	Franzstraße 21 47198, Duisburg Deutschland
E-mail	rehansiddiqui@hotmail.de

Studium:

06/2001 – 06/2003	Master of Science in Industrial Chemistry am A. M. University, Aligarh, India.
06/1998 – 06/2001	Bachelor of Science in Industrial Chemistry am A. M. University, Aligarh, India.
06/1994 – 05/1996	Hochschulreife: Senior Secondary School certificate am A. M. University, Aligarh, India.

Veröffentlichungen:

1. M. Aslam Siddiqi, Rehan A. Siddiqui, Burak Atakan
   "Thermal stability, sublimation pressures and diffusion coefficients of some metal acetylacetonates", **Surface and Coating Technology**, 201, (2007) 9055.

2. Andreas Schneider, Nadejda Popovska, Illona Jipa, Burak Atakan, M. Aslam Siddiqi, Rehan Siddiqui, and Ulrich Zenneck
   "Minimizing the Carbon Content of Thin Ruthenium Films by MOCVD Precursor Complex Design and Process Control", **Chemical Vapor Deposition**, 13, (2007) 389.

3. C. Pflitsch, R. A. Siddiqui and B. Atakan
   "Phosphorescence properties of sol–gel derived ruby measured as functions of temperature and Cr^{3+} content", **Applied Physics A: Materials Science & Processing**, 90, (2008) 527.

4. C. Pflitsch, R. A. Siddiqui and B. Atakan
   "Sol–Gel Deposition of Chromium Doped Aluminium Oxide Films (Ruby) for Surface Temperature Sensor Application", **Chemistry of Materials**, 20, (2008) 2773.

5. M. Aslam Siddiqi, Rehan A. Siddiqui, Burak Atakan
"Thermal stability, sublimation pressures and diffusion coefficients of anthracene, pyrene and some metal ß-diketonates" **Journal of Chemical Engineering Data**, (2009) *ASAP* (*DOI*:10.1021/je9001653).

6. M. Aslam Siddiqi, Rehan A. Siddiqui, Burak Atakan
"Thermal stability, sublimation pressures and diffusion coefficients of some metal 2,2,6,6.-tetramethyl-3,5-heptadionate[$M(tmhd)_n$] compounds" **Journal of Chemical Engineering Data**, (2009) submitted.